Identification and characterisation of the Pex3-Inp1 complex as the first peroxisome-plasma membrane tether

Georgia Elizabeth Hulmes, MBiolSci (Hons)

This thesis is submitted to the University of Sheffield for the degree of Doctor of Philosophy

The University Of Sheffield.

Faculty of Science
Department of Molecular Biology and Biotechnology

August 2020

Abstract

Eukaryotic cells have evolved molecular mechanisms that control organelle size, number and position. Molecular tethers are required for organelle positioning, multiplication and establishment of interorganellar contact sites. The balance between organelle tethering and motility determines the intracellular distribution of organelles and their segregation during cell division. In *Saccharomyces cerevisiae*, correct peroxisome distribution is achieved by the opposing processes of cortical anchoring in the mother cell and Myosin-dependent transport towards the bud. The Inp1-Pex3 tethering complex is required for peroxisome retention during cell division and for peroxisome positioning along the mother cortex.

As has been postulated for other organelles, yeast peroxisomes interact with many cellular structures including the plasma membrane, ER, vacuole, mitochondria and lipid bodies. Components of some interorganellar peroxisomal contact sites have recently been identified whereas others are still completely uncharacterised including the plasma membrane-peroxisome (PM-PER) contact site. The work presented in this thesis identifies Inp1 as the first known plasma membrane-peroxisome (PM-PER) tether by demonstrating that Inp1 meets the predefined criteria which a contact site tether protein must adhere to.

This thesis first describes a conserved Pex3 binding motif in the C-terminal region of Inp1. This motif bears a striking resemblance to the Pex3 binding site present on Pex19 and both *in vitro* and *in vivo* evidence is presented which illustrates that Pex19 and Inp1 can compete for binding to Pex3. In addition, the N-terminal 100 amino acids of Inp1 are shown to localise to the plasma membrane, bind to phosphatidylinositol 4,5-bisphosphate ($PI(4,5)P_2$) and, when artificially attached to the peroxisomal membrane, restore retention by relocating peroxisomes to the cell periphery in *inp1Δ* cells.

In this study, Inp1 is shown to be present in the correct sub-cellular location to interact with both the plasma membrane and peroxisomal membrane and the data illustrates the structural and functional capacity of Inp1 to be a PM-PER tether. Through detailed analysis of the molecular function of Inp1, the work in this thesis identifies a novel role for Inp1 as a PM-PER tether and concludes that tethering of peroxisomes to the plasma membrane is required for peroxisome retention. This is the first molecular characterisation of the PM-PER tether and has allowed for the proposal of a new model for peroxisome retention.

Acknowledgements

“If it was easy, everyone would do it.”

Firstly, I would like to express my deepest gratitude to Dr Ewald Hettema who has not only been my supervisor throughout my PhD but has also been my mentor, valued colleague and friend. Without his endless encouragement, support, enthusiasm and guidance, this work would not have been possible and I would not have grown into the scientist I am today.

I have been extremely lucky to have worked alongside many fantastic members of the Hettema Lab, both past and present. My PhD journey wouldn’t have been the same without their help, support and friendship. Special thanks to Dr John Hutchinson, for his friendship, patience and for his work that paved the way for me and made this study possible. I am also thankful to Dr Joanne Lacey, Dr Nadal Al-Saryi, Dr Donald Watts and Dr Lakhan Ekal who were wonderful lab colleagues and taught me much of what I know today. Thanks also to Dr James Nuttall who I have only ever met once but indirectly and unknowingly taught me so much and also made much of this thesis possible. Finally, thanks to the current members of E28, Sondos, Selva, Quentin, Abdulaziz, Tarad, Yousef, Nourah and Afroza for their ongoing friendship and support, it has been a pleasure to work with you all.

I would also like to pay my special regards to Dr Ellen Allwood for her invaluable help with the liposome binding assays which helped to elevate this work. I would also like to extend my thanks to all the members of the Ayscough lab who were so friendly and warmly welcomed me into their lab and coffee mornings.

Special thanks to Rob for the encouragement, patience and love that he gives me in all aspects of my life, but especially during my PhD. In many ways this wouldn’t have been possible without his selfless support for the last 8 years and I’ll be forever grateful.

Last but certainly not least, thank you to my ever-loving and supportive family. I would be nothing without my team of cheerleaders, celebrating every high and supporting me through every low. My achievements are a reflection of the endless love and encouragement they have shown to me through my PhD, and always.

Table of Contents

Abbreviations

BFP - Blue fluorescent protein
cER – Cortical ER
CHO – Chinese hamster ovary
Drp – Dynamin related protein
ECL - Enhanced Chemi-Luminescence
EPCON - ER-Peroxisome CONtact site
ERMES - ER-mitochondrial encounter structure
ESCRT – Endosomal sorting complexes required for transport
GET – Guided entry of Tail-anchors
Gpd1 - Glyercol-3-phosphate dehydrogenase 1
GST - Glutathione S-transferase
IPTG - Isopropyl-β-D-galactopyranoside
IRD – Infantile Refsum disease
Inp1 – inheritance of peroxisomes 1
LiAc – Lithium acetate
LTP – Lipid transport protein
MBP - Maltose binding protein
MCS – Membrane contact site
Mdh3 - Malate dehydrogenase 3
MECA – Mitochondrial endoplasmic reticulum cortical anchor
MHD – Middle homology domain
mPTS – Membrane peroxisome targeting signal
NALD – Neonatal adrenoleukodystrophy
OD – Optical density
ORF – Open reading frame
PBD – Peroxisome biogenesis disorder
PBS - Phosphate buffer saline
PC - Phosphatidylcholine
PCR – Polymerase chain reaction
PE - Phosphatidylethanolamine
PED – Peroxisomal enzyme deficiencies
PEG – Polyethylene glycol
pER – Peroxisomal endoplasmic reticulum
PEX – Peroxin
PH – Plekstrin homology
PI – Phosphoinositide
PI(4)P - Phosphatidylinositol 4-phosphate
$PI(4,5)P_2$ - Phosphatidylinositol 4,5-bisphosphate

PM – Plasma membrane
PMP – Peroxisomal membrane protein
PM-PER - Plasma membrane-peroxisome
PMSF - Phenylmethylsulfonyl fluoride
pPV – Pre-peroxisomal vesicle
PS - Phosphatidylserine
PTS – Peroxisome targeting signal
PTS1 - Peroxisomal targeting signal type I
PTS2 - Peroxisomal targeting signal type II
SDS-PAGE - Sodium dodecyl sulphate polyacrylamide gel electrophoresis
TCA - Trichloroacetic acid
UV - Ultraviolet
VAMP - Vesicle associated membrane protein
VLCFA – Very long chain fatty acid
YM1 - Yeast minimal medium 1
YM2 - Yeast minimal medium 2
ZS – Zellweger syndrome
ZSD – Zellweger spectrum disorder

List of Figures

Chapter 1

Chapter 2

Chapter 3

Chapter 4

Chapter 5

Chapter 6

List of Tables

Chapter 1 - Introduction

1.1 Peroxisomes

Peroxisomes are single-membrane bound organelles and are present in almost all eukaryotic cells. Their discovery is attributed to Rhodin who, in 1954, observed cytoplasmic particles in mouse renal cells which he morphologically described as 'microbodies' (Rhodin, 1954). These sub-cellular particles were later isolated in equilibrium density gradients and assigned a biochemical identity by Christian de Duve and his group. Enzymes were identified within the microbodies which catalyse reactions resultant in the production and subsequent degradation of hydrogen peroxide, for example catalase, hence the term 'peroxisome' was introduced (Baudhuin et al., 1965; De Duve and Baudhuin, 1966).

Peroxisomes are extremely plastic organelles and their size, number, contents and morphology can be rapidly altered in response to intracellular and extracellular changes. They have essential roles in a diverse array of biochemical pathways and contain a wide variety of enzymes which are required for a range of metabolic processes. Some peroxisomal reactions are organism specific such as in the firefly *Photinus pyralis* where luciferase, an oxidative enzyme which produces the bioluminescence which causes fireflies to 'glow', is localised to peroxisomes (Keller et al., 1987). Other peroxisomal pathways such as the degradation of fatty acids via the β-oxidation cycle are highly conserved across almost all eukaryotes (reviewed by Lazarow & Fujiki, 1985).

In plants and many fungi, β-oxidation of fatty acids occurs exclusively in peroxisomes whereas in higher eukaryotes, β-oxidation also takes place in the mitochondria. Until the 1980's it was assumed that mammalian peroxisomes are only required for β-oxidation of fatty acids when the oxidative capacity of the mitochondria within the cell is reached (Poirier et al., 2006). However, this idea was challenged upon observations that tissue from patients with peroxisomal disorders contains accumulations of very long chain fatty acids (VLCFA) (more than 22 carbon atoms in chain length) but not long or medium chain fatty acids. In the absence of functioning peroxisomes, VLCFA are not degraded by β-oxidation despite the presence of functioning mitochondria (Brown et al., 1982). It is now established that in higher eukaryotes, mitochondria and peroxisomes exhibit differential substrate specificity of the fatty acids they β-oxidise (reviewed by Wanders and Waterham, 2006).

The importance of peroxisomes in relation to human health is evidenced by the number of diseases which are resultant of an absence of functioning peroxisomes. Peroxisomal disorders arise when peroxisomal biogenesis or function is impaired and are generally classified into two distinct groups, peroxisome biogenesis disorders and single enzyme deficiencies (reviewed by Wanders, 2014).

1.2 Peroxisomal disorders

1.2.1 Peroxisome biogenesis disorders

The most severe of the peroxisomal diseases are peroxisome biogenesis disorders (PBDs), a group of heterogeneous, autosomal recessive diseases. The most common subtype of PBD is the Zellweger spectrum disorders (ZSD) (reviewed by Waterham et al., 2016). The Zellweger spectrum can be divided into several phenotypes ranging from mild to severe: Heimler syndrome, Infantile Refsum disease (IRD), Neonatal adrenoleukodystrophy (NALD) and Zellweger syndrome (ZS). Initially these were clinically described as separate diseases, but biochemical characterization means that they are now recognised as different presentations of disorders on the same clinical spectrum (Poll-The et al., 1987; Klouwer et al., 2015).

In mammalian peroxisome biogenesis there are 16 *PEX* genes which encode PEX proteins (peroxins). These peroxins are highly conserved throughout eukaryotes from yeast to humans and their co-ordinated activity is required for peroxisome formation and peroxisomal protein import. Biallelic, pathogenic mutations in any one of 14 of these *PEX* genes (most commonly, *PEX1*) have been found to result in disorders of peroxisome assembly. A full or partial block in peroxisome biogenesis consequently impairs many metabolic pathways and so results in metabolic abnormalities within patients (reviewed by Braverman et al., 2013).

1.2.2 Peroxisomal enzyme/transporter deficiencies

Peroxisomal enzyme deficiencies (PEDs) arise when peroxisomes are intact but there is an absence or dysfunction of an enzyme or pathway resulting in a biochemical abnormality. These disorders often involve just one affected enzyme but the diseases which manifest may be as clinically severe as a PBD (reviewed by Fidaleo, 2010). PEDs affect metabolic pathways such as ether-phospholipid synthesis, peroxisomal α-oxidation and peroxisomal β-oxidation and can also be subdivided into distinct subgroups (reviewed by Wanders and Waterham, 2006).

1.3 Peroxins and peroxisome biogenesis

Research into peroxisome biogenesis was initiated upon the discovery that growing the budding yeast *Saccharomyces cerevisiae* on media containing oleic acid results in peroxisome proliferation (Veenhuis et al., 1987). Further research showed that peroxisomes are essential for growth of *S. cerevisiae* on media where oleic acid is the sole carbon source. This observation was able to form the basis of a negative selection assay whereby peroxisome biogenesis mutants devoid of peroxisomal structures could be identified due to their inability to grow on oleic acid medium (Erdmann et al., 1989). This research was furthered in other yeast species such as *Pichia pastoris* (Liu et al., 1992; Gould et al., 1992), and in CHO (Chinese hamster ovary) cells where peroxisomes are essential for plasmalogen biosynthesis, thus providing another negative selection screen for the identification of peroxisome biogenesis mutants (Tsukamoto et al., 1990; Morand et al., 1990).

Further peroxisome biogenesis mutants were identified using positive selection screens. In one such assay, a chimeric protein comprised of the bleomycin antibiotic resistance gene and the peroxisomal matrix enzyme luciferase, was expressed in *S. cerevisiae*. The assay worked on the premise that if the chimeric protein was transported into peroxisomes, the cells would not be resistant to phleomycin. In mutants devoid of peroxisomal structures, the chimeric phleomycin resistance protein would be present in the cytosol and so peroxisome biogenesis mutants could be positively selected due to their phleomycin resistance (Elgersma et al., 1993).

The genes identified over this period were initially named and characterised with respect to their function or the order in which they were identified. The system under which they are now recognised were summarised by Distel *et al*., and the proteins were named peroxins, encoded by *PEX* genes (Distel et al., 1996). Further identification of *PEX* genes has been achieved using DNA microarray techniques for oleic-induced yeast genes and proteomic approaches and to date, 36 peroxins have been identified. The peroxins which have been identified in *S. cerevisiae* are described with their associated functions in Table 1.1.

Table 1.1 - The known peroxins in *S. cerevisiae* and their associated functions. Modified from (Smith and Aitchison, 2013).

Peroxin	Functional category
Targeting of matrix proteins	
Pex5	PTS1 cargo shuttling receptor
Pex7	PTS2 cargo shuttling receptor
Pex18	PTS2 cargo co-receptor
Pex21	PTS2 cargo co-receptor
Pex9	PTS1 cargo shuttling receptor
Matrix protein import machinery	
Pex13, Pex14, Pex17	Receptor docking complex
Pex8	Bridging of the docking and export complex, assembly of importer
Pex4	Ubiquitylation in receptor export, ubiquitin conjugating enzyme
Pex22	Pex4 anchor, receptor export
Pex2, Pex10, Pex12	Form the RING finger complex, receptor export
Pex1, Pex6	AAA-type ATPase, receptor recycling
Pex15	Membrane receptor for Pex1 and Pex6
Direct targeting of peroxisomal membrane proteins	
Pex3	Docking of Pex19, insertion of PMPs
Pex19	Soluble PMP receptor and chaperone
Formation of peroxisomal membrane from the ER	
Pex3, Pex19	Forms a complex required for *de novo* biogenesis of peroxisomes
Pex25	Required for *de novo* biogenesis of peroxisomes
Pex30	Regulates *de novo* biogenesis of peroxisomes
Fission	
Pex11	Membrane elongation, recruits fission machinery
Pex25	Membrane elongation and remodelling

Pex27, Pex34	Positive regulators of peroxisome fission
Regulation of peroxisome biogenesis	
Pex28, Pex29, Pex31, Pex32	Forms a complex with reticulon homology domain-containing proteins, establishes peroxisome contact sites as ER subdomains
Pex35	Interacts with Arf1 and regulates peroxisome abundance

1.4 Peroxisomal matrix protein import

Peroxisomal matrix proteins are synthesised on cytosolic ribosomes and post-translationally imported into peroxisomes (reviewed by Lazarow and Fujiki, 1985). Most peroxisomal matrix proteins contain one of two peroxisomal targeting signal (PTS) sequences within their polypeptide chains. The most common is PTS1, a conserved, tripeptide consensus sequence of (S/A/C)-(K/R/H)-L which is found at the extreme C-terminus of matrix proteins (Gould et al., 1989). The PTS2 is much less common. It is found near the N-terminus of the protein and is comprised of the consensus sequence (R/K)-(L/V/I/Q)-X-X-(L/V/I/H/Q)-(L/S/G/A/K)-X-(H/Q)-(L/A/F) (Swinkels et al., 1992; Petriv et al., 2004). The addition of a PTS sequence is sufficient to target even non-peroxisomal proteins to the peroxisomal matrix. The PTS1 in particular is often exploited for the creation of fluorescent peroxisomal matrix markers by the addition of the amino acids -SKL to the extreme C-terminus of a fluorescent protein.

Matrix proteins with a PTS1 or PTS2 bind to the soluble cytosolic receptors Pex5 and Pex7 respectively. In *S. cerevisiae*, Pex7 interactions with PTS2 proteins also requires the partially redundant co-receptors Pex18 and Pex21 or the orthologue Pex20 in *Pichia pastoris* (Titorenko et al., 1998). In mammalian peroxisome protein import, the function of co-receptor for PTS2 proteins is fulfilled by alternative splicing of Pex5 into a long and short isoform, PEX5L and PEX5S. PEX5L binds to Pex7 and is the place of conversion between the PTS1 and PTS2 pathways in mammalian cells (Braverman et al., 1998).

PTS1 and PTS2 receptor-cargo complexes assemble in the cytosol and are targeted to the docking complex (Pex13/Pex14/Pex17) on the peroxisomal membrane (Urquhart et al., 2000). Once assembled with Pex14 at the docking complex, a transient pore is formed from either Pex5 (PTS1 pathway) or Pex18 (PTS2 pathway) (Gouveia et al., 2000; Erdmann and Schliebs, 2005) It is through this pore that cargo proteins are released into the peroxisomal lumen, although the exact mechanisms behind this are not known (Meinecke et al., 2010; reviewed by Meinecke et al., 2016).

The PTS receptors are then recycled. This occurs through mono-ubiquitination of the receptor at a conserved cysteine by the E2-enzyme complex Pex4/Pex22 and the E3-ligases of the RING complex which consists of Pex2, Pex10 and Pex12 (reviewed by Platta and Erdmann, 2007; Williams et al., 2008; Platta et al., 2009; El Magraoui et al., 2012). Ubiquitination of the receptors primes them for release from the peroxisomal membrane and their release to the cytosol is carried out by the AAA-peroxins Pex1 and Pex6 in an ATP-dependent manner (Miyata and Fujiki, 2005; Platta et al., 2005). Pex1 and Pex6 form an heterohexameric complex anchored to the peroxisomal membrane by Pex15 or the orthologue Pex26 in humans (Matsumoto et al., 2003; Birschmann et al., 2003). Finally, the ubiquitin moiety is removed and the receptor is free to bind to cargo for another round of import (Fig. 1.1).

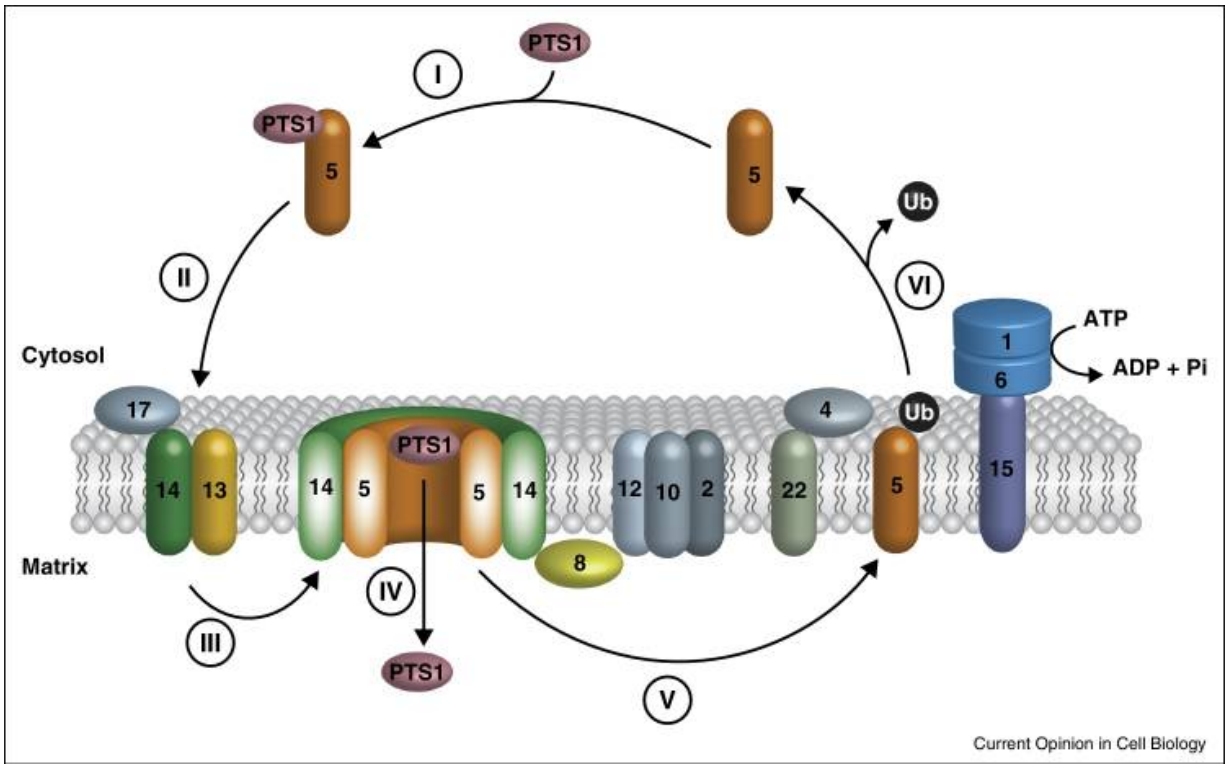

Figure 1.1 – A schematic diagram representing the model of events which are involved in the import of peroxisomal matrix proteins in *S. cerevisiae* (Hettema et al., 2014). (I) Proteins with a peroxisomal targeting signal of type 1 (PTS1) are recognised and bound by the import receptor Pex5 in the cytosol. (II) The cargo-loaded receptor is then directed to the peroxisomal membrane, binds to the docking complex and (III) forms a transient pore with Pex14. (IV) Cargo proteins are imported into the peroxisome in an unknown manner before being released from the receptor. (V) The import receptor is then mono-ubiquitinated and (VI) released from the peroxisomal membrane in an ATP-dependent manner.

1.5 Peroxisome membrane protein import

Peroxisomal membrane proteins (PMPs) have alternative pathways to peroxisomal matrix proteins for their insertion into the peroxisomal membrane. This is evident due to the existence of peroxisome 'ghosts' which were first observed in cells of Zellweger's patients. These empty peroxisomal membrane compartments contain PMPs but lack peroxisomal matrix proteins (Santos et al., 1988).

Pex3 and Pex19 are essential for peroxisomal membrane biogenesis and in cells where either of these genes are absent, there is a lack of typical peroxisomal membrane structures and most PMPs are mislocalised to the cytosol or other membrane compartments such as the ER or mitochondrial outer membrane (Gotte et al., 1998; Matsuzono et al., 1999; Hettema et al., 2000; Shimozawa et al., 2000; Muntau et al., 2000). In mammals and other higher eukaryotes, Pex16 is also found to play a key role in peroxisomal membrane biogenesis (Honsho et al., 1998; South and Gould, 1999). However, Pex16 is not functionally or structurally conserved and most yeast including *S. cerevisiae* lack a Pex16 orthologue.

Pex19 is a farnesylated protein which is predominantly found in the cytosol with a small amount present on the peroxisomal membrane (Gotte et al., 1998; Matsuzono et al., 1999; Sacksteder et al., 2000). Pex19 functions as both a PMP chaperone in the cytosol and an import receptor by binding to specific peroxisome targeting signals of PMPs known as membrane protein targeting signals (mPTSs) (Jones et al., 2004). These mPTSs generally consist of a stretch of hydrophobic and basic amino acids flanked by one or two transmembrane domains (Dyer et al., 1996; Honsho and Fujiki, 2001). Once bound to Pex19, the PMP is stabilised and released into the peroxisomal membrane bilayer when Pex19 docks with Pex3 on the peroxisomal membrane (Fig. 1.2) (Muntau et al., 2003; Fang et al., 2004; Matsuzono et al., 2006). The majority of PMPs are directly and post translationally inserted into peroxisomal membrane via Pex19 and these are referred to as Class I PMPs.

Class II PMPs are proposed to be targeted to the peroxisomal membrane via the ER, independent of Pex19. Of the few identified Class II PMPs, one of the best characterised is Pex3. Pex19 does not bind the mPTS of Pex3 and is not required for Pex3 import to peroxisomes, indicative that Pex3 is imported differently from other PMPs (Jones et al., 2004). This may be due to its essential role in peroxisome biogenesis, which is further discussed in the following section.

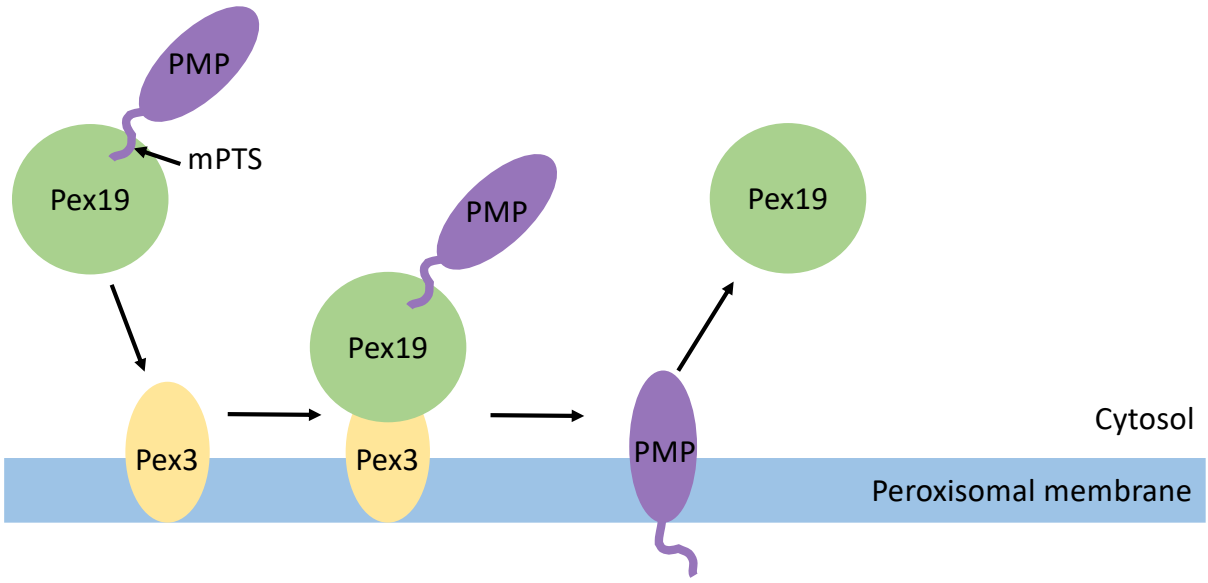

Figure 1.2 - The model of events which are involved in the import of peroxisomal membrane proteins into peroxisomes. In the cytosol, the peroxisomal membrane protein (PMP) docks with the chaperone protein Pex19 through interaction of its membrane PTS (mPTS). Pex19 chaperones the PMP through the cytosol before docking with Pex3 at the peroxisomal membrane via its conserved N-terminal domain. The PMP inserts into the peroxisomal membrane and Pex19 is released back to the cytosol. Diagram is not to scale.

1.6 Maintenance of peroxisomes and the role of Pex3

Pex3 is a highly conserved peroxisomal membrane protein and acts in a range of genetically separate, peroxisomal processes through its interactions with various proteins. It can be described as a hub-like protein, orchestrating diverse peroxisomal functions such as biogenesis, membrane protein import, retention and targeted degradation of peroxisomes (pexophagy) (Fig. 1.6).

1.6.1 Peroxisome biogenesis – Pex3 and Pex19

The biogenesis of peroxisomes has been a central theme of peroxisome research for several decades. This work has resulted in two main models of biogenesis for yeast peroxisomes which both centre around the emergence of peroxisomes from the ER and the essential interaction between the highly conserved peroxins Pex3 and Pex19. There is an additional model for mammalian peroxisome biogenesis which identifies a role for mitochondria. This work reports that peroxisomes can be derived from pre-peroxisomal vesicles which emerge from the ER and mitochondria (Sugiura et al., 2017). For the purpose of this thesis, the following sections will focus on the two models of yeast peroxisome biogenesis, with emphasis on the importance of the Pex3-Pex19 interaction.

The growth and division model

The growth and division model is based upon the idea that that peroxisomes form from pre-existing ones by growth from ER derived lipids, insertion of cytosolic PMPs into the peroxisomal membrane and subsequent fission to form a daughter peroxisome (Fig. 1.3) (Lazarow and Fujiki, 1985; Motley and Hettema, 2007). As described in Section 1.5, PMPs are synthesised in the cytosol and post-translationally chaperoned to peroxisomes by Pex19. Pex19 has a high affinity N-terminal binding site for Pex3 and docks with Pex3 at the peroxisomal membrane where Class I PMPs are subsequently inserted into the membrane bilayer (Fang et al., 2004; Matsuzono et al., 2006; Schmidt et al., 2010). The two proteins can form a structural and functional unit as the mPTS of Pex3 is different to the mPTS binding sites of other PMPs which allows for the formation of Pex3-Pex19-PMP complexes (Shibata et al., 2004). Furthermore, the amino acid domain required for Pex19 docking has been identified in Human Pex3 (Muntau et al., 2003; Fang et al., 2004).

To produce the daughter peroxisome, fission occurs via three steps, elongation, constriction and scission. The Pex11 family proteins, Pex11α, Pex11β and Pex11γ in mammalian cells and Pex11, Pex25 and Pex27 in *S. cerevisiae*, are central to this process (reviewed by Kiel et al., 2006). *S. cerevisiae* Pex11 and its mammalian α, β, γ-isoforms cause tubulation of peroxisomes during peroxisome elongation. Following constriction, Pex11 (or mammalian Pex11β) binds to the tail anchored adaptor protein Fis1 which in turn recruits the yeast peripheral membrane receptors Caf4 or Mdv1 or the mitochondrial fission factor Mff1 in mammalian cells (Motley et al., 2008; Gandre-Babbe and van der Bliek, 2008). The yeast dynamin-related protein (Drp) GTPase Dnm1, or mammalian Dlp1, are subsequently localised to the site of constriction and GTP hydrolysis leads to peroxisome scission (Li and Gould, 2003; Kuravi et al., 2006). In yeast, the Drp Vps1 is also recruited for fission and contributes more to peroxisome fission under normal growth conditions than Dnm1 based fission, but this occurs independently of Fis1 (Hoefpner et al., 2001; Motley et al., 2008).

The *de novo* biogenesis model

The importance of the Pex3-Pex19 interaction is highlighted when it is considered that cells lacking functional Pex3 or Pex19 are devoid of peroxisomes (Hettema et al., 2000). In peroxisome biogenesis mutants or peroxisome inheritance mutants that lack peroxisomes, complementation by the missing gene allows peroxisomes to form without pre-existing peroxisomal membrane structures (Höhfeld et al., 1991). This observation gave rise to the *de novo* peroxisome biogenesis model, a process by which peroxisomes are generated from domains in the ER in a Pex3 and Pex19 dependent manner (Fig. 1.4) (Hoepfner et al., 2005).

In the absence of peroxisomal structures, Pex3 accumulates in specialised domains of the ER referred to as the pre-peroxisomal ER (Hoepfner et al., 2005; Kragt et al., 2005; Tam et al., 2005; Motley and Hettema, 2007). Many PMPs including Pex3 itself are co-translationally inserted into the pre-peroxisomal subdomains of the ER by the Sec61 complex whilst peroxisomal tail anchored proteins are inserted post-translationally and dependent upon Get1, 2 and 3 of the GET complex (Guided Entry of Tail-anchors) and Pex19 (Schuldiner et al., 2008; Thoms et al., 2012; Mayerhofer et al., 2016).

The release of pre-peroxisomal vesicles from the ER is Pex19 dependent although the mechanisms by which Pex19 releases Pex3 are unknown and any other essential molecular machinery has yet to be characterised (Van Der Zand et al., 2010; Lam et al., 2011). The endosomal sorting complexes required for transport (ESCRT)-III proteins Vps20 and Snf7 are proposed to play a role in pre-peroxisome vesicle scission (Mast et al., 2018). The pre-peroxisomal vesicles then fuse with each other to form a pre-peroxisome which is capable of matrix protein import and can subsequently mature into a functional peroxisome (Van Der Zand et al., 2012).

Some studies do suggest that *de novo* formation of peroxisomes occurs in all cells (Kim et al., 2006; Van Der Zand et al., 2012), however the majority of yeast studies indicate that growth and division is the default mode of peroxisome multiplication and that *de novo* formation is observed when a cell is temporarily devoid of peroxisomes (Motley and Hettema, 2007; Knoblach et al., 2013; Motley et al., 2015).

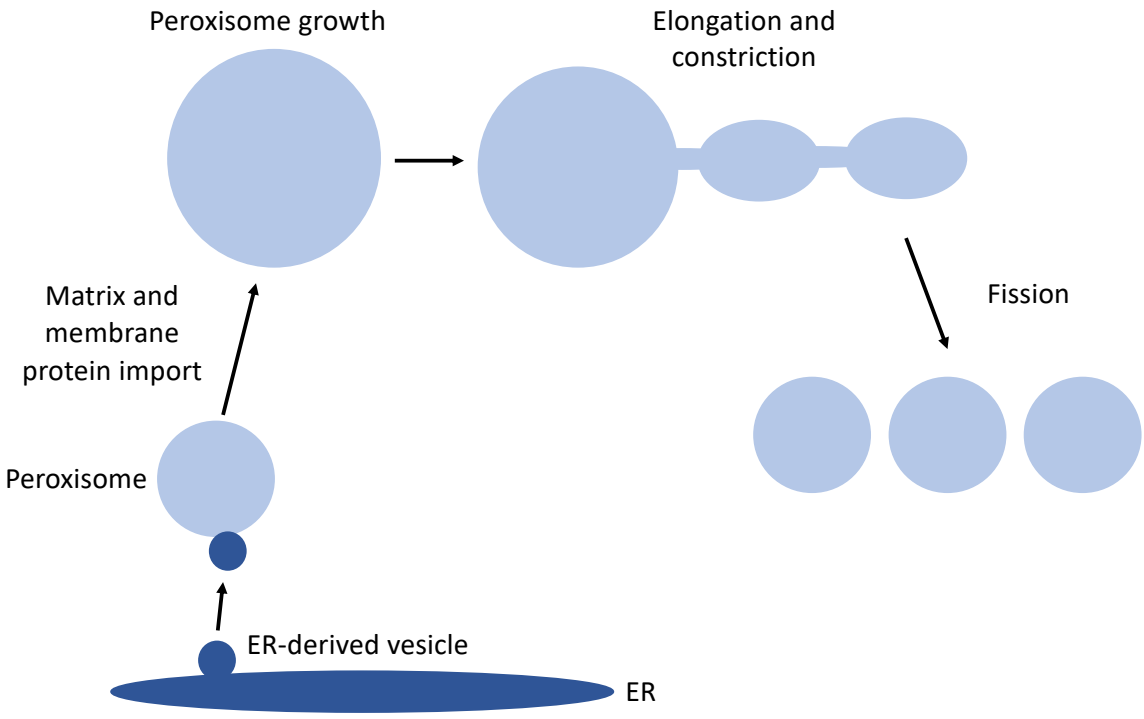

Figure 1.3 – The peroxisome growth and division model. The growth and division model proposes that peroxisomes receive lipids and a subset of PMPs from the ER via vesicular transport and fusion. Additionally, peroxisomes receive newly synthesised peroxisomal matrix and membrane proteins from the cytosol. These processes contribute to peroxisomal growth and so once a peroxisome reaches a certain size it undergoes elongation, constriction and fission. Diagram is not to scale.

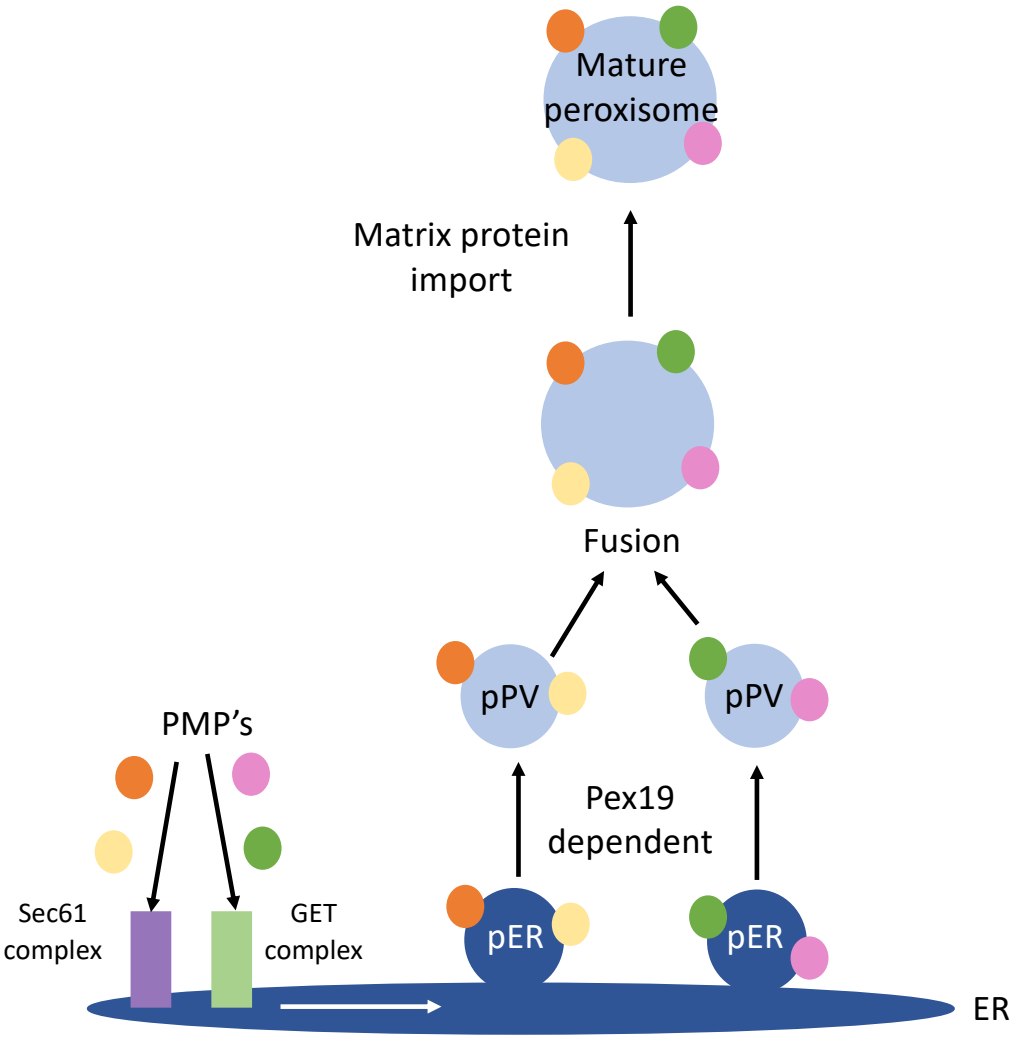

Figure 1.4 - The peroxisome *de novo* biogenesis model. PMPs are co-translationally inserted into the ER via the Sec61 complex or post-translationally inserted via the GET complex. The PMPs are targeted to sub-domains of the ER known as the peroxisomal ER (pER). These areas then form into pre-peroxisomal vesicles (pPV) which bud from the ER in a Pex19-dependent manner. The pre-peroxisomal vesicles are of two distinct types, one comprised of Pex3, Pex2 and Pex11 and the other comprised of Pex3, Pex13, Pex14, Pex17, Pex10 and Pex12. These pPVs then fuse with each other and form a pre-peroxisome which is capable of matrix protein import and can subsequently mature into a functional peroxisome. Diagram is not to scale.

1.6.2 Pexophagy – Pex3 and Atg36

Selective autophagic breakdown of peroxisomes, pexophagy, requires an interaction between Pex3 and Atg36 in *S. cerevisiae* and its orthologue Atg30 in *Pichia pastoris*. Atg36 and Atg30 function as specific pexophagy adaptors and through interactions with Atg8 and Atg11, couple peroxisomes to the autophagic machinery (Motley et al., 2012; Burnett et al., 2015). The interaction between Atg36 and Atg11 is dependent upon phosphorylation of Atg36 by Hrr25 but as yet, the exact mechanisms by which the Atg36-Pex3 interaction is regulated remain unclear and a higher eukaryotic orthologue of Atg36 is yet to be identified (Tanaka et al., 2014).

1.6.3 Peroxisome retention and inheritance

Pex3 and Inp1

A full complement of organelles is important for cellular function and eukaryotic cells have evolved molecular mechanisms that control organelle size, number and position. Molecular tethers are required for organelle positioning, multiplication and establishment of inter-organellar contact sites, a topic which will be further discussed in Section 1.7. Spatial and temporal control of organelle location requires a tightly regulated system and the balance between organelle tethering and motility determines the intracellular distribution of organelles and their segregation during cell division (Fagarasanu et al., 2010). The inheritance of some organelles during cell division is crucial, such as the mitochondria and nucleus which contain essential genetic material and cannot be formed *de novo*. Other organelles such as peroxisomes can be formed *de novo*, but as discussed in Section 1.6.1, this is not an energetically favourable process and does not appear to be the preferred process by which cells form peroxisomes.

S. cerevisiae is a budding yeast that undergoes asymmetric cell division during asexual reproduction. As such, organelles must be actively and vectorially transported to the growing bud. Correct peroxisome inheritance is achieved by a balance between the opposing processes of cortical anchoring in the mother cell and Myosin-dependent transport towards the bud (Hoepfner et al., 2001; Fagarasanu et al., 2006; Knoblach et al., 2013; Knoblach and Rachubinski, 2019). It is the direct interaction between Pex3 and Inp1 which is essential for retention of a subset of peroxisomes during cell division and correct peroxisome positioning along the mother cortex (Fagarasanu et al., 2005; Munck et al., 2009; Knoblach et al., 2013).

Inp1 (Inheritance of peroxisomes 1) is a peripheral membrane protein identified in yeast. It was first implicated in peroxisome retention as cells devoid of Inp1 have an abnormal distribution of peroxisomes, with almost all peroxisomes present in the bud. These cells also exhibit a phenotype of a reduced number of enlarged peroxisomes (Fagarasanu et al., 2005). Conversely, overexpression of Inp1 leads to almost all peroxisomes being retained in the mother cell (Fagarasanu et al., 2005). The recruitment of Inp1 to peroxisomes is due to its direct binding to Pex3 (Munck et al., 2009; Knoblach et al., 2013).

The current model for the peroxisome tethering function of Inp1 proposes that Inp1 acts as a molecular bridge between peroxisomes and the ER by interacting in *trans* with peroxisomal Pex3 and cortical ER-associated Pex3 via N and C-terminal Pex3 binding domains (Fig. 1.5) (Knoblach et al., 2013). However, recent work by the same group has shed doubt on the simplicity of this model with the suggestion that the ER-peroxisome tether is likely to involve additional cortical factors. The authors also suggest that contact sites between the ER and peroxisomes may occur independently of Inp1 and that Inp1 may function as a tether between peroxisomes and other organelles (Knoblach and Rachubinski, 2019).

Transport of peroxisomes to the bud is facilitated by Inp2, an integral peroxisomal membrane protein which functions antagonistically to Inp1 (Fagarasanu et al., 2006). Inp2 is a specific peroxisomal receptor for the class V myosin, Myo2, a myosin motor which binds to Inp2 via its C-terminal cargo binding domain (CBD) and transports peroxisomes along actin cables to the bud (Fig. 1.5) (Hoepfner et al., 2001; Sellers and Veigel, 2006; Fagarasanu et al., 2006; Knoblach and Rachubinski, 2015). As with Inp1, Inp2 is thought to be a poorly conserved protein with orthologues yet to be identified in higher eukaryotes. However, residues in the CBD of Myo2 which are considered relevant for its interaction with Inp2 have been found to be conserved in the CBD's of mammalian MyoVa and MyoVb. This implies a highly conserved function among class V myosin motors from yeast to humans and perhaps points to the existence of a human Inp2 equivalent (Nascimento et al., 2013).

In cells lacking Inp2, peroxisome inheritance is abolished or delayed and results in buds devoid of peroxisomes whilst overexpression of Inp2 results in a depletion of peroxisomes from mother cells as they are all transported into the bud (Fagarasanu et al., 2006). By anchoring peroxisomes at the cortex of the mother cell, it is ensured that a population of peroxisomes are retained in the mother. Additionally, anchoring of peroxisomes to the bud cortex, once transported there, prevents against backtracking of peroxisomes into the mother cell (Fagarasanu et al., 2005). Pex19 has also been shown to contribute to peroxisome delivery to the bud by binding to Inp2 and in *H. polymorpha,* Pex19 is essential for Inp2's interaction with Myo2 (Otzen et al., 2012; Saraya et al., 2010).

The peroxisomal locations of Inp1 and Inp2 during growth, division and fission have been distinguished using the mutant *Δdnm1/Δvps1*. In these cells peroxisome fission is abolished, and peroxisomes appear elongated and 'sausage-like'. On these peroxisomes, Inp1 is observed at the tip of the peroxisome proximal to the mother cell whilst Inp2 is present on the tip of the peroxisome which resides in the bud (Knoblach et al., 2013).

Cortical tethering of peroxisomes and active transport of peroxisomes to the bud are required during asymmetric cell division to ensure that the peroxisomal population is properly maintained as cell division occurs. Inp1 and Inp2 are central to this process as they define the spatial and temporal distribution of peroxisomes by performing antagonistic functions and ensuring proper peroxisome segregation along the mother-bud axis (Fagarasanu et al., 2005; A. Fagarasanu et al., 2006; M. Fagarasanu et al., 2006).

Pex3 and Myo2 in *Yarrowia lipolytica*

At present, there are no identified higher eukaryotic orthologues of Inp1, but orthologues of Inp1 are present in other yeasts such as *Yarrowia lipolytica*. *Yl*Inp1 has also been shown to be required for peroxisome retention, although it has not been shown that this is due to a direct interaction with *Yl*Pex3 (Chang et al., 2007). *Y. lipolytica* is unique in that it contains Pex3 and a paralogue of Pex3 which has been named Pex3B. *Yl*Pex3 and *Yl*Pex3B have been shown to bind to the class V Myosin MyoV and are reported to have roles as peroxisome-specific myosin adaptors which contribute to the transport of peroxisomes to the bud during cell division. Additionally, *Yl*Pex3 and *Yl*Pex3B are able to interact with *Sc*Myo2 which is suggestive that they are functional equivalents of Inp2 in *S. cerevisiae* (Chang et al., 2009). It is reasonable to predict that, as is known for other orthologues of Inp1, *Yl*Inp1 directly interacts with a paralogue of *Yl*Pex3. This therefore implies that in *Y. lipolytica*, Pex3 is directly involved in both peroxisome retention and transport. Due to the evolution of two members of the Pex3 protein family, *Y. lipolytica* allows for the unique observation of the contribution of Pex3 to the movement of peroxisomes. Although it is not yet reported in any other species, the observations made in *Y. lipolytica* give rise to the idea that Pex3 is able to play a direct role in both peroxisome retention and transport in other species.

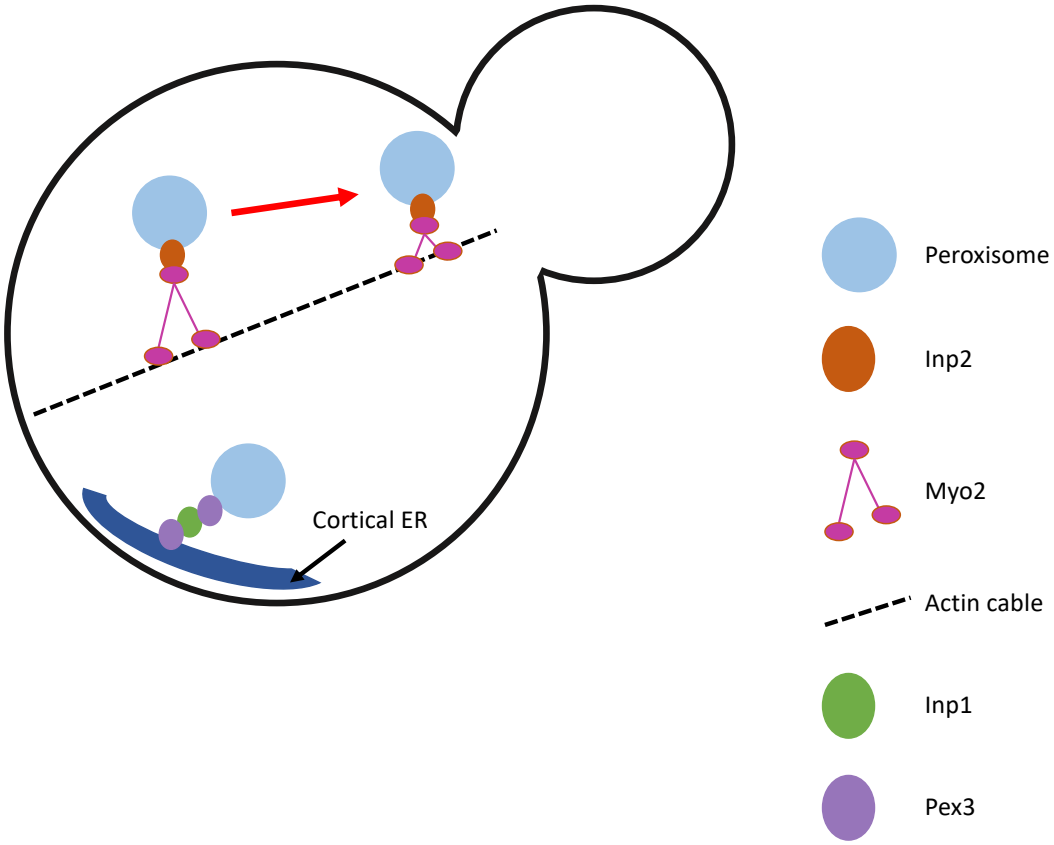

Figure 1.5 – The existing model of peroxisome inheritance and retention in *S. cerevisiae*. Transport of peroxisomes to the bud requires Inp2 (orange) which is a peroxisome-specific receptor for the Class V Myosin, Myo2 (pink). The myosin motor binds to Inp2 through its C-terminal cargo binding domain and transports peroxisomes along actin cables towards the bud. Retention of peroxisomes is currently proposed to occur via Inp1 (green) which binds to peroxisomal and cortical ER-associated Pex3 (purple) in trans. It is suggested that by acting as a molecular bridge, Inp1 ensures peroxisome retention at the mother cell cortex during asymmetric cell division. Diagram is not to scale.

1.6.4 Pex3 and the vacuole

A recent study in the yeast *Hansenula polymorpha* implicated Pex3 as a factor involved in the formation of peroxisome-vacuole contact sites under conditions of rapid peroxisome development. Pex3 accumulates at sites of vacuole-peroxisome contact during growth on methanol and overexpression of Pex3 was found to result in the formation of peroxisome-vacuole contact sites in conditions where these sites do not usually occur (Wu et al., 2019). Whether Pex3 directly interacts with proteins or lipids on the vacuolar membrane is unclear but this gives rise to an additional role of Pex3 in organelle contact site formation, a topic which is further discussed in Section 1.7.

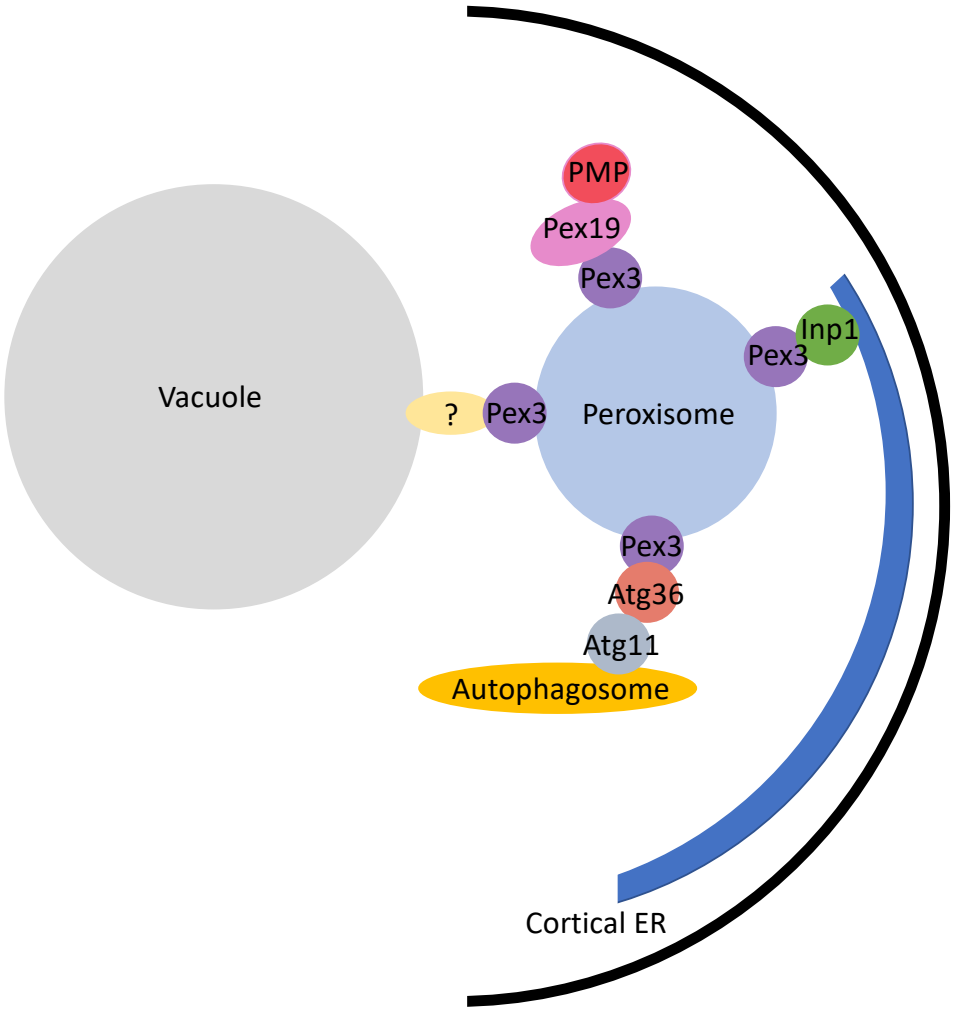

Figure 1.6 – Pex3 is central to a range of roles in peroxisome biology. This schematic diagram represents the role of *S. cerevisiae* Pex3 in peroxisome membrane import via Pex19, peroxisome retention via Inp1, peroxisome autophagy via Atg36 and peroxisome-vacuole contact site formation via as yet unidentified factors. Diagram is not to scale. Modified from (Wu et al., 2019).

1.7 Organelle contact sites

A distinguishing feature of eukaryotic cells is their compartmentalisation into distinct, membrane-bound organelles. This creates a diverse range of microenvironments and increases the efficiency of sub-cellular reactions but also means that there are physical barriers which could create obstacles as molecules move around the cell. In the mid-20th century, electron microscopy studies observed that organelles were frequently found in close apposition to each other with defined focal points of contact (Bernhard and Rouiller, 1956; Copeland and Dalton, 1959; Gray, 1963). These studies gave the first indications that organelles could communicate through direct contact with each other, however, it was widely believed that diffusion, active transport and vesicular trafficking through the cytoplasm were the primary methods by which inter-organellar exchange of cellular materials occurred. However, over recent years it has become increasingly obvious that organelles are not isolated structures and that cross-membrane communication and organelle functionality are frequently facilitated by physical contact between organelles at membrane contact sites (MCS). Membrane contact sites can be defined as domains where membranes from two intracellular compartments are tethered in close proximity by protein or lipid interactions, resulting in the function of one or both organelles being affected (Prinz, 2014; Shai et al., 2018; Prinz et al., 2020). Every organelle has now been shown to have at least one functional MCS with another organelle and most organelles have more than one (Valm et al., 2017; Shai et al., 2018).

Membrane contact sites are extremely diverse. The distance between organelles can be fixed or variable and where it varies, the range of distance between two organelles can be very broad. In *S. cerevisiae* the distance between the ER and the plasma membrane (PM) at MCS can range from 16-60nm (West et al., 2011). The stability of MCS also varies widely, some contacts are extremely stable and persist for the lifetime of the cell while others are much more transient and last for less than 1 second (Lewis et al., 2016). Some organelles share multiple physically and functionally distinct MCS at the same time. For example distinct contact sites between the ER and PM have been shown to co-exist to facilitate the functionally different processes of what appears to be cholesterol exchange and store-operated calcium entry (Besprozvannaya et al., 2018).

Membrane contact sites are not restricted to just two different organelles and there are several examples of three-way organelle contact sites. For example, the ER is present at contact sites between the plasma membrane and mitochondria as part of a multi-subunit complex termed MECA (mitochondrial ER cortical anchor) (Lackner et al., 2013). Additionally, in *S. cerevisiae* the ER protein Mdm1 has been proposed to associate with lipid droplets and the vacuole, creating a three-way junction between the organelles (Hariri et al., 2019). Another form of MCS are intraorganellar membrane contact sites. In the ER, Atlastin has been identified as a tether protein which creates junctions within the ER (Wang et al., 2016).

1.7.1 Roles of contact sites

Membrane contact sites have been shown to have a wide range of roles with the best characterised being non-vesicular transport of metabolites such as lipids and cell communication and signalling pathways. Intracellular lipid transport by non-vesicular lipid

exchange is facilitated by lipid transport proteins (LTPs). LTPs are often enriched at MCS and bind to MCS-associated proteins. Lipid exchange at MCS serves to alter lipid compositions of specific membranes or organelles and to regulate lipid-based signalling pathways such as phosphoinositide (PI) based signalling at the ER-PM membrane contact site (reviewed by Cockcroft and Raghu, 2018). MCSs can serve as signalling hubs in response to external stimuli such as stress or nutrition. Phosphatidylinositol is synthesised in the ER but the kinases that convert it to phosphoinositides such as PI(4)P or PI(4,5)P_2 are present in other organelles such as the plasma membrane or Golgi (Agranoff et al., 1958; Walch-Solimena and Novick, 1999; Audhya and Emr, 2002). Hence, the formation of MCS between the ER and other organelles allows for differential amounts of PI to be produced or depleted dependent on the cell's needs (Kim et al., 2011). These phosphoinositides then have downstream functions in a broad range of cellular processes such as cell signalling, regulation of ion channel activity, endocytosis and vesicular transport (reviewed by Balla et al., 2009 and Dickson and Hille, 2019).

MCSs also allow for the efficient exchange of metabolites such as calcium ions between organelles. This increases reaction rates and prevents loss of metabolites to the surrounding areas of the cell. For example, there is an enrichment of ER Ca^{2+} channels at ER-Mitochondria MCS which results in a higher concentration of Ca^{2+} at these sites and hence increases the efficiency of metabolite transfer between the two organelles (Rizzuto et al., 1993; Csordás et al., 2010).

1.8 Organelle positioning and tethering

1.8.1 Mitochondrial tethering

MCS are required for regulation of organelle inheritance and retention and this has been shown in *S. cerevisiae* with mitochondria, peroxisomes and lipid droplets. During asymmetric cell division, the correct positioning of mitochondria at the cell periphery is mediated by at least three known MCSs. Cortical mitochondrial anchorage occurs via the mitochondrial ER cortex anchor (MECA), a multi-subunit protein complex (Lackner et al., 2013). The core component of MECA is Num1, a cortical associated protein which binds to the mitochondrial outer membrane and the plasma membrane via two distinct lipid binding domains (Lackner et al., 2013; Ping et al., 2016). Although MECA is reported to be a tether between three organelle membranes, the molecular mechanisms for MECA association with the ER remain poorly understood. The plasma membrane has been further implicated in mitochondrial tethering via site-specific mitochondrial anchorage at the mother cell tip via Mfb1 (Pernice et al., 2016). In the bud, the mitochondrial Myo2 receptor-related protein Mmr1 mediates ER-Mitochondria MCS to anchor mitochondria to the bud cell tip (Swayne et al., 2011). The various MCS between mitochondria, the PM and the ER ensure that functional organelles are both retained by mother cells and inherited by daughter cells.

1.8.2 Peroxisome contact sites

Peroxisome – ER

In mammalian cells, nearly 90% of peroxisomes contact the ER (Valm et al., 2017). The proteins which tether the ER and Peroxisomes at their MCS in mammalian cells were described by two independent groups. The ER resident proteins known as Vesicle associated membrane protein (VAMP)-associated proteins A and B (VAP-A and VAP-B) interact with the FFAT-like motifs of the peroxisomal membrane proteins ACBD4 and ACBD5 in mammalian cells (Loewen and Levine, 2003; Hua et al., 2017; Costello et al., 2017a; Costello et al., 2017b). Absence or disruption of these tethers results in decreased plasmalogen, cholesterol and fatty acid β-oxidation levels and implies that ER-peroxisome contact is important in lipid transport (Hua et al., 2017; Yagita et al., 2017).

In yeast, several membrane contact sites between the ER and Peroxisome have so far been described. One such MCS plays a role in peroxisome retention and requires Inp1 and Pex3. This is fully described in Section 1.6.3. Peroxisome-ER contact in *S. cerevisiae* also involves the Pex23 family proteins Pex29 and Pex30 which form a complex with ER-localised reticulon homology proteins Rtn1 and Yop1 and create an ER-Peroxisome CONtact site (EPCON). The ER domains enriched for Pex29 and Pex30 dynamically associated with peroxisomes during growth on glucose and stably associate during growth on oleate. It is suggested that the EPCON plays a role in *de novo* biogenesis of peroxisomes (David et al., 2013; Mast et al., 2016; Joshi et al., 2016; Joshi et al., 2018). Similar observations have recently been made in *H. polymorpha* where it was shown that the Pex23 family peroxins Pex24 and Pex32 function as tethers to mediate peroxisome-ER contact sites. Deletion of *Hp*Pex24 or *Hp*Pex32 results in disruption of peroxisome-ER contacts and impairs peroxisome biogenesis and normal peroxisome segregation between mother cells and buds (Wu et al., 2020).

Peroxisome – Mitochondria

Peroxisomes and mitochondria co-operate closely in β-oxidation of fatty acids and share proteins required for their respective division machineries, a relationship which implies the need for close contact between the two organelles (reviewed by Schrader et al., 2012). Sites of close proximity between peroxisomes and mitochondria have been observed in *S. cerevisiae* and mammalian cells with several different tether complexes proposed in *S. cerevisiae* (Fan et al., 2016; Shai et al., 2018).

The peroxisomal membrane protein Pex34 and the mitochondrial outer membrane mitofusin protein Fzo1 are proposed to exist as distinct tether complexes. They are enriched at peroxisome-mitochondria MCS and their overexpression enhances the number of contact sites between the two organelles. However, the identities of their counterpart binding partners remains unclear. Associations between peroxisomes and mitochondria are assumed to allow efficient transport of metabolites to enhance metabolism as it is proposed that Pex34 functions in the transfer of β-oxidation intermediates between the two organelles (Shai et al., 2018). In mammalian cells it is suggested that peroxisome-mitochondria MCS allow for interorganellar exchange of steroid biosynthesis metabolites (Fan et al., 2016). Pex11 has also been identified as a potential peroxisome-mitochondria tether through direct interaction

with Mdm34, a component of the ERMES (ER-mitochondrial encounter structure) complex (Ušaj et al., 2015). Pex11 interacts directly with Fis1, a shared component of both peroxisomal and mitochondrial fission and as such the Pex11-Mdm34 MCS could have a role in peroxisome fission (Koch et al., 2010; Joshi et al., 2012).

Peroxisome – Lipid droplets

Growth of yeast on oleate induces peroxisome proliferation and has also been shown to increase the number and stability of peroxisome-lipid droplet contact sites (Binns et al., 2006). Contact between these two organelles is assumed to be mainly for lipid transfer. In addition to observations made in fungal cells, lipid droplets have also been observed to form contact sites with peroxisomes in mammalian cells through the peroxisomal membrane protein ABCD1 and the lipid droplet protein M1 Spastin (Chang et al., 2019).

Peroxisome – Vacuole

Membrane contact sites between the vacuole and peroxisome have been observed in the budding yeast *S. cerevisiae* using split-GFP technology (Shai et al., 2018; Kakimoto et al., 2018). These MCS are further described in the yeast *Hansenula polymorpha* where Pex3 is implicated to play a crucial role in the formation of Peroxisome-Vacuole contact sites (Wu et al., 2019).

1.8.3 Defining a tether

After the identification of MCS by electron microscopy, further studies went on to find proteins which were present at the sites of contact between interorganellar membranes and were involved in physically bridging the opposing membranes (Kawamoto et al., 1986; Pan et al., 2000). It is now established that contact between organellar membranes is achieved through proteins or protein complexes known as 'tethers' due to their functional and structural capacity to physically tether organelles together. Some tethers actively participate in the specific function of the interorganellar MCS whilst others adapt the size and number of MCS in response to environmental stimuli (Kornmann et al., 2011; Prinz, 2014). Other tethers serve as molecular bridges, physically attaching the membranes together (Csordás et al., 2006).

The list of interorganellar contact sites is expanding all the time and it is clear that the proteins which reside in these contact sites and are implicated in interorganellar tethering roles may contribute to any of several molecular functions. The recent increase in the identification of contact site proteins has led to a formal consensus of criteria that a protein should adhere to in order to be formally classified as an MCS tether (Eisenberg-Bord et al., 2016; Scorrano et al., 2019).

1) Defined location: A tether must reside exclusively in or be enriched in a contact site.

2) Structural capacity: A tether or tether complex must have the ability to mediate binding to the opposing membranes.

3) Functional activity: A tether must exert a tethering force. This can be measured by observing the effect that loss of or overexpression of a tether has on the extent of a contact site. It can also be assayed with the use of artificial tethers and their capability to rescue tether loss.

1.9 Aims

The molecular interaction between Inp1 and Pex3 was first described by the Hettema lab, (Munck et al., 2009) and the current model of Inp1/Pex3-mediated peroxisome retention was established in 2013 (Knoblach et al., 2013). This model was widely accepted by the cell biology community until fairly recently when the authors (Knoblach and Rachubinski, 2019), shed doubt on the mechanisms of their own model with the suggestion that additional components are required for peroxisome tethering to the cell cortex and that Inp1 may function as a tether between peroxisomes and other organelles.

The original aim of this study was to functionally characterise Inp1 in molecular detail, however the data obtained led to an investigation into the role of Inp1 as a potential membrane contact site tether between peroxisomes and another organelle, the plasma membrane. This study now aims to present evidence that Inp1 is the first identified peroxisome-plasma membrane tether and proposes a new model for peroxisome retention during asymmetric cell division in yeast.

Chapter 3 aims to confirm the preliminary characterisation of the Inp1-Pex3 interaction and further previously obtained data (Hutchinson, 2016). Both *in vivo* and *in vitro* techniques are employed to reveal the molecular mechanisms by which Inp1 interacts with peroxisomal Pex3. Chapter 4 aims to elucidate the role of the N-terminal domain of Inp1 and through *in vitro* liposome binding assays, investigates how, if not via ER-bound Pex3, Inp1 tethers peroxisomes to the mother cell cortex during asymmetric cell division. Chapter 5 serves to explore the identity of Inp1 as a membrane contact site tether protein between the plasma membrane and peroxisomes. The evidence presented illustrates that Inp1 adheres to the criteria which allow a protein to be formally classified as a tether (Eisenberg-Bord et al., 2016). Finally, Chapter 6 aims to discuss the data obtained throughout the study and concludes with a new model for peroxisome retention which involves MCS between peroxisomes and the plasma membrane.

Chapter 2 - Materials and Methods

2.1 Chemicals and enzymes

Most of the chemicals, primers and materials used throughout this study were supplied by MERCK (Formerly Sigma-Aldrich). Restriction enzymes and buffers were supplied by New England Biolabs (NEB). PCR buffers, dNTPs, DNA polymerases and Miniprep kits were supplied by Bioline UK. Gel extraction kits were supplied by Qiagen.
Growth media components were supplied by Difco Laboratories and ForMedium. D-Glucose was provided by Fisher Scientific UK.
Equipment used for DNA and protein work was supplied by BioRad. Buffers for protein work were provided by Geneflow.

2.2 Strains and plasmids

2.2.1 Strains

Table 2.1 - The yeast strains used in this study. Gene deletions or modifications were performed as described in (Longtine et al., 1998).

Strain	Genotype	Source
BY4741 WT	*MATA his3-1 leu2-0 met15-0 ura3-0*	Euroscarf
BY4742 WT	*MATα his3-1 leu2-0 lys2-0 ura3-0*	Euroscarf
inp1Δ	*MATA his3-1 leu2-0 met15-0 ura3-0 inp1::KanMX4*	Euroscarf
inp1/pex3Δ	*MATA his3-1 leu2-0 met15-0 ura3-0 inp1::KanMX4 pex3::hphMX6*	Hettema Lab
inp1/inp2Δ	*MATA his3-1 leu2-0 met15-0 ura3-0 inp1::KanMX4 inp2::hphMX6*	Hettema Lab
pex3Δ	*MATA his3-1 leu2-0 met15-0 ura3-0 pex3::KanMX4*	Euroscarf
pex19Δ	*MATα his3-1 leu2-0 lys2-0 ura3-0 pex19::KanMX4*	Euroscarf
atg36Δ	*MATA his3-1 leu2-0 met15-0 ura3-0 atg36Δ::KanMX4*	Euroscarf
mdh3/gpd1Δ	*MATA his3-1 leu2-0 met15-0 ura3-0 gpd1Δ::KanMX4 mdh3Δ::SpHis5*	(Al-Saryi et al., 2017)

mdh3/gpd1/pex3Δ	*MATA his3-1 leu2-0 met15-0 ura3-0 gpd1Δ::KanMX4 mdh3Δ::SpHis5 pex3Δ::HphMX6*	(Al-Saryi et al., 2017)
sac1Δ	*MATA his3-1 leu2-0 met15-0 ura3-0 sac1::KanMX4*	Euroscarf
rtn1/rtn2/yop1Δ	*MATA his3-1 leu2-0 met15-0 ura3-0 rtn1::KanMX4 rtn2::KanMX4 yop1::KanMX4*	(Voeltz et al., 2006)
rtn1/rtn2/yop1/inp1Δ	*MATA his3-1 leu2-0 met15-0 ura3-0 rtn1::KanMX4 rtn2::KanMX4 yop1::KanMX4 inp1::URA3*	This study
scs2/scs22/ist2/tcb1/tcb2/tcb3Δ	*MATA leu2-3,112 ura3-52 his3-Δ 200 trp1-Δ901 lys2-801 suc2-Δ9 ist2::HISMX6 scs2::TRP1 scs22::HISMX6 tcb1::KANMX6 tcb2::KANMX6 tcb3::HISMX6*	(Manford et al., 2012)
scs2/scs22/ist2/tcb1/tcb2/tcb3/inp1Δ	*MATA leu2-3,112 ura3-52 his3-Δ 200 trp1-Δ901 lys2-801 suc2-Δ9 ist2::HISMX6 scs2::TRP1 scs22::HISMX6 tcb1::KANMX6 tcb2::KANMX6 tcb3::HISMX6 inp1::URA3*	This study
Plasma membrane-Peroxisome reporter	*his3delta1 leu2delta0 lys2+/lys+ met15delta0 ura3delta0 can1Δ::STE2pr-sp HIS5 lyp1Δ::STE3pr-LEU2; KAN::Tef2pr-Vn-Pmp3; Pex11-VC-His*	This study
ER-Peroxisome reporter	*his3delta1 leu2delta0 lys2+/lys+ met15delta0 ura3delta0 can1Δ::STE2pr-sp HIS5 lyp1Δ::STE3pr-LEU2; Sec63-VC-His; Pex3-VN-Kan*	(Shai et al., 2018)
Mitochondria-Peroxisome reporter	*his3delta1 leu2delta0 lys2+/lys+ met15delta0 ura3delta0 can1Δ::STE2pr-sp HIS5 lyp1Δ::STE3pr-LEU2; Tom20-VC-His; Pex11-VN-Kan*	(Shai et al., 2018)
Vacuole-Peroxisome reporter	*his3delta1 leu2delta0 lys2+/lys+ met15delta0 ura3delta0 can1Δ::STE2pr-sp HIS5 lyp1Δ::STE3pr-LEU2; Zrc1-VC-His; Pex25-VN-Kan*	(Shai et al., 2018)

Table 2.2 – The *Escherichia coli* strains used in this study. The strain, genotype, purpose and source of each *E. coli* strain are shown.

***E. coli* strain**	**Genotype**	**Purpose**	**Source**
DH5α	*supE44 ΔlacU169 (Φ80 lacZ ΔM15) hsdR17 recA1 endA1gyrA96 thi-1 relA1*	Amplification of plasmids and recovery of plasmid DNA from *S. cerevisiae* following *in vivo* homologous recombination	(Hanahan, 1983)
BL21 DE3	*hsdS gal (λcIts857 ind1 Sam7 nin5 lacUV5-T7 gene 1)*	Expression of GST, MBP and 6xHis fusion proteins	(Studier and Moffatt, 1986)

2.2.2 Plasmids

The plasmids used in this study are shown in Table 2.3. Plasmids were made by restriction digest and ligation followed by transformation into *E. coli* or by homologous recombination in *S. cerevisiae*. For *E. coli* expression, the parental vectors pET42a and pET30a were used (Rosenberg et al., 1987). For plasmids expressed in yeast, the parental vectors Ycplac33 and Ycplac111 were used which contain the multiple cloning site shown below (Gietz and Sugino, 1988). Promoters, terminators, recombinant tags and open reading frames were introduced into the restriction sites.

EcoRI SacI KpnI SmaI BamHI XbaI SalI PstI SphI HindIII

gaa ttc gag ctc ggt acc cgg gga tcc tct aga gtc gac ctg cag gca tgc aag ctt

Table 2.3 - Plasmids used in this study. The description, parental plasmid, primer codes, restriction enzymes and vector backbone are shown.

Plasmid	**Made from**	**Primers (F + R)**	**Enzymes**	**Vector**
Plasmids used in truncation screen				
GAL1 Inp1-GFP	*GAL1* GFP	VIP55 + VIP 167	BamH1/Sal 1	ycplac111
GAL1 Inp1 1-400 GFP	*GAL1* Inp1-GFP	VIP49 + VIP556	EcoR1/Pst1	ycplac111
GAL1 Inp1 1-370 GFP	*GAL1* Inp1-GFP	VIP49 + VIP604	EcoR1/Pst1	ycplac111
GAL1 Inp1 1-340 GFP	*GAL1* Inp1-GFP	VIP49 + VIP603	EcoR1/Pst1	ycplac111
GAL1 Inp1 1-315 GFP	*GAL1* Inp1-GFP	VIP49 + VIP602	EcoR1/Pst1	ycplac111
GAL1 Inp1 1-282 GFP	*GAL1* Inp1-GFP	VIP49 + VIP 557	EcoR1/Pst1	ycplac111
GAL1 Inp1 100-420 GFP	*GAL1* Inp1-GFP	VIP648 + VIP643	Sac1/Pst1	ycplac111
GAL1 Inp1 170-420 GFP	*GAL1* Inp1-GFP	VIP649 + VIP643	Sac1/Pst1	ycplac111

GAL1 Inp1 240-420 GFP	*GAL1* Inp1-GFP	VIP650+ VIP643	Sac1/Pst1	ycplac111
GAL1 Inp1 295-420 GFP	*GAL1* Inp1-GFP	VIP642 + VIP643	Sac1/Pst1	ycplac111
GAL1 Inp1 300-420 GFP	*GAL1* Inp1-GFP	VIP644 + VIP 643	Sac1/Pst1	ycplac111
GAL1 Inp1 311-420 GFP	*GAL1* Inp1-GFP	VIP645 + VIP643	Sac1/Pst1	ycplac111
GAL1 Inp1 315-420 GFP	*GAL1* Inp1-GFP	VIP625 + VIP 643	Sac1/Pst1	ycplac111
GAL1 Inp1 281-400 GFP	*GAL1* Inp1-GFP	VIP605 + VIP556	Sac1/Pst1	ycplac111
GAL1 Inp1 311-370 GFP	*GAL1* Inp1-GFP	VIP645 + VIP604	Sac1/Pst1	ycplac111
GAL1 Inp1 315-400 GFP	*GAL1* Inp1-GFP	VIP625 + VIP556	Sac1/Pst1	ycplac111
GAL1 Inp1 315-370 GFP	*GAL1* Inp1-GFP	VIP625 + VIP604	Sac1/Pst1	ycplac111
Point mutation plasmids				
Inp1-GFP	GFP	VIP261 + VIP167	EcoR1	ycplac33
Inp1 DD>AA-GFP	Inp1-GFP	VIP2617 + VIP2618		ycplac33
Inp1 L>A-GFP	Inp1-GFP	VIP1722 + VIP1723		ycplac33
Inp1 NY>AA-GFP	Inp1-GFP	VIP3664 + VIP3665		ycplac33
Inp1 LL>AA-GFP	Inp1-GFP	VIP1724 + VIP1725		ycplac33
Inp1 DEE>AAA-GFP	Inp1-GFP	VIP1778 + VIP1779		ycplac33
Inp1 Δmotif-GFP	Inp1-GFP	VIP3663 + VIP3664		ycplac33
Tpi-Inp1	Tpi-MCS	VIP55 + VIP56	BamH1/Sal 1	ycplac111
Tpi-Inp1 LL>AA	Tpi-MCS	VIP1722 + VIP1723		ycplac111
GFP-Pex19	Tpi GFP-Pex19	VIP1819 + VIP1792	EcoR1/Bam H1	ycplac111
GFP-Pex19 L>A	GFP-Pex19	VIP1780 + VIP1781		ycplac111
GFP-Pex19 LL>AA	GFP-Pex19	VIP1782 + VIP1783		ycplac111
GFP-Pex19 DD>NY	GFP-Pex19	VIP3657 + VIP3658		ycplac111
Expression vector plasmids				
His-Pex3 (40-441)	pET30a	VIP235 + VIP237	BamH1/Sal 1	pET30a
MBP-Inp1	pMAL-c5x	VIP2485 + VIP2488	Nde1/Bam H1	pMAL-c5x
MBP-Inp1 1-280	pMAL-c5x	VIP2485 + VIP2486	Nde1/Bam H1	pMAL-c5x
MBP-Inp1 281-420	pMAL-c5x	VIP2487 + VIP2488	Nde1/Bam H1	pMAL-c5x

GST-Inp1	pGEX6p-2a	VIP55 + VIP56	BamH1/Sal 1	pGEX6p-2a
GST-Inp1 Δmotif	GST-Inp1	VIP3663 + VIP3664		pGEX6p-2a
GST-Inp1 LL>AA	GST-Inp1	VIP1724 + VIP1725		pGEX6p-2a
Artificial/minimal tether plasmids				
Inp1-GFP-Pex15	GFP-Pex15	VIP49 + VIP272	EcoR1/Sac1	ycplac111
Inp1 Δmotif-GFP-Pex15	GFP-Pex15	VIP49 + VIP272	EcoR1/Sac1	ycplac111
Inp1 1-280-GFP-Pex15	GFP-Pex15	VIP49 + VIP3755	EcoR1/Sac1	ycplac111
Inp1 281-420-GFP-Pex15	GFP-Pex15	VIP3756 + VIP272	EcoR1/Sac1	ycplac111
Inp1 1-100-GFP-Pex15	GFP-Pex15	VIP49 + VIP2090	EcoR1/Sac1	ycplac111
Inp1 101-280-GFP-Pex15	GFP-Pex15	VIP3764 + VIP3755	EcoR1/Sac1	ycplac111
GFP-Pex15	GFP-MCS	VIP1119 + VIP1120	BamH1	ycplac111
Inp1 100-420-GFP	Inp1 prom-MCS-GFP	VIP3764 + VIP3741	Sac1/Sal1	ycplac33
Num1 PH (2563-2692) GFP-Pex15	Inp1 prom-MCS-GFP-Pex15	VIP3909 + VIP3911	Sac1	ycplac111
TPI1 Inp1 1-100 mRFP-Pex15	mRFP-Pex15	VIP49 + VIP3972	EcoR1	ycplac111
GAL1 Inp1 1-100-GFP	Tpi Inp1 1-100-GFP	VIP49 + VIP2090	EcoR1/Pst1	ycplac33

2.3 Growth media

All components of cell growth media were dissolved in Millipore water, mixed with a magnetic stirrer and autoclaved to sterilisation at 121°c. Where antibiotics or amino acid stocks were required, these were added to their final concentration when the autoclaved media had cooled to at least 50°c. The reagents required to make growth media are listed in Table 2.4.

Table 2.4 - Growth media. Antibiotic and amino acid concentrations are final concentrations.

Culture Media	Description
2TY	1.6% Bacto-tryptone, 1% yeast extract, 0.5% NaCl. Where required, ampicillin or kanamycin was added to autoclaved media to final concentrations of 75µg/ml and 50µg/ml respectively.
YPD	2% Bacto-peptone, 2% D-Glucose, 1% yeast extract.
Yeast minimal medium 1 YM1 (For selection of all auxotrophic markers)	0.17% yeast nitrogen base (without amino acids and ammonium sulphate), 0.5% ammonium sulphate, 2% D-Glucose, raffinose or galactose. Adjusted to pH 6.5 with NaOH. Relevant amino acid stocks added after autoclaving.
Yeast minimal medium 2 YM2 (For selection of Uracil auxotrophic marker)	0.17% yeast nitrogen base (without amino acids and ammonium sulphate), 0.5% ammonium sulphate, 2% D-Glucose, raffinose or galactose, 1% casamino acids. Adjusted to pH 6.5 with NaOH. 30ng/ml Leucine added after autoclaving.
Amino acid and Uracil stocks	Amino acid/Uracil stocks were added to YM1 and YM2 as required from 100x stocks to final concentrations of 20ng/ml (Uracil, Tryptophan, Methionine, Histidine-HCl) or 30ng/ml (Leucine, Lysine-HCl). Sometimes amino acids were added before autoclaving in the form of dropout supplements from ForMedium.
Solid Media	2% (w/v) agar was added to liquid growth media prior to autoclaving. Once autoclaved and cooled, media was poured into sterile petri dishes (Sterilin) and left to set at room temperature. Once prepared, plates were stored at 4°C

2.4 *S. cerevisiae* protocols

2.4.1 Yeast growth and maintenance

Yeast strains were grown at 30°C on either solid media or in liquid media on an oscillating shaker at 200 rpm. Amino acids and uracil were added to media for auxotrophic strains as required. Antibiotics were used to select for cassettes conferring resistance. For strains containing a plasmid with an inducible *GAL1/10* promoter, cells were grown overnight in selective medium containing 2% raffinose then transferred to YM2 + 2% galactose for the time stated, for induction of gene expression. For long term storage, cells were grown up overnight and 15% v/v glycerol stocks were prepared in cryogenic vials (Nunc) and stored at -80°C.

2.4.2 One step transformation

Yeast strains were transformed with plasmid DNA using the One Step method (Chen et al., 1992). Cells were inoculated into 3ml of appropriate media (usually YPD) and grown overnight at 30°C on a shaker at 200 rpm. The next day, 200µl of the culture was harvested by centrifugation for 1 minute at 12,000 rpm in an Eppendorf table top centrifuge. The supernatant was removed and 1µl plasmid DNA (100ng-400ng), 5µl (50µg) of single stranded DNA (ssDNA) from Salmon sperm and 50µl one step buffer (0.2M LiAc pH 5.0, 40% (w/v) PEG 4000 (polyethylene glycol), 0.1M DTT) were added to the cell pellet and mixed by vortexing. The tube was incubated at room temperature for 3-5 hours with occasional vortexing. The tube was then heat shocked at 42°C in a water bath for 30 minutes, vortexed again and the cell suspension was plated onto relevant selective solid media. Plates were incubated at 30°C for 2-3 days then stored at room temperature once colonies had appeared.

2.4.3 High efficiency transformation

High efficiency yeast transformations were performed to create knockout strains and plasmids. This was according to the Lithium Acetate protocol (Gietz and Woods, 2002) using the reagents listed in Table 2.5. Yeast strains were grown overnight in 3ml YPD liquid medium at 30°C with shaking at 200 rpm. The following morning, the optical density ($O.D._{600}$) of the culture was measured in a Jenway spectrophotometer at 600nm wavelength and the appropriate amount of overnight culture was added to 5ml YPD to give an OD of 0.1. Cells were grown at 30°C on an oscillating shaker at 200 rpm until they reached exponential phase ($O.D._{600}$=0.5). The cells were then centrifuged at 2500 rpm for 5 minutes at room temperature and the supernatant was discarded. The pellet was washed in 1ml sterile water, centrifuged as before then washed in 1ml 1xTE/LiAc solution. The supernatant was completely removed and the pellet was resuspended in 50µl 1xTE/LiAc.
5µl digested vector (0.2-0.5µg), 5µl PCR product, 5µl (50µg) ssDNA and 300µl 40% PEG 4000 was added to 50µl resuspended pellet in an Eppendorf tube. The reaction was left at room temperature for 30 minutes, incubated at 30°C for 30 minutes then heat shocked in a 42°C water bath for 15 minutes. The cells were harvested by centrifuging for 30 seconds at 8000 rpm, the supernatant discarded and the pellet resuspended in 50µl 1xTE. The cells were then plated on selective agar media and incubated for 3 days at 30°C.

Table 2.5 – Components of the solutions required for high efficiency yeast transformation. Solutions were prepared from sterile stocks of the reagents listed.

Solution	Stock reagents used
1xTE/Lithium Acetate solution	1ml 10x TE (0.1M Tris-HCl and 0.01M EDTA) (pH 7.4) 1ml 1M Lithium Acetate solution (pH 7.5) 8ml dH_20
40% Polyethylene Glycol solution	3.2ml 50% (w/v) PEG 4000 dissolved in Millipore water 0.4ml 10x TE (0.1M Tris-HCl and 0.01M EDTA) (pH 7.4) 0.4ml 1M Lithium Acetate (pH 7.5)
1x TE	1ml 10xTE (0.1M Tris-HCl and 0.01M EDTA) (pH 7.4) 9ml dH_20

2.4.4 Yeast genomic DNA isolation

Transformed yeast cells were scraped from a selective plate and centrifuged in a 2ml screw cap tube with 1ml sterile water at 12,000 rpm for 1 minute. For each sample, 200µl of TENTS solution (20mM Tris/HCl pH 8.0, 1mM EDTA, 100mM NaCl, 2% Triton X-100, 1% SDS), 200µl glass beads and 200µl phenol/chloroform was added. Samples were placed in a bead beater for 45 seconds at full speed and then centrifuged at 12,000 rpm for 1 minute. A further 200µl TENTS solution was added and the mixture was vortexed. The sample was then centrifuged at 12,000 rpm for 5 minutes. 350µl supernatant was removed and transferred to a fresh Eppendorf tube. 200µl phenol/chloroform was added, the sample was vortexed and centrifuged as before. 300µl supernatant was removed and transferred to a fresh Eppendorf tube, the nucleic acids were then precipitated using 30µl 3M Sodium acetate and 750µl 100% ethanol. The sample was vortexed and stored at -20°C for an hour.
The sample was then centrifuged at 12,000 rpm for 10 minutes. The supernatant was removed and the pellet washed in 250µl 70% ethanol before the sample was again centrifuged at 12,000 rpm for a further 10 minutes. The supernatant was removed, the pellet was resuspended in 200µl 1xTE pH 8.0 and 2µl RNAse was added. After 10 minutes incubation at room temperature, 20µl 3M Sodium acetate and 500µl 100% ethanol was added, the sample was vortexed and stored at -20°C for a further hour. Centrifugation was then carried out as before and the remaining pellet was washed in 70% ethanol, left to air dry then resuspended in a final volume of 50µl 1xTE pH 8.0.

2.4.5 Epitope tagging or gene knockout in the genome

Epitope tags or knockout cassettes with selective markers were amplified by PCR. Forward primers were designed to contain 50 nucleotides identical to the region immediately upstream of the open reading frame (ORF) (for gene deletion) or stop codon (for epitope tagging) and reverse primers were designed to contain 50 nucleotides downstream of the stop codon (Fig. 2.1). PCR fragments were transformed into yeast by high efficiency transformation (Section 2.4.3) and grown on appropriate selective medium. Correct clones were confirmed by PCR, Western blotting and fluorescence microscopy.

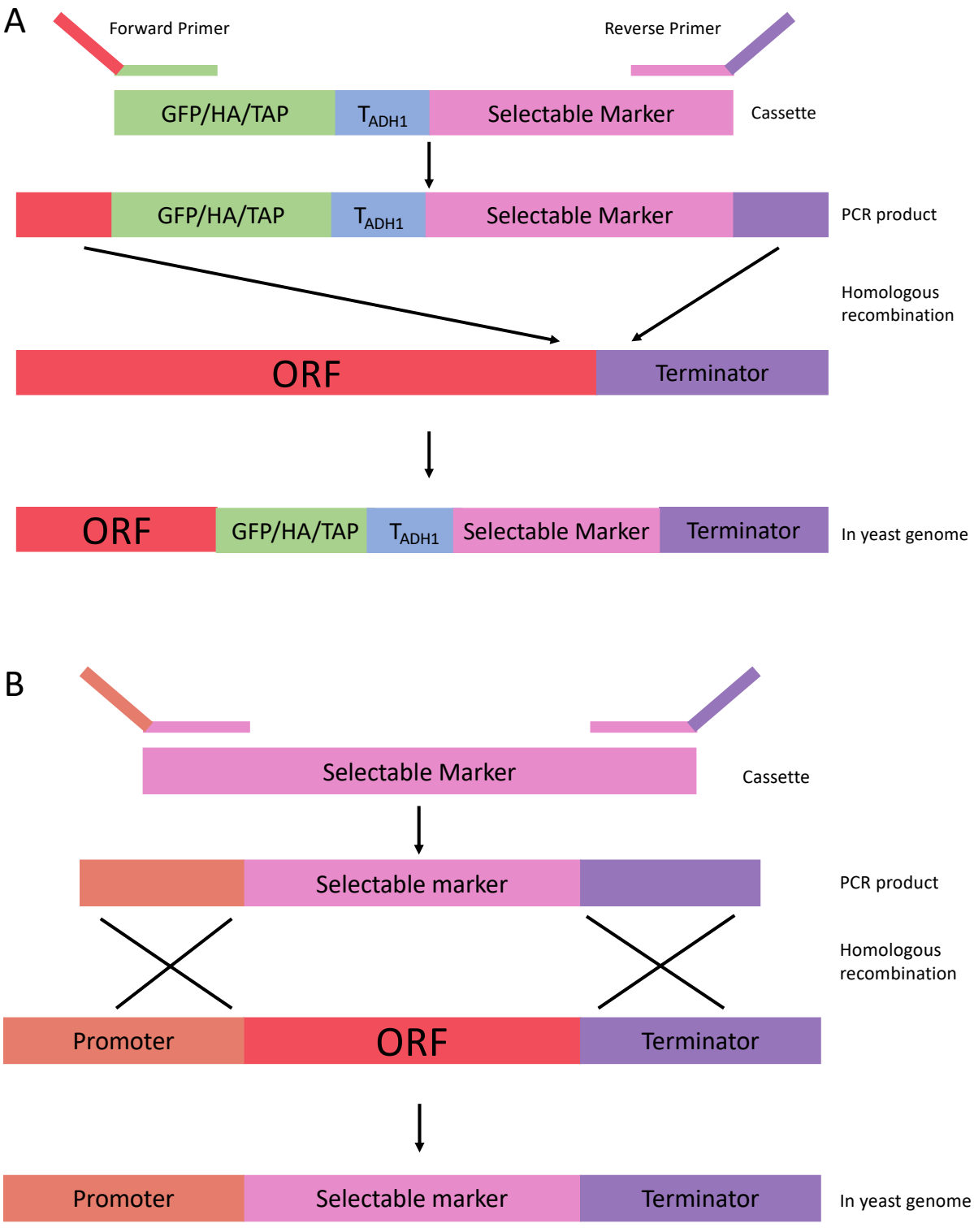

Figure 2.1 – Schematic representations of the methods used to modify genes in the yeast genome. (A) Method for epitope tagging at the C-terminus of open reading frames (ORF). (B) Method for gene deletion. PCR products were transformed into yeast strains by the high efficiency transformation protocol to obtain the desired genetically modified strains. T_{ADH1} indicates *ADH1* terminator.

2.4.6 Mating assays

Cells of each mating type were grown to logarithmic phase on YPD. Cells were then mixed, pelleted, and spotted onto a pre-warmed YPD plate and incubated at 30°C for the times indicated. Cells were harvested from the plate by scraping, resuspended into selective growth medium and analysed by fluorescence microscopy.

2.4.7 Fluorescence microscopy

Cells were analysed with a microscope (Axiovert 200M; Carl Zeiss, Inc.) equipped with Exfo X-cite 120 excitation light source, band-pass filters (Carl Zeiss, Inc. and Chroma), a Plan-Fluar 100x/1.45 NA or Plan-Apochromat 63x 1.4 NA objective lens (Carl Zeiss, Inc.) and a digital camera (Orca ER; Hamamatsu Phototonics). Image acquisition was performed using Volocity software (PerkinElmer). Fluorescence images were routinely collected as 0.5 µm z-stacks and several layers were merged into one plane in Openlab (PerkinElmer) (except where it is indicated that single focal planes are shown). Images were then processed further in Photoshop (Adobe) by adjusting brightness and contrast levels where appropriate. Brightfield images were processed where necessary to illustrate the circumference of cells by increasing the contrast of the image in the blue RGB channel on Photoshop. For linescan analyses, lines were drawn through a region of interest on ImageJ/FIJI to generate intensity profiles across the line for each channel. In order to categorise peroxisomes as 'peripheral' (For example in Fig. 5.3), the individual z-stack layers of relevant images were carefully analysed in order to determine the location of individual peroxisomes in relation to the periphery of the cell. Experimental and control cells were scored in a consistent way.

2.5 *E. coli* protocols

2.5.1 *E. coli* growth and maintenance

E. coli was inoculated into 4ml liquid 2TY medium and incubated at 37°C overnight on an oscillating shaker at 200 rpm or spread onto 2TY agar plates and grown at 37°C. In order to select for transformants, the media was supplemented accordingly with 75µg/ml ampicillin or 50µg/ml kanamycin.

2.5.2 Production of chemically competent *E. coli* cells

E. coli DH5α cells were thawed from -80°C, streaked onto a 2TY plate and incubated overnight at 37°C. The following day a single colony was inoculated into 4ml of 2TY and grown overnight at 37°C on an oscillating shaker at 200 rpm. The next morning, a secondary culture of 200ml 2TY in a 1 litre flask was inoculated to give an $O.D._{600}$ of 0.1. Cells were grown at 37°C on an oscillating shaker at 200 rpm until they reached exponential phase ($O.D._{600}$=0.5) then placed on ice for 10 minutes.
The culture was divided between 4, 50ml sterile falcon tubes and centrifuged for 10 minutes at 3000 rpm at 4°C (Sigma4-16K). The supernatant was discarded, and the pellets were resuspended in 35ml of RF1 (See Table 2.6). 2 tubes were combined to make 2 70ml tubes, left on ice for 20 minutes then centrifuged as before. The supernatant was discarded and 8ml

of RF2 (See Table 2.6) was used to resuspend each pellet before combining the two to give 16ml. 200µl aliquots were taken and put into pre-cooled Eppendorf tubes before flash freezing in liquid N_2 and storing at -80°C.

Table 2.6 – The components of the solutions RF1 and RF2. Required for the production of chemically competent (RbCl) *E. coli* DH5α cells.

RF1 (pH 5.8)	RF2 (pH 6.8)
100mM RbCl	10mM MOPS
50mM $MnCl_2$	10mM RbCl
30mM Potassium acetate	75mM $CaCl_2$
10mM $CaCl_2$	15% (v/v) Glycerol
15% (v/v) Glycerol	

2.5.3 Production of electrocompetent *E. coli* cells

E. coli DH5α cells were thawed from -80°C, streaked onto a 2TY plate and incubated overnight at 37°C. The following day a single colony was inoculated into 4ml of 2TY and grown overnight at 37°C on an oscillating shaker at 200 rpm. The next morning, the appropriate amount of overnight culture was added to 1L 2TY to give a secondary culture with an $O.D._{600}$ of 0.1. Cells were then grown at 37°C on an oscillating shaker at 200 rpm. When exponential phase was reached ($O.D._{600}$=0.5) the culture was divided between two 500ml, sterile centrifuge buckets and centrifuged at 3000 rpm for 15 minutes at 4°C (Sigma 4-16K). The supernatant was removed and each pellet was resuspended in 250ml of ice cold 10% (v/v) glycerol. The cells were centrifuged twice more as before with the pellets being resuspended first in 125ml ice cold 10% (v/v) glycerol and then in 50ml ice cold 10% (v/v) glycerol after which both cultures were transferred to 50ml falcon tubes. After a final centrifugation (as before) the supernatant was removed and both pellets were resuspended in 0.35ml of ice cold 10% (v/v) glycerol and then combined to give a 0.7ml suspension. 40µl aliquots were taken and put into pre-cooled Eppendorf tubes before flash freezing in liquid N_2 and storing at -80°C.

2.5.4 Transformation of chemically competent *E. coli*

50µl chemically competent DH5α or BL21 DE3 cells per transformation were removed from storage at -80°C and thawed on ice. 1µl plasmid DNA or 10µl ligation mixture was added to 50µl cells in an Eppendorf tube and the tube was left on ice for 20 minutes. The cells were heat shocked in a 42°C water bath for 2 minutes then transferred back onto ice for 5 minutes. 900µl 2TY was added to each transformation and the tube was incubated at 37°C for 45 minutes. The tube was then centrifuged at 13,000 rpm for 1 minute and 850µl supernatant was removed leaving approximately 50µl 2TY media and cells. The cells were resuspended gently then plated onto the relevant selective agar media and incubated overnight at 37°C before being stored at 4°C.

2.5.5 Transformation of electrocompetent *E. coli*

40µl electrocompetent cells per transformation were removed from storage at -80°C and thawed on ice. 10µl of 10x diluted gDNA was added to the electrocompetent cells and the reaction mixture was transferred to a 2mm electroporation cuvette (Fisher) on ice. The cuvette was loaded into the Biorad MicroPulser and the cells were electroporated with one pulse on the setting EC2 (V=2.5kV). 600µl 2TY was immediately added and the cells were transferred to a fresh 1.5ml Eppendorf tube and incubated at 37°C for 45 minutes. The tube was then centrifuged for 1 minute at 5000 rpm, the supernatant was removed and the cell pellet was plated onto relevant selective agar media and incubated overnight at 37°C before being stored at 4°C.

2.6 DNA procedures

2.6.1 Polymerase Chain Reaction (PCR)

PCR was used to amplify specific regions of DNA or whole plasmids for Site Directed Mutagenesis (SDM). ACCUZYME™ or VELOCITY™ DNA polymerase were used to amplify DNA when proof-reading activity was required. MyTaq™ DNA polymerase was used for colony PCR. Biovision Pfu was used for SDM PCR. 25µl reactions were made up in PCR tubes. The reagents used are detailed in Table 2.7.

Table 2.7 – PCR reaction mixture compositions. PCR reactions were prepared with the detailed reagents on ice with the DNA polymerase added last. For colony PCR, DNA templates were obtained by using a sterile pipette tip to pick individual colonies and inoculate the PCR reaction mixture.

ACCUZYME™ DNA polymerase	**MyTaq™ DNA polymerase**	**VELOCITY™ DNA polymerase**	**Pfu DNA polymerase**
2.5µl 10x ACCUZYME™ reaction buffer	5µl 5x MyTaq™ reaction buffer	5µl 5x Hi-Fi buffer	2.5µl 10x Pfu buffer
2.5µl forward primer (5µM)	2.5µl forward primer (5µM)	2.5µl forward primer (5µM)	2.5µl forward primer (5µM)
2.5µl reverse primer (5µM))	2.5µl reverse primer (5µM)	2.5µl reverse primer (5µM)	2.5µl reverse primer (5µM)
1.5µl 2.5mM dNTP's (0.15mM)	-	1.5µl 2.5mM dNTP's (0.15mM)	1.5µl 2.5mM dNTP's (0.15mM)
0.75µl 50mM $MgCl_2$ (1.5mM)	-	-	-
1µl 1/50 diluted plasmid DNA (5-10ng) or 1µl gDNA	DNA template acquired by inoculating with an individual bacterial colony	1µl 1/50 diluted plasmid DNA (5-10ng) or 1µl gDNA	1µl 1/5 diluted plasmid DNA (30-50ng)

0.5µl ACCUZYME™ DNA polymerase (1.25 unit)	0.25µl MYTAQ™ DNA polymerase (1.25 unit)	0.25µl VELOCITY™ polymerase (1.25 unit)	0.5µl Pfu polymerase (1 unit)
13.75µl dH_20	14.75µl dH_20	12.25µl dH_20	14.5µl dH_20

PCR reactions were run in a thermocycler with the lid preheated to 100°C to prevent condensation in the PCR tubes. The PCR conditions used are detailed in Table 2.8.

Table 2.8 – PCR conditions. PCR conditions were set up as detailed. The annealing temperature was calculated depending on the AT/GC content of the individual primers used. Steps 2-4 were repeated for 30 cycles in each PCR reaction.

	ACCUZYME™ DNA polymerase	**MyTaq™ DNA polymerase**	**VELOCITY™ DNA polymerase**	**Pfu DNA polymerase**
1 - Initial DNA denaturing	95°C 3 min	95°C 3 min	95°C 3 min	95°C 3 min
2 – DNA denaturing	95°C 30 sec	95°C 30 sec	95°C 30 sec	95°C 30 sec
3 – Annealing of primers	50-65°C 30 sec	50-65°C 30 sec	50-65°C 30 sec	50-65°C 1 min
4 – Elongation	72°C 2min/kb	72°C 30sec/kb	72°C 15sec/kb	68°C 2min/kb
5 – Final extension	72°C 10 min	72°C 10 min	72°C 10 min	68°C 20 min

Annealing temperature was dependent upon the nucleotide composition of each individual primer. These were calculated using the following equation: Annealing temperature (°C) = Melting temperature (°C) - 5°C where Melting temperature = 4(#G + #C) + 2(#A + #T). The primers used in this study are listed in Table 2.9.

Table 2.9 – Primers used in this study. F = Forward and R = Reverse. Sequences are 5’ to 3’.

Nº	**Description**	**Sequence 5'-3'**
49	M13 in ycplac F	GTTTTCCCAGTCACGACG
167	Inp1-GFP R	AGCACCCGCCCCTGCTCCAAGGTCGCCAAGACCAG
644	*GAL1* Inp1 300- F	CAAGGAGAAAAAACTATAGAGCTCAAAATGAACGATGATGATGATGATAA
643	Inp1-GFP R	AGCACCCGCCCCTGCTCCCTGCAGAAGGTCGCCAAGACCAGATATG
625	Inp1 315-420-GFP F	CAAGGAGAAAAAACTATAGAGCTCAAAATGTTGCTGGATGAAGAATACG
556	Inp1 -400-GFP R	AGCACCCGCCCCTGCTCCCTGCAGCGGGGGAGAGTCGATAAAAGG
604	Inp1 -370-GFP R	AGCACCCGCCCCTGCTCCCTGCAGAGGAGCGGTTCGTCTGATAGC
603	Inp1 -340-GFP R	AGCACCCGCCCCTGCTCCCTGCAGATTTAGATTAGAGCAAGTGTTCG

602	Inp1 -325-GFP R	AGCACCCGCCCCTGCTCCCTGCAGCAAGTAATTAAGGTCGTCATC
557	Inp1 -282-GFP R	AGCACCCGCCCCTGCTCCCTGCAGAGGCGGCAGTTTGAATTTATC
648	*GAL1* Inp1 100- F	CAAGGAGAAAAAACTATAGAGCTCAAAATGAATGATATTCCGAATAGCAG
649	*GAL1* Inp1 170- F	CAAGGAGAAAAAACTATAGAGCTCAAAATGCCCTTTCAAAAATCTAGTAA
650	*GAL1* Inp1 240- F	CAAGGAGAAAAAACTATAGAGCTCAAAATGTCAGAGTTGGAAAATAGTG
642	*GAL1* Inp1 295- F	CAAGGAGAAAAAACTATAGAGCTCAAAATGAATAATGATGATGATAACGA
645	*GAL1* Inp1 311- F	CAAGGAGAAAAAACTATAGAGCTCAAAATGGACCTTAATTACTTGCTGG
605	*GAL1* Inp1 281- F	CAAGGAGAAAAAACTATAGAGCTCAAAATGCCTACTTCGGACATAGAGC
261	600bp upstream *INP1*	GTAAAACGACGGCCAGTGAATTCATTGCTGACCATTTGGTTGG
2617	Inp1 DD>AA SDM F	GATGATAATTATGATGATGCCGCCCTTAATTACTTGCTGGATG
2618	Inp1 DD>AA SDM R	CATCCAGCAAGTAATTAAGGGCGGCATCATCATAATTATCATC
1722	Inp1 L>A SDM F	GATAATTATGATGATGACGACGCTAATTACTTGCTGGATGAAG
1723	Inp1 L>A SDM R	CTTCATCCAGCAAGTAATTAGCGTCGTCATCATCATAATTATC
3664	Inp1 NY>AA SDM F	GATAATTATGATGATGACGACCTTGCTGCTTTGCTGGATGAAGAATAC
3665	Inp1 NY>AA SDM F	GTATTCTTCATCCAGCAAAGCAGCAAGGTCGTCATCATCATAATTATC
1724	Inp1 LL>AA SDM F	GATGACGACCTTAATTACGCTGCAGATGAAGAATACGAACAAGG
1725	Inp1 LL>AA SDM R	CCTTGTTCGTATTCTTCATCTGCAGCGTAATTAAGGTCGTCATC
1778	Inp1 DEE>AAA SDM F	CGACCTTAATTACTTGCTGGCTGCAGCATACGAACAAGGATGTACAG
1779	Inp1 DEE>AAA SDM R	CTGTACATCCTTGTTCGTATGCTGCAGCCAGCAAGTAATTAAGGTCG
3662	Inp1 Δmotif SDM F	GATAATTATGATGATGACGACGATGAAGAATACGAACAAGGATGTACAG
3663	Inp1 Δmotif SDM R	CTGTACATCCTTGTTCGTATTCTTCATCGTCGTCATCATCATAATTATC
1722	Inp1 L>A SDM F	GATAATTATGATGATGACGACGCTAATTACTTGCTGGATGAAG
1819	500bp upstream of *PEX19*	GTAAAACGACGGCCAGTGAATTCTACACGTTTGGATGATAAAATCCGGC
1792	Pex19 R	GTTCTTCTCCTTTACTCATGAGCTCTACTTCGTGTTGTATGTTTGGC
1780	Pex19 L>A SDM F	CGAGTACGATAATTTTGATGATGCGGATGACCTTTTAGATGAAGATCC
1781	Pex19 L>A SDM R	GGATCTTCATCTAAAAGGTCATCCGCATCATCAAAATTATCGTACTCG
1782	Pex19 LL>AA SDM F	GATGATTTGGATGACGCTGCAGATGAAGATCCCAC
1783	Pex19 LL>AA SDM R	GTGGGATCTTCATCTGCAGCGTCATCCAAATCATC
235	His Pex3 (40-441) F	GAGCTCGGTACCCGGGGATCCAAGAGATGGTTGTATAAACAGC
237	His Pex3 (40-441) R	AAGCTTGCATGCCTGCAGGTCGACTTATCTAGAAGGCTTGAAGGAAAACG AGC

2485	MBP-Inp1 F	ACTGCATATGGTTTTATCAAGGGGAG
2488	MBP-Inp1 R	TGACGGATCCTCAAAGGTCGCCAAGACCAG
2486	MBP-Inp1 1-280 R	ACTGGGATCCCTACAGTTTGAATTTATCGCTC
2487	MBP-Inp1 281-420 F	ACTGCATATGCCGCCTACTTCGGACATAGAGC
55	GST-Inp1 F	GAGGGATCCGGTATGGTTTTATCAAGGGGAG
56	GST-Inp1 R	GAGGTCGACTCAAAGGTCGCCAAGACCAG
2090	Inp1 1-100 GFP R	AGCACCCGCCCCTGCTCCCTGCAGCTGCAGATTATGAATGGGAACGAATG
3764	*INP1* promoter-Inp1 101- F	CAGGAAATTAAACAAAGTGGTGAGCTCATGGATATTCCGAATAGCAGTTG C
3755	Inp1 -280 GFP R	GTTCTTCTCCTTTACTCATTGCACCCGCCCCTGCTCCCAGTTTGAATTTATCG CTC
1119	GFP-Pex15 F	TGGATGAACTATACAAAGGATCCATGGCTGCAAGTGAGATAATG
1120	GFP-Pex15 R	ATCGATAAGCTTGCATGCCTGCAGTCATATACTCGCTAGAAG
3741	Inp1 R	GCATGCCTGCAGGTCGACAAGGTCGCCAAGACCAGATATGG
3909	*INP1* promoter-Num1 (2563-2692) F	CTCAGGAAATTAAACAAAGTGGTATGAACGAACCAAGCATAATACCC
3911	Num1 PH (2563-2692)-GFP R	CTTCTCCTTTACTCATTGCACCCGCCCCTGCTCCCTCTAAACTTATCCCTTGC
3972	Inp1 1-100-mRFP R	GACGTCCTCGGAGGAGGCCATTGCACCCGCCCCTGCTCCATTATGAATGG GAACGAATG

2.6.2 Restriction digest

Each restriction digest was carried out in a volume of 20µl and contained 2µl 10x NEB CutSmart™ Buffer, 0.5µl each restriction enzyme required and 0.5-2µg plasmid DNA. The volume was made up to 20µl with dH_20. Restriction digests were prepared on ice and incubated at 37°C for a minimum of 2 hours but usually overnight.

2.6.3 Agarose gel electrophoresis

DNA samples were analysed by agarose gel electrophoresis. 1% (w/v) agarose gels were prepared by dissolving high grade agarose powder in 1x TBE buffer solution (0.1M Tris-Base, 0.1M Boric acid, 10mM EDTA, pH 8) and Ethidium bromide (final concentration 0.5µg/ml). Samples were loaded alongside Bioline Hyperladder I DNA ladder to determine DNA fragment size and 6x loading buffer (0.25% bromophenol blue, 0.25% xylene cyanol FF, 30% (v/v) glycerol) was added to samples to give a 1x final concentration.

Agarose gels were run at a constant voltage of 90V for 35 minutes in 1xTBE buffer solution. Gels were analysed by viewing with an ultraviolet (UV) transilluminator imaging system (GeneSys).

2.6.4 DNA gel extraction

DNA was run on an agarose gel as detailed in Section 2.6.3 and visualised on a long wavelength UV transilluminator. The relevant DNA bands were excised from the gel using a sterile scalpel and gel extractions were performed using the QIAquick gel extraction kit (Qiagen) according to the manufacturer's instructions.

2.6.5 Ligation

Each ligation reaction was made in a final volume of 20µl. A 3:1 insert:vector molar ratio was used with 50ng digested, gel extracted vector added to the relevant amount of digested, gel extracted insert. 2µl 10x ligase buffer and 0.5µl T4 DNA ligase (Promega) was added and the reactions were made up to 20µl with dH_20. Ligation reactions were incubated for at least 2 hours at room temperature but were preferentially left overnight for optimal ligation and transformed into chemically competent *E. coli* cells the following day.

2.6.6 Site directed mutagenesis

Site directed mutagenesis was carried out with Pfu DNA polymerase as described in Section 2.6.1. The PCR product was digested with DpnI for 1 hour at 37°C then analysed on a gel by agarose gel electrophoresis. 1µl of PCR was transformed into electrocompetent *E. coli* cells and individual colonies were grown in selective overnight cultures of 2TY for miniprep purification of plasmids. Several plasmid clones were sent for sequencing to check for the presence of desired mutations.

2.6.7 Plasmid Miniprep

Plasmids were isolated from 4ml selective overnight cultures of *E. coli* using the Bioline miniprep kit according to the manufacturer's instructions. Plasmid DNA was eluted into a 1.5ml Eppendorf and the concentration of the sample was subsequently measured using a Nanodrop.

2.6.8 Homologous Recombination based cloning

Homologous recombination in *S. cerevisiae* was used for gene cloning to introduce open reading frames or tags into a vector (Fig. 2.2). Target open reading frames were first amplified by PCR. The primers used were designed to ensure that the PCR product was flanked by at least 18 nucleotides which were homologous to the insertion sites in the vector. The vector was digested using restriction enzymes at the insertion site and the PCR fragment and linearised vector were transformed to yeast by high efficiency yeast transformation (Section 2.4.3). Upon homologous recombination, gap repair occurs which circularises the vector, incorporating the PCR product. Yeast cells containing recombinant plasmids were then identified by growth on selective yeast medium.

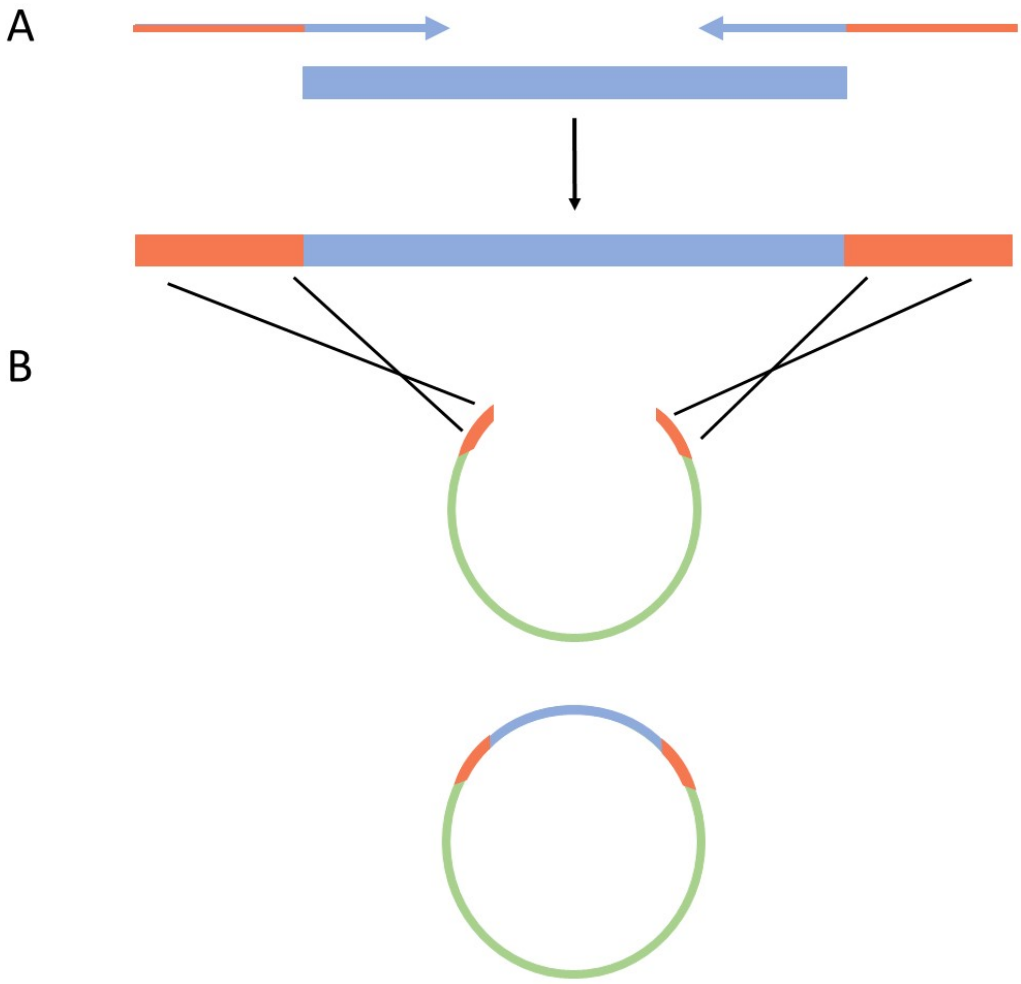

Figure 2.2 – Homologous recombination in *S. cerevisiae* was one method used to construct plasmids. A) Primers (represented by the orange and blue arrows) were designed to create a PCR product of the desired DNA insert (blue) flanked by approximately 18 nucleotides homologous to sequences in the vector (orange). B) The vector was digested with the appropriate restriction enzymes and was transformed into *S. cerevisiae* together with the PCR product. Homologous recombination then took place, producing a recombinant vector.

2.6.9 DNA sequencing

Plasmids were sequenced by Source Bioscience using their Sanger sequencing service. The data was analysed using SnapGene and the online multiple sequence alignment tool ClustalW.

2.7 Protein procedures

2.7.1 SDS-PAGE

Sodium dodecyl sulphate polyacrylamide gel electrophoresis (SDS-PAGE) was performed as described by (Sambrook and Russell, 2006). 8-12% gels were prepared using the reagents shown in Table 2.10. Protein loading dye was added to protein samples at 1X final concentration before loading onto the gel. Gels were then run at constant voltage (90-120V) until the dye front ran off the bottom of the gel.

Protein running buffer (10X): 30.28g Tris Base, 144.13g Glycine, 1% (w/v) SDS, dH_20 up to 1L. Protein loading dye (4X): 250mM Tris pH 6.8, 9.2% (w/v) SDS, 40% (w/v) Glycerol, 0.2% (w/v) Bromophenol brilliant blue, 100mM DTT.

Table 2.10 – SDS-PAGE gel reagents. Volumes of each reagent used to make a 12% gel are shown.

Reagents	Resolving gel (12%)	Stacking gel (4%)
Protogel (Acrylamide, Bis-acrylamide mix) 30% stock	4ml	0.67ml
Resolving buffer 4X stock	2.5ml	-
Stacking buffer 4X stock	-	1.25ml
APS 10% (w/v) stock	100µl	50µl
TEMED 1000X stock	10µl	5µl
dH_20	3.39ml	3.025ml
Total volume	10ml	5ml

2.7.2 Protein induction

Primary *E. coli* cultures were inoculated in 4ml 2TY containing the appropriate antibiotic and incubated overnight at 37°C on a shaker at 200 rpm. Secondary cultures were inoculated the following day in larger volumes of 2TY + antibiotic (usually 1 litre) to give a starting $O.D._{600}$ of 0.1. Cells were grown to $O.D._{600}$ 0.6-0.8 before protein induction was performed through the addition of Isopropyl-β-D-galactopyranoside (IPTG) to a final concentration of 1mM. Cells were grown for a further 3-4 hours at 37°C on a shaker at 200 rpm before cells were harvested through centrifugation at 8000 rpm for 15 minutes. Bacterial pellets were then stored at -80°C until required.

2.7.3 Protein purification

Bacterial cell pellets were resuspended in 1ml ice cold 1xPBS, 1mM phenylmethylsulfonyl fluoride (PMSF) and EDTA-free protease inhibitor cocktail (Roche). Cells were subjected to 1x 30sec, 2x 15sec sonication at an amplitude of 12 µm and samples were kept on ice throughout. 1% Triton X-100 was added to the lysates (except when lysate contained Pex3) and incubated at 4°C for 30 minutes with end over end turning. Lysates were subsequently centrifuged at 20,000 *g* for 5 minutes at 4°C and the supernatant retained. To purify tagged proteins, Glutathione Sepharose 4B (GE Healthcare), Amylose (New England Biolabs) or Ni-Sepfast (BioToolomics) beads were prewashed in 1xPBS and added to relevant fusion protein lysates before incubation at 4°C with end over end mixing for 30 minutes. The beads were then washed twice with 1xPBS + 0.05% Igepal CA-630 (Sigma-Aldrich).

2.7.4 Protein binding assays

In vitro binding assays

GST-Inp1, MBP-Inp1 and His-Pex3 proteins were expressed in *E. coli* BL21 DE3 and purified on Glutathione Sepharose 4B, Amylose or Ni-Sepfast beads prewashed in 1xPBS as described above (Section 2.7.2/2.7.3). The beads were washed twice with 1xPBS + 0.05% Igepal CA-630 (Sigma-Aldrich) before relevant secondary *E. coli* lysates were added. Samples were then incubated for 2 hours at 4°C with end over end mixing. The beads were washed 4 times with 1xPBS + 0.05% Igepal CA-630. The second wash included 500 mM KCl as this was found to be sufficient to remove any non-specific binding to bead only controls without affecting binding, as previously described (Munck et al., 2009). Bound material was eluted with SDS-PAGE sample loading buffer, resolved by SDS-PAGE and analysed by Coomassie staining.

In vitro competition assay

MBP-Inp1, GST-Pex19 and His-Pex3 proteins were expressed in *E. coli* BL21 DE3. Cells were grown, induced and lysates prepared as above (Section 2.7.2/2.7.3). Total lysates containing GST-Pex19 were incubated with washed glutathione Sepharose 4B beads at 4°C for 30 minutes. Total lysates containing His-Pex3 and MBP-Inp1 proteins were mixed together and incubated at 4°C for 30 minutes. The glutathione Sepharose beads were washed twice with 1xPBS + 0.05% Igepal CA-630 before the His-Pex3/MBP-Inp1 lysate mixtures were added. Samples were then incubated for 2 hours at 4°C with end over end mixing. The total unbound fraction was removed from the glutathione Sepharose beads and added immediately to Amylose resin beads. These samples were then incubated for a further 1 hour at 4°C with end over end mixing. All beads were washed 4 times with 1xPBS + 0.05% Igepal CA-630, with the second wash containing 500 mM KCl (as described above). Bound fractions were eluted from the glutathione Sepharose beads using SDS-PAGE sample loading buffer. Bound fractions were eluted from Amylose beads with maltose buffer (20 mM Tris-HCl pH7.4, 200 mM NaCl, 1 mM EDTA, 10 mM maltose). All samples were resolved by SDS-PAGE and analysed by Coomassie staining. For detection of His-Pex3-MBP-Inp1 complexes, immunoblot analysis was carried out with the monoclonal anti-polyhistidine peroxidase antibody.

2.7.5 TCA protein extraction

Yeast cultures were grown overnight in selective medium and 10 $O.D._{600}$ units of cells were harvested at 12,000 rpm for 1 minute. The supernatant was removed and the pellet was resuspended in 500µl TCA lysis buffer (0.2M NaOH, 0.2% β-Mercaptoethanol) before being incubated on ice for 10 minutes. Subsequently, 71µl of 40% (w/v) TCA (Trichloroacetic acid) solution was added and the mixture was again left on ice for 10 minutes. The sample was then centrifuged at 13,000 rpm for 5 minutes at 4°C and the supernatant was aspirated leaving behind the precipitated protein pellet. The pellet was neutralised by adding 10µl of 1M Tris-HCl pH 9.4 before 90µl of 1X SDS protein loading buffer was added. Samples were boiled for 10 minutes at 95°C before loading onto SDS-PAGE gel (1-2 $O.D._{600}$ equivalent).

2.7.6 Western blot analysis

Protein samples were separated by SDS-PAGE and transferred onto a nitrocellulose membrane using a Biorad Mini Trans-Blot Electrophoretic transfer cell. Samples were transferred at a constant 200mA current for 2 hours in transfer buffer (25mM Tris pH 8.3, 150mM Glycine, 40% (v/v) methanol). Protein transfer was checked using Ponceau S solution (0.1% (w/v) Ponceau S in 5% (v/v) acetic acid). Blots were blocked overnight at 4°C in blocking buffer comprised of 2% (w/v) fat-free Marvel milk in TBS–Tween 20 (50 mM Tris-HCl, pH 7.5, 150 mM NaCl, and 0.1% (v/v) Tween 20). Membranes were incubated with primary and secondary antibodies for 1 hour at room temperature in blocking buffer with wash steps of at least 30 minutes between incubations using TBS-Tween20 (without milk). Antibodies were used at the given dilutions: anti-GFP (1:3000), anti-His (1:10000), anti-PGK1 (1:3000). Secondary antibody was HRP-linked anti-mouse polyclonal (1:10000). Blots were developed using Enhanced Chemi-Luminescence (ECL) substrates and tagged proteins were detected and imaged using a Syngene GBox imaging system and Genesys software.

2.7.7 Liposome binding assays

For Folch liposomes, 22 µl of a 25 mg/ml solution of Folch fraction-1 (Sigma-Aldrich) was dried under nitrogen, then resuspended in 200 µl liposome buffer (20 mM HEPES pH 7.2, 100 mM KCl, 2 mM MgCl2, 1 mM DTT) at 60°C for 30 minutes with gentle agitation. For preparation of synthetic liposome solutions, 40µl of 25 mg/ml PC solution, 4.6µl of 25 mg/ml PE solution and 307 µl of 1 mg/ml $PI(4,5)P_2$ or PI(4)P solution or 12.3 µl 25 mg/ml PS solution (Avanti Polar Lipids, dissolved in chloroform) were dried under nitrogen then resuspended in 400 µl liposome buffer. Purified protein was pre-spun at 350,000 *g* for 15 minutes (Beckman Ultra centrifuge, TL100 rotor) then immediately added to 10 µl of liposome solution and made up to final volume 50 µl with maltose buffer. The mixture was incubated at room temperature for 30 minutes before pelleting the liposomes at 280,000 *g* for 15 minutes. After centrifugation, supernatants were removed and pellets were resuspended in 50 µl liposome buffer. 10 µl Strataclean resin (Stratagene) was added to each sample to concentrate the protein. This was pelleted by spinning at 8000 *g* in a table top microcentrifuge for 2 minutes. Supernatants were removed and the pellet of each sample was resuspended in 15 µl SDS-PAGE loading buffer. Samples were then analysed by SDS-PAGE and Coomassie staining.

Chapter 3 – Inp1 and Pex19 compete for binding to Pex3

3.1 Introduction

S. cerevisiae cells divide asymmetrically and the balance between organelle tethering and motility determines the intracellular distribution of organelles. Faithful segregation of peroxisomes between the mother cell and growing bud requires a careful balance between the opposing processes of cortical anchoring in the mother cell and Myosin-dependent transport towards the bud. These processes rely on Inp1 and Inp2, proteins which perform antagonistic functions and ensure proper peroxisome segregation along the mother-bud axis (Hoepfner et al., 2001; Fagarasanu et al., 2005; Fagarasanu et al., 2010).

Peroxisomes in *Δinp1* cells have increased mobility and aren't retained in fixed cortical positions in mother cells or larger buds as they are in wild type cells. By anchoring peroxisomes at the cortex of the mother cell, it is ensured that a sub-population of peroxisomes are retained in the mother. The exact mechanisms by which Inp1 functions in peroxisome retention at the cell cortex remain poorly understood. The existing model postulates that Inp1 acts as a 'molecular hinge' that simultaneously binds to both peroxisomal and cortical ER-localised Pex3 (Knoblach et al., 2013). However, further research by the same group has since shed doubt on the simplicity of this model with the suggestion that additional components are required for tethering of peroxisomes to the cell cortex and that contact between peroxisomes and the ER may occur independent of Inp1 (Knoblach and Rachubinski, 2019).

The molecular interaction between Inp1 and Pex3 was first described by the Hettema lab, (Munck et al., 2009) and has since been further studied by John Hutchinson (Hutchinson, 2016). This subsequent work has led to the identification of a conserved, leucine-based motif present in the C-terminal region of Inp1. Furthermore, it has been noted that this motif bears a striking similarity with the established Pex3 binding site present in human Pex19, leading to the idea that Inp1 and Pex19 could compete for binding to Pex3 with their analogous, leucine-based motifs (Sato et al., 2010; Schmidt et al., 2010; Schmidt et al., 2012). In Chapter 3, the preliminary characterisation of the Inp1-Pex3 interaction is confirmed and furthered in order to elucidate the molecular mechanisms by which Inp1 interacts with peroxisomal Pex3.

3.2 Confirmation that a C-terminal motif in Inp1 is required for binding to Pex3

3.2.1 A C-terminal region of Inp1 is required for its peroxisomal localisation

Previous studies by the Hettema lab have uncovered that the C-terminal region of Inp1 is required for its interaction with peroxisomal Pex3. This was first elucidated by a genome wide yeast two-hybrid screen using the cytosolic domain of Pex3 as bait (amino acids 40-441) (Motley et al., 2012). This screen identified interactions between Pex3 and 10 different Inp1 protein fragments encoded by 14 independent Inp1 DNA clones. The smallest fragment of

Inp1 that interacted with Pex3 comprised amino acids 300-378 and this region was common to all hits (Fig. 3.1A).

In order to confirm earlier work that this minimal region of Inp1 is sufficient to associate with peroxisomes, a library of galactose-inducible Inp1-GFP truncations were co-expressed in *Δinp1* or *Δinp1/Δpex3* cells with a peroxisomal matrix marker consisting of a fluorescent protein appended with a peroxisomal targeting signal type I (*Hc*Red-PTS1) (Fig. 3.1B, C). Analysis by fluorescence microscopy revealed that, as expected, full length Inp1-GFP was present in punctate structures which co-localised with *Hc*Red-PTS1 when expressed in *inp1Δ* cells and was cytosolic in *Δinp1/Δpex3* cells where peroxisomes are absent. This localisation pattern was observed for truncations of Inp1-GFP up to and including amino acids 300-420. However, when Inp1 was further truncated (amino acids 315-420) it was no longer associated with peroxisomes. Further fine mapping revealed that the minimal region that still associated with peroxisomes comprises residues 311-370, a region which is corroborated by the yeast two-hybrid data.

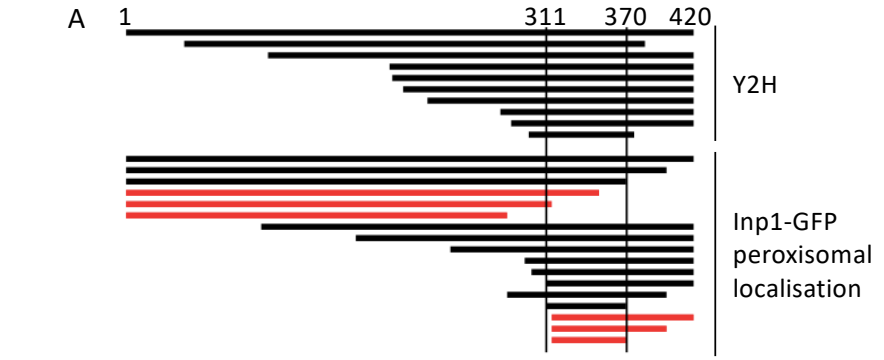
A
1
311
370
420
Y2H
Inp1-GFP
peroxisomal
localisation

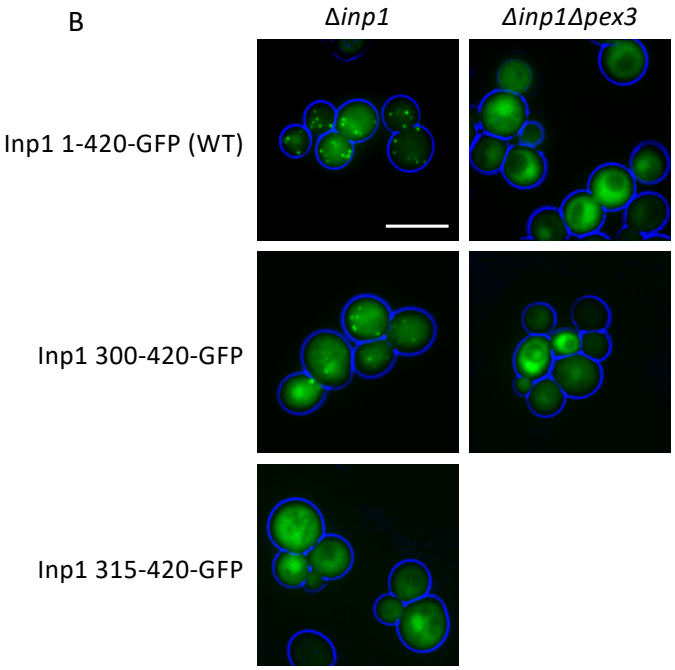
B
Δinp1
Δinp1Δpex3
Inp1 1-420-GFP (WT)
Inp1 300-420-GFP
Inp1 315-420-GFP

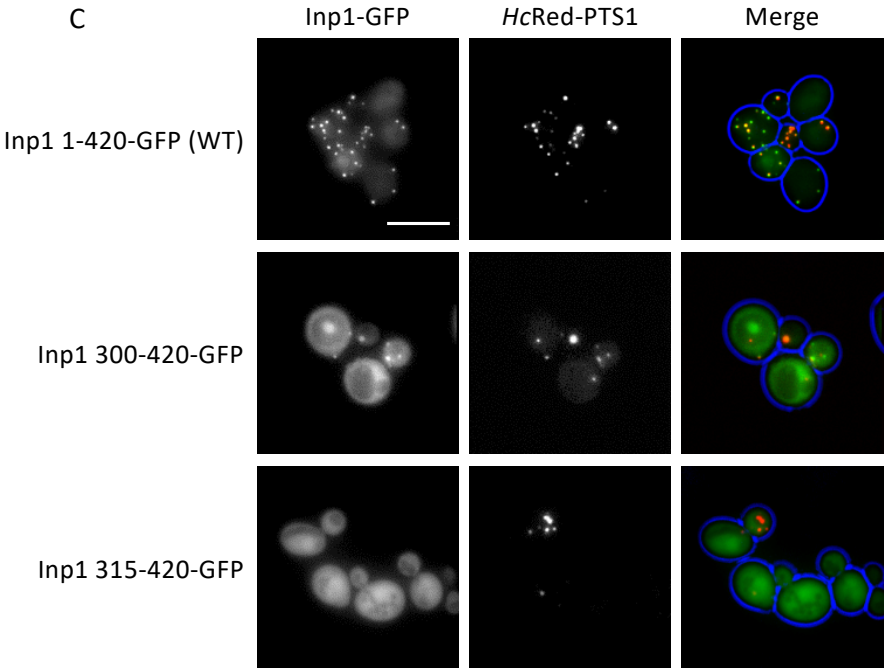
C
Inp1-GFP
HcRed-PTS1
Merge
Inp1 1-420-GFP (WT)
Inp1 300-420-GFP
Inp1 315-420-GFP

Figure 3.1 – Summary of the yeast two-hybrid and *in vivo* Inp1-GFP truncation screens. A) The upper panel is a line diagram showing the truncations of Inp1 identified by a genome wide yeast two-hybrid screen with the cytosolic domain of Pex3 (40-441) as bait (performed by Motley et al., 2012). The lower panel shows the truncations of Inp1-GFP which localise to peroxisomes (black lines) or do not localise to peroxisomes (red lines). The vertical black lines indicate the minimal region required for Inp1-GFP localisation to peroxisomes. Truncations shown in the lower panel are as follows (from top to bottom) amino acids 1-420, 1-400, 1-370, 1-315, 1-282, 100-420, 170-420, 240-420, 295-420, 300-420, 311-420, 315-420, 281-400, 311-370, 315-420, 315-400, 315-370. B) Truncations of Inp1-GFP under the control of the *GAL1/10* inducible promoter were expressed in *Δinp1* or *Δinp1/Δpex3* cells and analysed by fluorescence microscopy. C) Truncations of Inp1-GFP under the control of the control of the *GAL1/10* inducible promoter were co-expressed in *Δinp1* cells with the peroxisomal matrix marker *Hc*Red-PTS1 and analysed by fluorescence microscopy. Bars, 5 µm.

3.2.2 The C-terminus of Inp1 binds to Pex3 *in vitro*

Previously, it has been shown that Inp1 interacts directly with Pex3 (Munck et al., 2009). To further investigate the regions of Inp1 required for this interaction, an *in vitro* binding assay was performed (Fig. 3.2). Previous studies have interpreted secondary structure analysis of Inp1 to predict that the protein can be roughly divided into "two globular domains", an N-terminal domain comprised of amino acids 1-280 and a C-terminal domain comprised of amino acids 281-420 (Knoblach et al., 2013). We used these same domains to carry out experiments in this study (Fig. 3.2). Maltose binding protein (MBP) fusions of the N- or C-terminal domains of Inp1 were expressed in *E. coli* and bound to amylose beads. Subsequently, total *E. coli* lysates expressing the cytosolic domain of Pex3 (40-441) with a 6x-His tag (His-Pex3) or a His tag only, were added to and incubated with the samples. The His-Pex3 lysate was also incubated with the MBP alone, bound to amylose beads. After extensive washing with 1x phosphate buffer saline (PBS) including a PBS + 0.5M KCl wash, bound protein was eluted from the amylose beads with 1x protein loading buffer. The binding of His-Pex3 to the MBP-Inp1 truncations was subsequently analysed by SDS-PAGE, Coomassie staining of the gel and western blotting. Anti-His tag antibody was used to confirm the presence His-Pex3 bound to MBP-Inp1 C.

A direct interaction was found between His-Pex3 and the C-terminal domain of Inp1 (MBP-Inp1 281-420). His-Pex3 did not bind to the N-terminal domain of Inp1 (MBP-Inp1 1-280) nor MBP alone, thus suggesting that the direct interaction between Pex3 and the Inp1 is dependent on the C-terminal domain of Inp1. This is in agreement with the *in vivo* data obtained from the Inp1-GFP truncation screen and yeast two-hybrid assay.

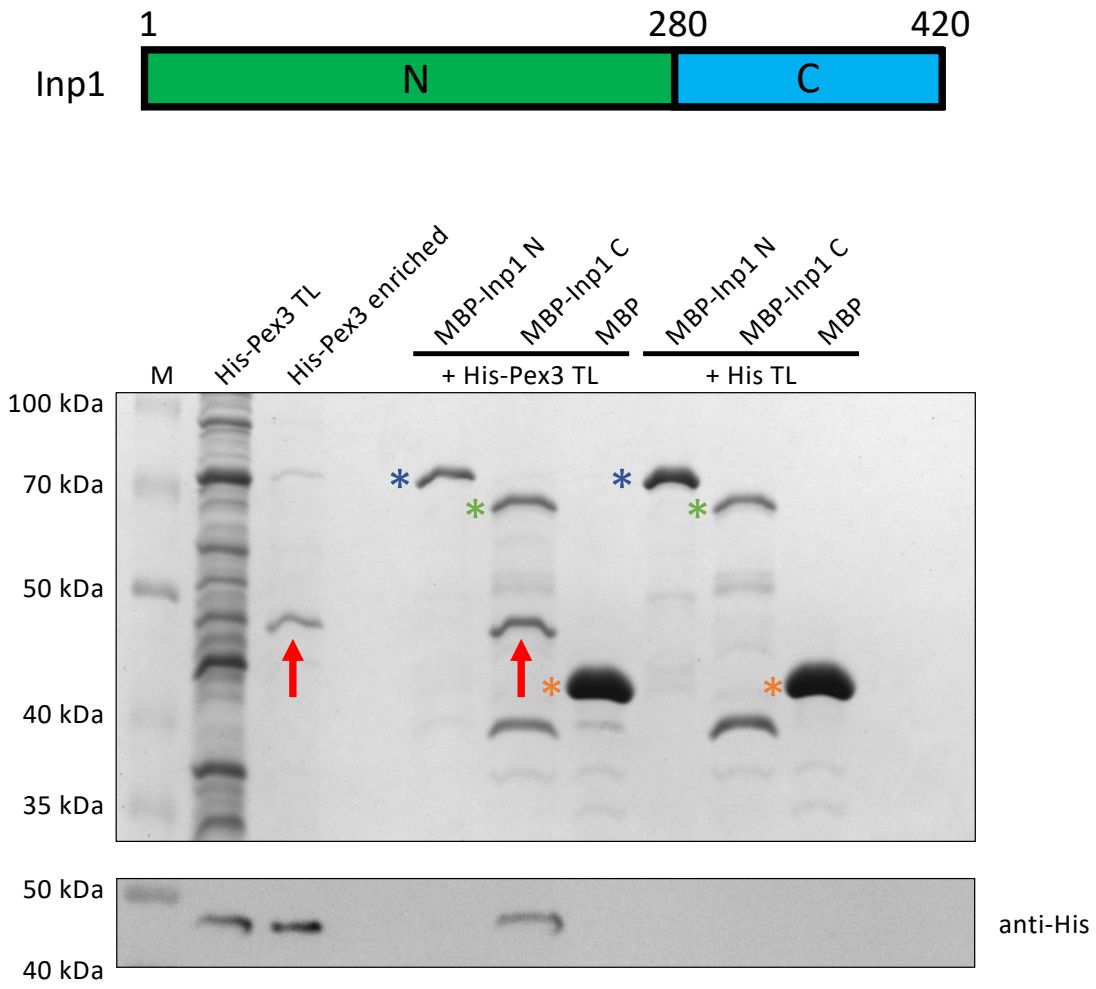

Figure 3.2 – The C-terminus of Inp1 binds directly to Pex3 *in vitro*. The schematic diagram illustrates how Inp1 was considered as two domains as in (Knoblach et al., 2013). The N-terminal domain comprises amino acids 1-280, the C-terminal domain comprises amino acids 281-420. *E. coli* expressed MBP-Inp1 N (blue asterisk, amino acids 1-280), MBP-Inp1 C (green asterisk, amino acids 281-420) or MBP only (orange asterisk) were bound to amylose beads and incubated with a total lysate of *E. coli* expressing either 6xHis-Pex3 (40-441) or 6xHis-tag only. After extensive wash steps, bound protein fractions were analysed with SDS-PAGE followed by Coomassie staining (upper gel) and western blotting (lower panel). A lane was included with enriched His-Pex3 as a control. M, molecular weight marker. TL, total lysate. Red arrows indicate His-Pex3.

Previously, it has been reported that both the N- and C-terminal domains of Inp1 bind directly to Pex3 *in vitro* (Knoblach et al., 2013). Specific binding of the N-terminal domain of Inp1 to Pex3 was not able to be repeated under our assay conditions. The first explanation for this could be due to the inclusion of a high salt wash (PBS + 0.5M KCl) during the extensive wash steps. A wash with PBS + 0.5M KCl was found to be sufficient to remove non-specific binding to bead only controls without affecting binding, as previously described (Munck et al., 2009). A second explanation could be the omission of detergent, specifically Triton X-100, from any *E. coli* lysates containing His-Pex3. It has been shown that the cytosolic domain of Pex3 can be purified from *E. coli* in the absence of detergent and that it aggregates in the presence of Triton X-100 (Pinto et al., 2009). The binding assay performed by Knoblach *et al.* does include the incubation of Triton X-100 with Pex3 lysates and does not include a high salt wash. Detergent-dependent aggregation of Pex3, non-specific binding or a combination of the two could form a plausible explanation as to why Pex3 binding to MBP-Inp1 1-280 is reported in their assay but not observed here.

3.2.3 Confirmation of the identity of the LXXLL motif in Pex19 and Inp1

Bioinformatic analysis of the amino acid sequences of Inp1 orthologues in other budding yeast species highlighted a highly conserved leucine-based motif flanked by negatively charged residues (Fig. 3.3). This motif corresponds to amino acids 312-316 and so is present within the minimal region of Inp1 that was confirmed as necessary for localisation to peroxisomes *in vivo* and binding to Pex3 *in vitro* (amino acids 311-370).

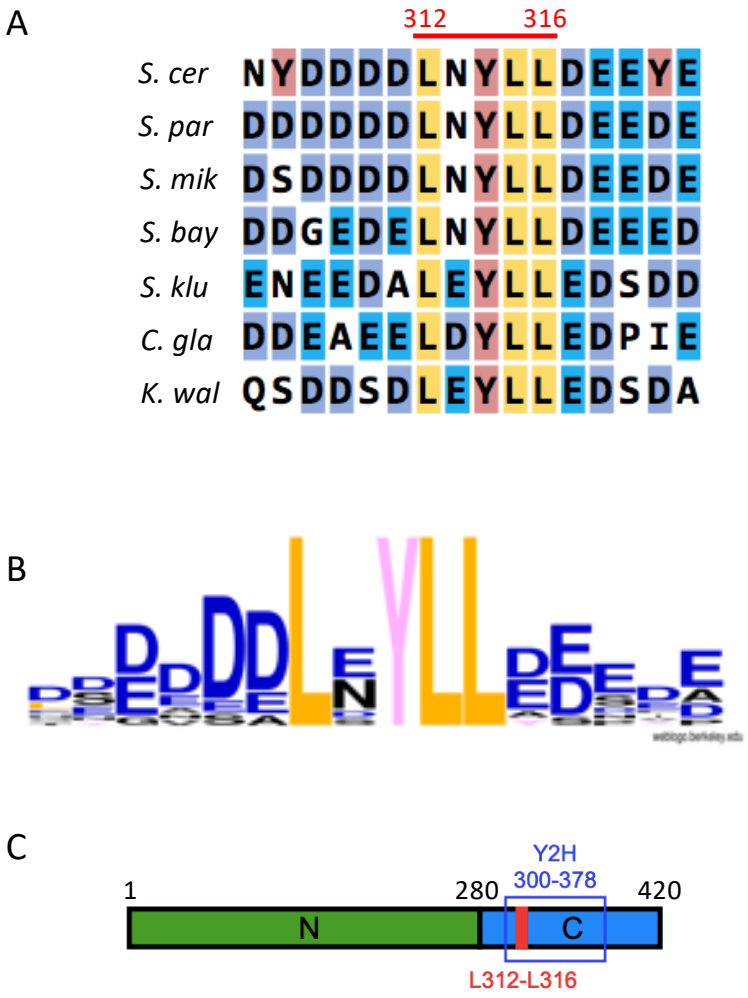

Figure 3.3 - Bioinformatic analysis of Inp1 revealed a conserved LXXLL motif. A) ClustalW was used to create a multiple sequence alignment of the conserved motif region of Inp1 orthologues of species closely related to *S. cerevisiae* (*S. cer*). *S. paradoxus* (*S. par*), *S. mikatae* (*S. mik*), *S. bayanus* (*S. bay*), *S. kluyveri* (*S. klu*), *Candida glabrata*, (*C. gla*), *Kluyveromyces waltii* (*K. wal*). The residues numbered in red highlight the conserved leucine motif with amino acid numbers corresponding to those in *Sc*Inp1. B) A consensus sequence of the motif region of interest shown in A. The height of letters within the stack indicates the relative frequency of each amino acid at that position. C) A schematic diagram showing an overview of the hypothetical Inp1 domain structure. Green, N-terminal domain 1-280. Blue, C-terminal domain 281-420. Red, conserved leucine motif. Y2H box, the smallest region of Inp1 found to bind to Pex3 in a yeast two-hybrid screen.

It was noted that the identified motif (which will be referred to as LXXLL) bears a striking similarity to the designated Pex3 binding motif of Pex19 (Fig. 3.4A). The interaction between Pex3 and Pex19 has been well characterised (Sato et al., 2010; Schmidt et al., 2010; Agrawal et al., 2017), and a "leucine triad" motif in human Pex19 has been identified as being critical for Pex3 binding and peroxisome biogenesis. Substitution of the leucine residues in the LXXLL motif of human Pex19 have been shown to result in decreased affinity for Pex3 (Sato et al., 2010; Schmidt et al., 2012). We tested the functional importance of the leucine triad in the *S. cerevisiae* orthologue of Pex19 (*Sc*Pex19) using an alanine scan. The Pex19 mutants were co-expressed under the control of the *PEX19* promoter in *Δpex19* cells with the peroxisomal matrix marker *Hc*Red-PTS1. Cells devoid of functional Pex19 are blocked in peroxisome formation and consequently mislocalise peroxisomal matrix proteins to the cytosol (Götte et al., 1998). Substitutions of the leucine residues for alanines resulted in the cytosolic localisation of *Hc*Red-PTS1 (Fig. 3.4B). This indicates a loss of functional Pex19 although the *Sc*Pex19 mutants were well expressed (Fig. 3.4C). This confirms that as in human Pex19, the LXXLL motif of *Sc*Pex19 is required for function.

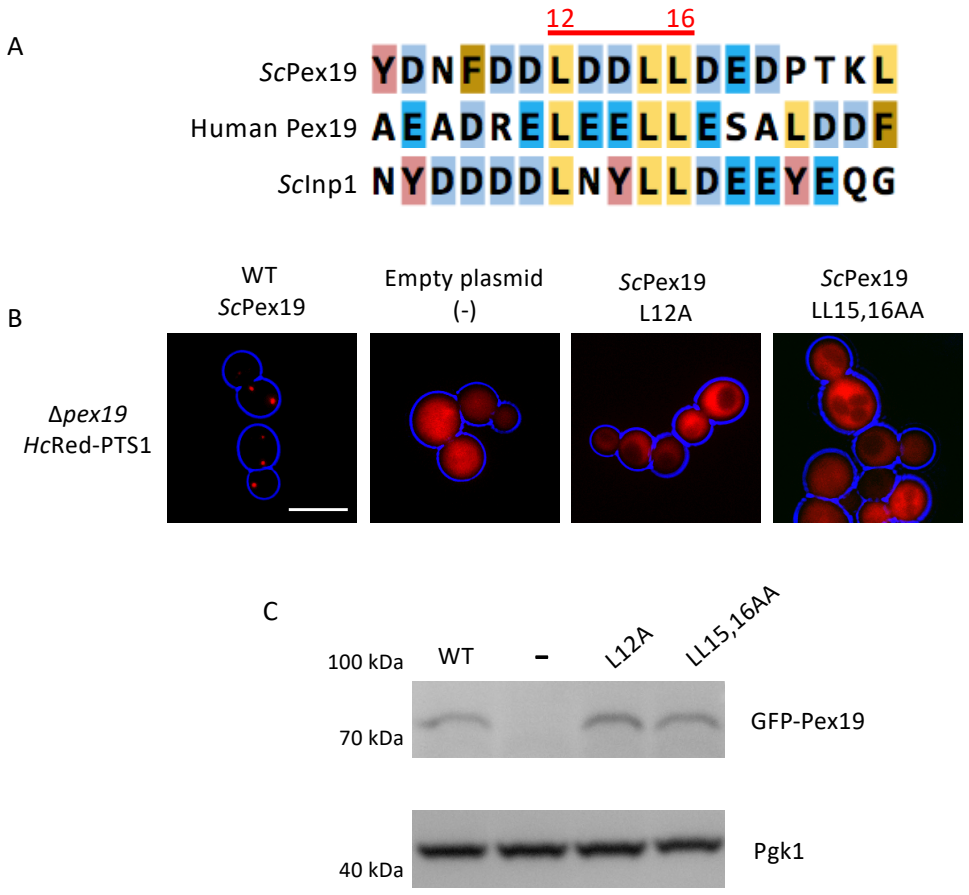

Figure 3.4 – *Sc*Pex19 also contains an LXXLL motif required for function. A) ClustalW was used to create a multiple sequence alignment of *Sc*Pex19 amino acids 6-23, human Pex19 amino acids 12-29 and *Sc*Inp1 amino acids 306-323. Residues numbered in red highlight the conserved leucine motif with amino acid numbers corresponding to those in *Sc*Pex19. B) Wildtype *Sc*Pex19 (WT) or *Sc*Pex19 leucine motif mutants were expressed with the *PEX19* promoter in *Δpex19* cells co-expressing *Hc*Red-PTS1. Bar, 5 µm. C) Immunoblot analysis of *Sc*Pex19 mutants. (-), empty plasmid control. *PGK1* loading control.

In order to determine if the LXXLL motif of Inp1 is also important for its function, the LXXLL motif of Inp1 was subsequently targeted for mutagenesis. A loss of functional Inp1 is easily assayed in *S. cerevisiae* by observing the distribution of peroxisomes in budding cells. In cells lacking functional Inp1, peroxisomes are not retained at the mother cell cortex and so there is an abnormal distribution of peroxisomes between mother cells and their buds with almost all peroxisomes present in the bud. Additionally, in peroxisome retention mutants (devoid of functional Inp1), cells have a phenotype of reduced numbers of enlarged peroxisomes (Fagarasanu et al., 2005) (Fig. 3.5A). First, the LXXLL motif was deleted in Inp1-GFP (Inp1 L312_L316-GFP) and this Δmotif mutant was co-expressed under the control of the endogenous *INP1* promoter in *Δinp1* cells with *Hc*Red-PTS1 (Fig. 3.5B, C). Inp1 Δmotif-GFP was stably expressed but no longer localised to peroxisomes and failed to rescue the *Δinp1* peroxisome retention defect phenotype.

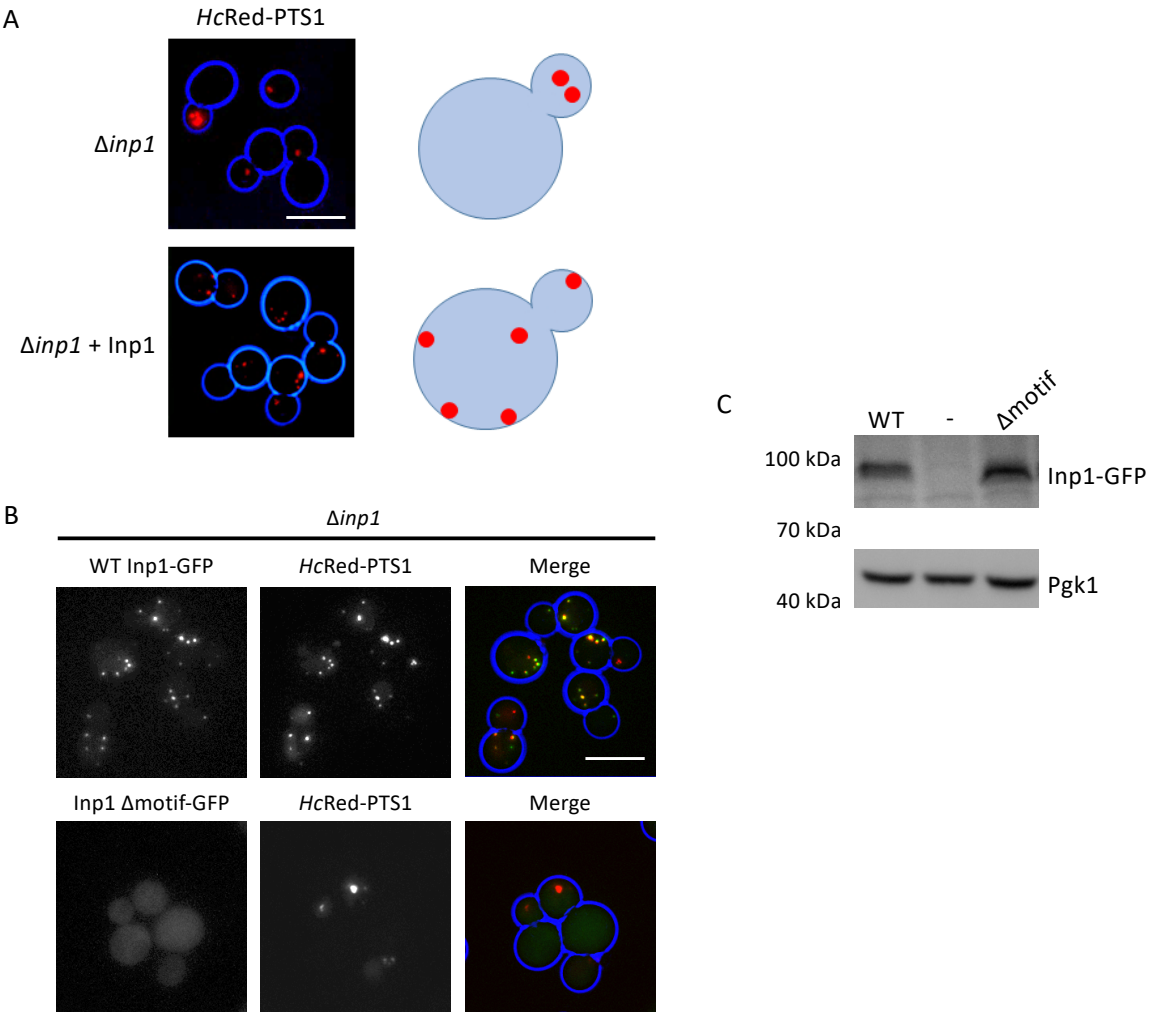

Figure 3.5 – Deletion of the LXXLL motif of Inp1 results in a loss of peroxisomal localisation and function. A) HcRed-PTS1 was expressed in Δinp1 cells in the presence or absence of Inp1 and analysed by fluorescence microscopy. The schematic diagrams represent the peroxisomal phenotypes observed when INP1 is absent or present in budding S. cerevisiae cells. B) Inp1-GFP and a leucine motif deletion mutant (Δmotif) were expressed under control of the INP1 promoter with HcRed-PTS1 and analysed by fluorescence microscopy. Bars, 5 µm. C) Immunoblot analysis of Inp1 Δmotif-GFP. (-), empty plasmid control. *PGK1* loading control.

The LXXLL motif sits in a highly acidic region of Inp1. From amino acids 285-326 there are 20 acidic residues (D/E) and none with a positive charge. In order to further characterise the functionality of the LXXLL motif, an alanine scan of the motif and its adjacent acidic residues (amino acids 310-319) was carried out in Inp1-GFP (Fig. 3.6). Most mutants behaved as wild type Inp1 with peroxisomal localisation and complementation of the *Δinp1* phenotype. However, substitution of the three leucine residues L312, L315 and L316 resulted in a loss of peroxisomal localisation of Inp1-GFP and a peroxisome retention defect indicative of a lack of functional Inp1, as was observed for the Inp1-Δmotif mutant (Fig. 3.6A, B). This is the first detailed alanine scan analysis which includes the acidic residues within a Pex3 binding motif and from this experiment, it was established that it is the leucine residues that are important for the peroxisomal localisation and function of Inp1. Inp1 mutants with reduced peroxisomal localisation were no longer concentrated in punctate structures and difficult to visualise with fluorescence microscopy due to them being expressed from their endogenous promoter. Western blot analysis showed that all of the mutants were stably expressed (Fig. 3.6C).

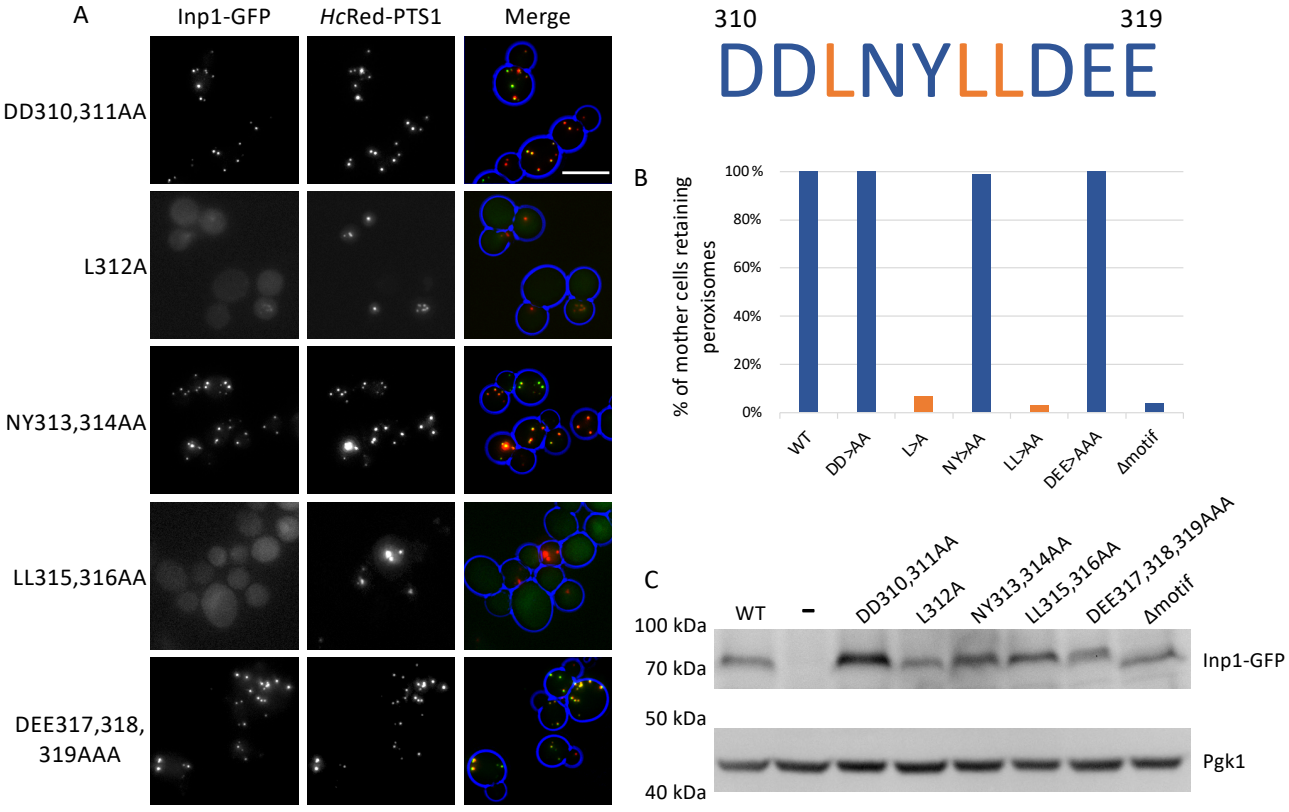

Figure 3.6 – An alanine scan of the LXXLL motif region found that it is the leucine residues which are required for the peroxisomal localisation and function of Inp1. A) Alanine scan of Inp1-GFP region amino acids 310-319. Mutants were expressed under control of the *INP1* promoter in *Δinp1* cells co-expressing *Hc*Red-PTS1. Bar, 5 µm. B) Quantitative analysis of peroxisome retention in alanine scan mutants. Budding cells were scored for the presence or absence of peroxisomes in the mother cell. At least 100 budding cells were quantified for each mutant. The motif region targeted for mutagenesis, amino acids 310-319, is shown. C) Immunoblot analysis of Inp1-GFP mutants. (-), empty plasmid control. *PGK1* loading control.

3.2.4 The LXXLL motif of Inp1 is involved in direct binding to Pex3

The Inp1 Δmotif-GFP and Inp1 LL315,316AA-GFP (LL>AA) mutants had the strongest effect on peroxisomal localisation and function of Inp1-GFP and so these mutants were tested for their binding to the cytosolic domain of Pex3 (40-441) in an *in vitro* binding assay. Glutathione S-transferase tag (GST) fusions of wild type Inp1, Inp1 Δmotif or Inp1 LL>AA were expressed in *E. coli* and bound to glutathione Sepharose beads. Subsequently, total *E. coli* lysates expressing the cytosolic domain of Pex3 (40-441) with a 6x-His tag (His-Pex3) or a His tag only, were incubated with the beads. The His-Pex3 lysate was also incubated with the GST tag alone. After extensive wash steps, bound fractions were analysed by SDS-PAGE followed by Coomassie staining.

As reported previously, (Munck et al., 2009), His-Pex3 directly interacts with GST-Inp1. Conversely, both GST-Inp1 motif mutants were strongly compromised in direct binding to His-Pex3. Mutation of the two leucine residues (LL>AA) massively reduces the interaction between Inp1 and His-Pex3 whilst deletion of the motif appears to completely prevent His-Pex3 from binding to Inp1. From the *in vivo* and *in vitro* data obtained, it can be concluded that Inp1 contains an LXXLL motif that is required for its function as it is involved in direct binding to Pex3 and localisation to peroxisomes. During the course of this work, an independent study reported a random Inp1 mutant in this motif (LXXLP) which also blocked recruitment of Inp1 to peroxisomes and interfered with Inp1 function (Knoblach and Rachubinski, 2019). This further supports the conclusion that the LXXLL motif plays an important role in Inp1 function.

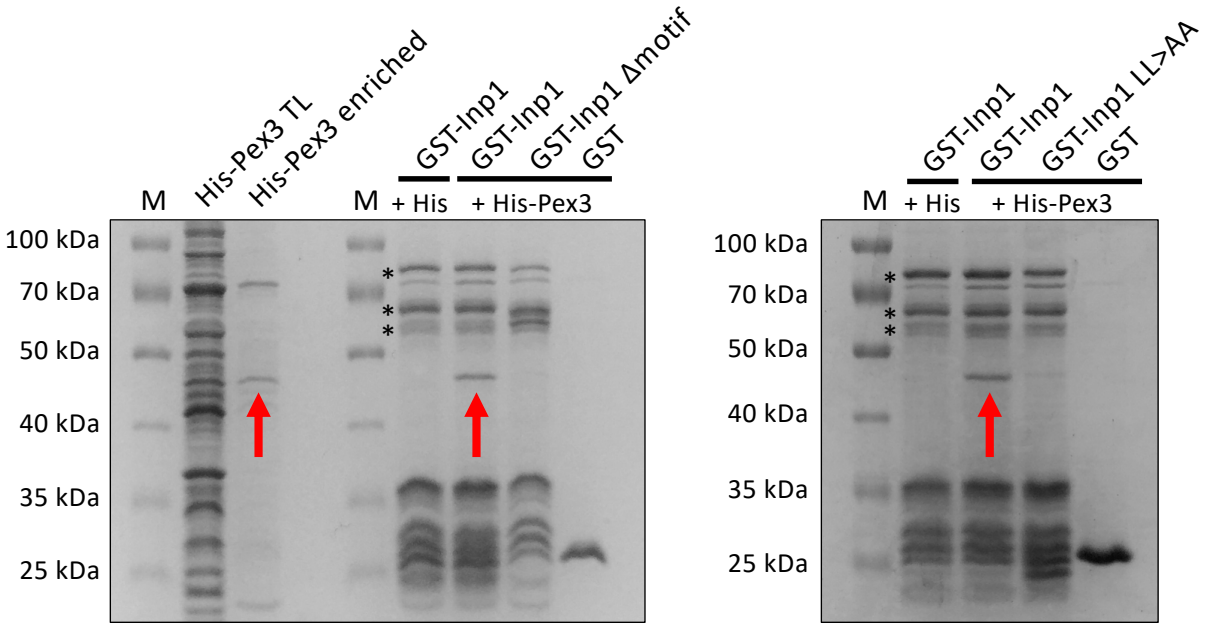

Figure 3.7 – Mutation of the LXXLL motif of Inp1 disrupts its direct binding to Pex3. *E. coli* expressed GST-Inp1, GST-Inp1 Δmotif, GST-Inp1 LL>AA and GST were bound to glutathione Sepharose beads and incubated with a total lysate of E. coli expressing either His-Pex3 (40-441) or His-tag only. After extensive washing with 1x PBS including a PBS + 0.5M KCl wash, bound protein was eluted from the glutathione Sepharose beads with 1x protein loading buffer and analysed by SDS-PAGE and Coomassie staining of the gel. A lane was included with enriched His-Pex3 as a control. M, molecular weight marker. TL, total lysate. Red arrows indicate His-Pex3. Asterisks indicate multiple GST-Inp1 fragments.

3.3 Inp1 competes with Pex19 for binding to Pex3

3.3.1 Overexpression of Inp1 results in a loss of peroxisomal structures

Initially, overexpression of Inp1 results in an increase in the number of peroxisomes which are retained at the mother cell periphery. Peroxisomes are prevented from being normally transported to the bud which results in buds being devoid of peroxisomes and an observable over-retention of peroxisomes in the mother cell (Fagarasanu et al., 2005). However, it has also been observed that constitutive overexpression of Inp1 under control of the *TPI1* promoter, leads to mislocalisation of a peroxisomal matrix marker to the cytosol (Munck, 2008) (Fig. S3 of Knoblach et al., 2013). Mislocalisation of a peroxisomal matrix protein can be the result of a block in matrix protein import or peroxisomal membrane biogenesis, excessive peroxisome degradation (pexophagy) or mis-segregation of peroxisomes.

To confirm the overexpression phenotype, Inp1 was constitutively overexpressed under the control of the *TPI1* promoter in wild type cells (Fig. 3.8). As expected, GFP-PTS1 was

mislocalised to the cytosol and the peroxisomal membrane marker Pex11-GFP no longer displayed a punctate pattern but appeared as a tubular network. These phenotypes resemble those seen in *Δpex3* and *Δpex19* cells where matrix proteins and Pex11 mislocalise to the cytosol and mitochondria, respectively, due to the absence of peroxisomal membrane structures (Motley et al., 2015). This suggests that typical peroxisomal structures are absent upon overexpression of Inp1. The same phenotypes were also observed when the experiment was repeated in *Δatg36* cells, a mutant which is deficient in pexophagy. This confirmed that the phenotypes observed are not a result of excessive peroxisomal degradation.

In order to investigate the role of the LXXLL motif in this overexpression phenotype of Inp1, the experiment was repeated with the double leucine mutant Inp1 LL>AA. Overexpression of Inp1 LL>AA did not affect localisation of GFP-PTS1 nor Pex11-GFP. This implies that the loss of typical peroxisomal membranes upon overexpression of Inp1 is dependent upon its LXXLL motif.

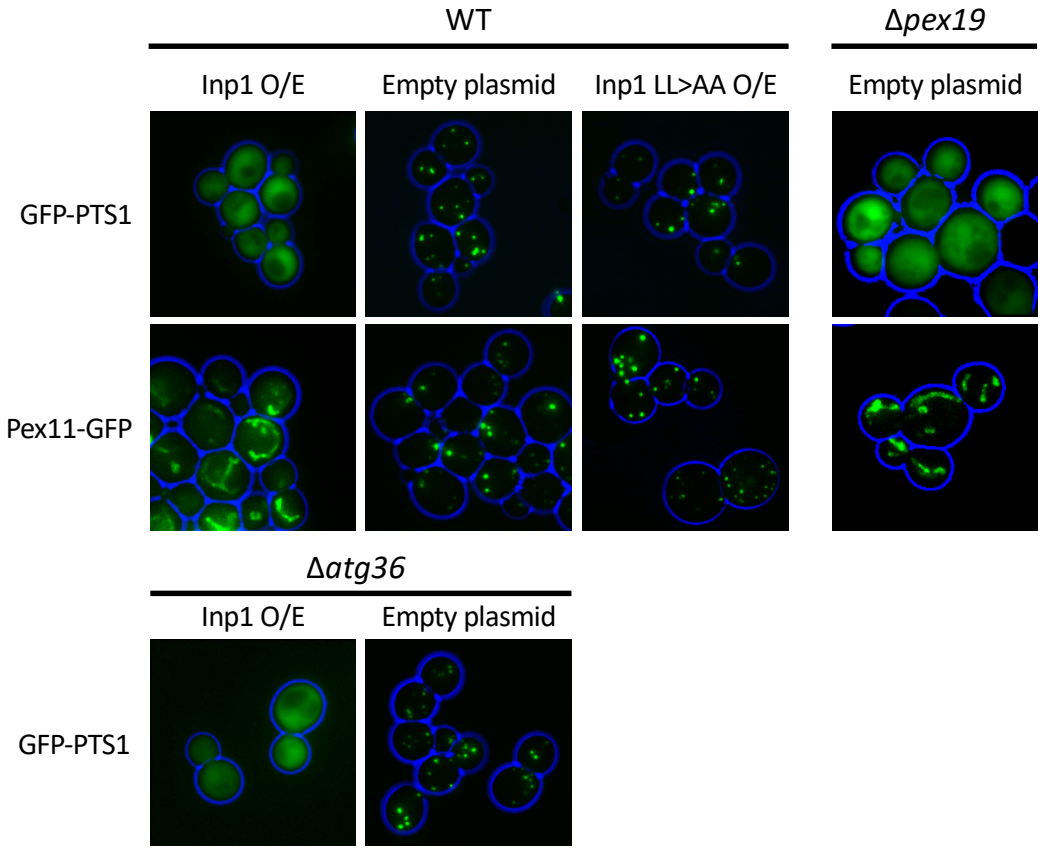

Figure 3.8 – Overexpression of Inp1 results in a loss of peroxisomal membrane structures. Fluorescence microscopy images of WT cells overexpressing Inp1 or Inp1 LL>AA under control of the TPI1 promoter with either GFP-PTS1 or the peroxisomal membrane marker Pex11-GFP. An empty plasmid was used as a control. Δpex19 cells were transformed with GFP-PTS1 or Pex11-GFP to show the location of these proteins in the absence of typical peroxisomal structures. Inp1 was also overexpressed in Δatg36 cells co-expressing GFP-PTS1 to show that the loss of peroxisomal structures is not due to increased pexophagy. Bar, 5 µm.

The loss of peroxisomal structures upon Inp1 overexpression was further tested using an assay developed in the Hettema lab. Previously, it has been reported that the last step in the lysine biosynthesis pathway, the conversion of saccharopine to lysine by Lys1, occurs in peroxisomes (Al-Saryi et al., 2017). This reaction requires regeneration of NAD^+ from NADH which also occurs intraperoxisomally and is mediated by peroxisomal malate dehydrogenase (Mdh3) and glyercol-3-phosphate dehydrogenase (Gpd1). As such, *Δmdh3/Δgpd1* mutants are unable to synthesise lysine and so show strong growth defects when grown on lysine deficient medium. This growth deficiency can be overcome when Lys1 is mislocalised from peroxisomes to the cytosol for example, in mutants where peroxisomes are absent due to a peroxisome biogenesis defect such as in *Δmdh3/Δgpd1/Δpex3* cells (Al-Saryi et al., 2017). This simple growth assay can be exploited to screen for mutants with peroxisome biogenesis defects.

Overexpression of Inp1 in *Δmdh3/Δgpd1* cells restored their growth on lysine deficient medium. This implies that upon overexpression of Inp1, Lys1 is mislocalised to the cytosol due to a loss of peroxisomal structures and confirms the phenotypes observed in Fig. 3.8. Conversely, overexpression of the motif mutant Inp1 LL>AA did not restore growth of *Δmdh3/Δgpd1* cells on lysine deficient medium, indicating that peroxisomes remained intact. This again supports the idea that the loss of peroxisomal membranes upon Inp1 overexpression is dependent on its LXXLL motif.

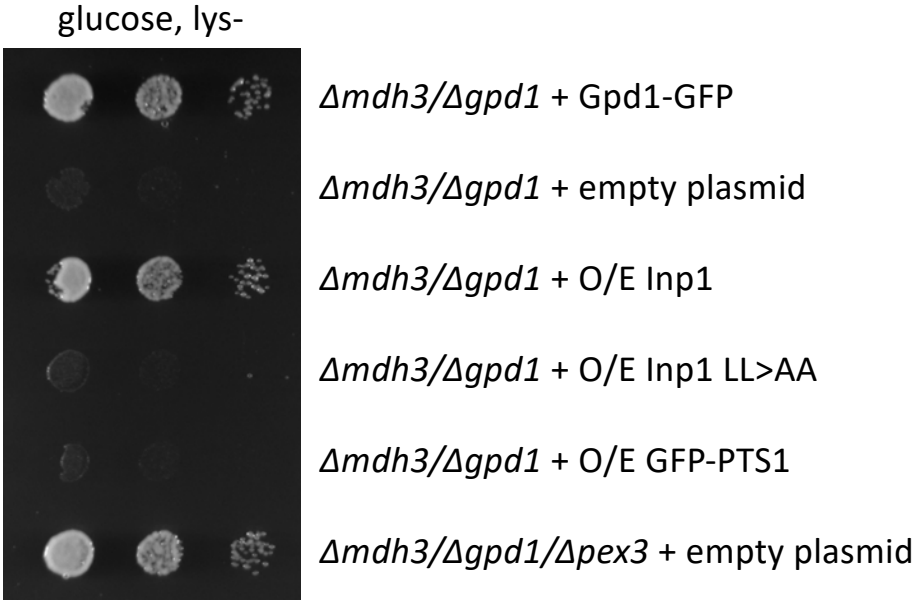

Figure 3.9 – Growth of *Δmdh3/Δgpd1* cells on lysine deficient medium can be used as an assay to show that overexpression of Inp1 results in loss of peroxisomal structures. The strains indicated were grown on solid complete synthetic glucose medium in the absence of L-lysine for 2 days at 30°C. Growth of cells overexpressing Inp1 indicates that there is a loss of peroxisomal structures.

3.3.2 Overexpression of Inp1 blocks *de novo* biogenesis of peroxisomes

Since both Inp1 and Pex19 have an LXXLL motif required for their respective functions and both bind to Pex3 to perform these functions, it is a logical prediction that they compete for binding to Pex3. The crystal structure of the soluble domain of human Pex3 has been resolved and so predictions can be made about the structure of *Sc*Pex3 due to the high levels of conservation between the two proteins (Schmidt et al., 2010). Mutation of a conserved Tryptophan (W104) in human Pex3 results in a loss of interaction with Pex19 and hence a block in peroxisome formation (Sato et al., 2008). Mutagenesis of the homologous residue W128 to Alanine in *Sc*Pex3 has also been shown to block peroxisomal formation and prevent co-localization between Pex3 and Inp1 foci (Knoblach et al., 2013). This data supports the idea that both Inp1 and Pex19 interact with a similar region of Pex3.

The loss of peroxisomal structures upon overexpression of Inp1 also supports this theory. As mentioned previously, the absence of peroxisomes in cells overexpressing Inp1 could initially be a result of peroxisome over-retention, with buds failing to inherit peroxisomes and so peroxisome-containing cells slowly being diluted out of the population (Fagarasanu et al., 2005; Fig. S1B of Munck et al., 2009). Under these circumstances, cells are able to reform peroxisomes *de novo*, a process reliant on the direct interaction between Pex3 and Pex19 (Hoepfner et al., 2005; Motley and Hettema, 2007). In cells overexpressing Inp1, it appears that this *de novo* synthesis pathway of peroxisome formation is blocked as even after several hours of growth, no peroxisomes are present. To directly test this, an assay for *de novo* peroxisomes formation was carried out based on the mating of *Δpex3* and *Δpex19* cells (Motley and Hettema, 2007).

Both *Δpex3* and *Δpex19* cells are devoid of typical peroxisomal membrane structures (Hettema et al., 2000). In *Δpex19* cells, Pex3 accumulates in the ER and so upon mating, the soluble Pex19 from the *Δpex3* mating partner should diffuse into the *Δpex19* cell and initiate the exit of Pex3 from the ER. This will then lead to the *de novo* formation of peroxisomes within 4-6 hours of mating. Haploid *Δpex3* cells labelled with GFP-PTS1 were mated with *Δpex19* cells constitutively overexpressing Inp1 under control of the *TPI1* promoter or *Δpex19* cells containing an empty plasmid and hence with endogenous levels of Inp1. Within 6 hours of mating, peroxisomes were formed *de novo* in the control cells, but GFP-PTS1 remained cytosolic in mated cells in which Inp1 was overexpressed as peroxisomes failed to form. The experiment was then repeated with constitutive overexpression of Inp1 LL>AA in the *Δpex19* mating cells. Within 6 hours, peroxisomes were formed *de novo* as in the control (Fig. 3.10).

Taken together, the data presented in Sections 3.2.1 and 3.2.2 show that constitutive overexpression of Inp1 prevents the *de novo* synthesis of peroxisomes and that this is dependent on the LXXLL motif. This strongly supports the idea that the overexpression of Inp1 prevents Pex19 from interacting with Pex3, hence blocking peroxisome biogenesis, and that Inp1 and Pex19 compete for binding to Pex3 with their respective LXXLL motifs.

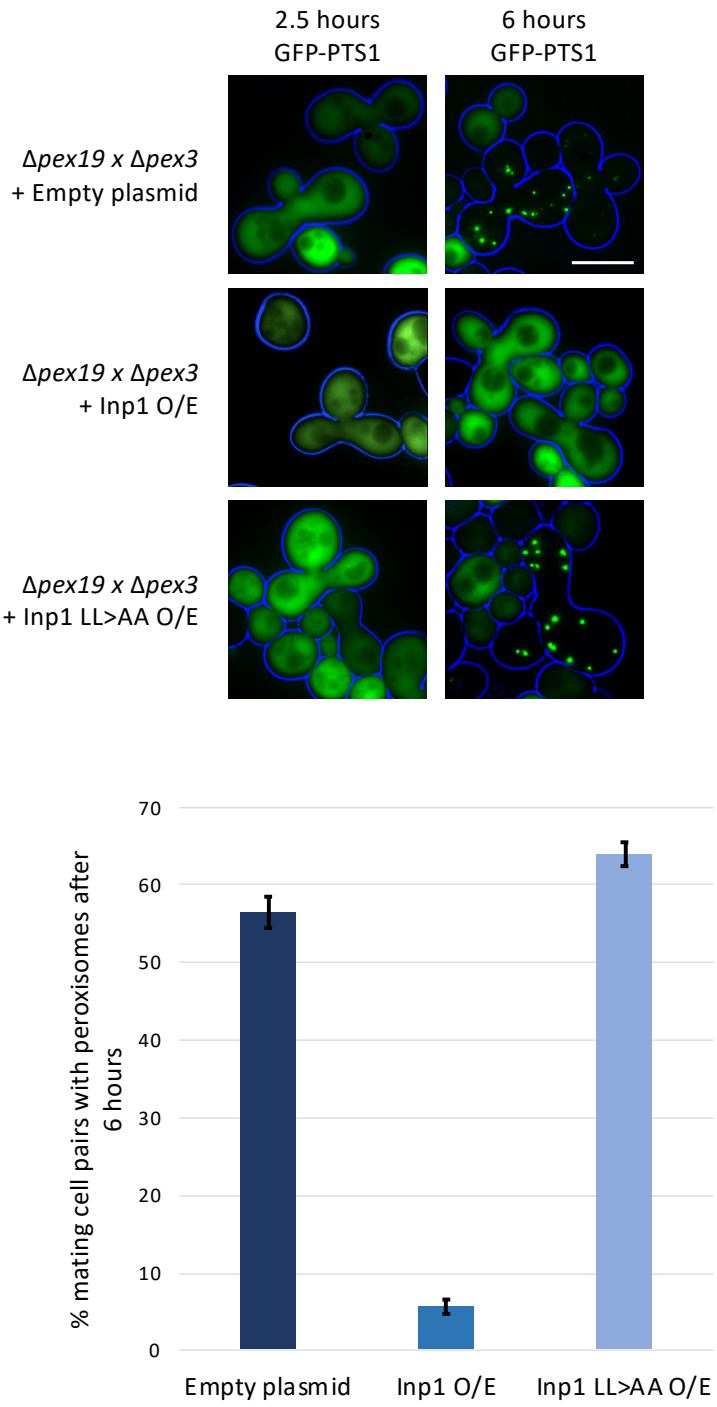

Figure 3.10 – Overexpression of Inp1 blocks *de novo* formation of peroxisomes. *Δpex3* (MATa) cells expressing GFP-PTS1 were mated with *Δpex19* (MATα) cells expressing an empty plasmid of overexpressing either Inp1 or Inp1 LL>AA (under control of the *TPI1* promoter). Cells were imaged after 2.5 or 6 hours to check for de novo formation of peroxisomes. The graph represents quantitative analysis of the mating assay. Mating cell pairs were scored for the presence or absence of peroxisomes after 6 hours. At least 100 mating cell pairs were quantified for each assay. Error bars represent SEM. Bar, 5 µm.

3.3.3 Inp1 prevents Pex3 from binding to Pex19 *in vitro*

In order to further investigate the theory that Inp1 and Pex19 can bind to the same binding site on Pex3, *in vitro* binding assays were performed (Fig. 3.11 and 3.12). First, a total lysate of *E. coli* cells expressing His-Pex3 was preincubated with a total lysate of *E. coli* cells expressing MBP-Inp1 in order to allow Pex3 to bind to Inp1. This unpurified mixture was then poured over *E. coli* expressed GST-Pex19 fusions, immobilised on glutathione Sepharose beads. After further incubation, the beads were extensively washed with 1x PBS including a PBS + 0.5M KCl wash and protein was eluted from the glutathione Sepharose beads with 1x protein loading buffer. The binding of His-Pex3 to GST-Pex19 was subsequently analysed by SDS-PAGE and Coomassie staining of the gel.

Where MBP-Inp1 had been preincubated with His-Pex3, His-Pex3 was prevented from binding to the immobilised GST-Pex19. When the *E. coli* lysate containing the MBP tag only was preincubated with His-Pex3, no competition was observed. This demonstrates that Pex19 cannot bind to Pex3 *in vitro* in the presence of Inp1 (Fig. 3.11).

The competition assay was then repeated with MBP fusions of the N- or C-terminal domains of Inp1 (amino acids 1-280 and 281-420, respectively, as described in Fig. 3.2) (Fig. 3.12). His-Pex3 was found to bind directly to GST-Pex19, except where it had been preincubated with the C-terminus of Inp1. This suggests that a complex had formed between Pex3 and the C-terminus of Inp1 (281-420) during the preincubation and supports earlier experiments described in Fig 3.2, that the C-terminus of Inp1 binds directly to Pex3. The N-terminus of Inp1 (1-280) did not disrupt binding of GST-Pex19 to His-Pex3 indicating that the N-terminus of Inp1 does not compete with Pex19 for Pex3 binding. This is probably because, as seen previously (Fig. 3.2), under these experimental conditions, the N-terminus of Inp1 does not directly bind to Pex3. To confirm this, the unbound fractions of the competition assay were further analysed. After incubation with GST-Pex19 immobilised on glutathione Sepharose beads, the unbound fractions were removed and incubated with amylose beads to which the MBP-fusions bind. The proteins were subsequently eluted from the amylose beads with 10mM maltose buffer. Due to breakdown bands of MBP-Inp1, the bound His-Pex3 is not easily distinguishable by Coomassie staining and so a western blot with Anti-His tag antibody was done. This confirmed the presence of His-Pex3 bound to MBP-Inp1 C and also showed that MBP-Inp1 N does not compete with GST-Pex19 as no His-Pex3 was bound in that fraction.

These results show that the C-terminus of Inp1 competes with Pex19 for binding to Pex3 and reinforce that the C-terminus of Inp1 binds directly to Pex3. This supports a hypothesis that it is the LXXLL motif in this region that directly competes with Pex19 for a binding site on peroxisomal Pex3.

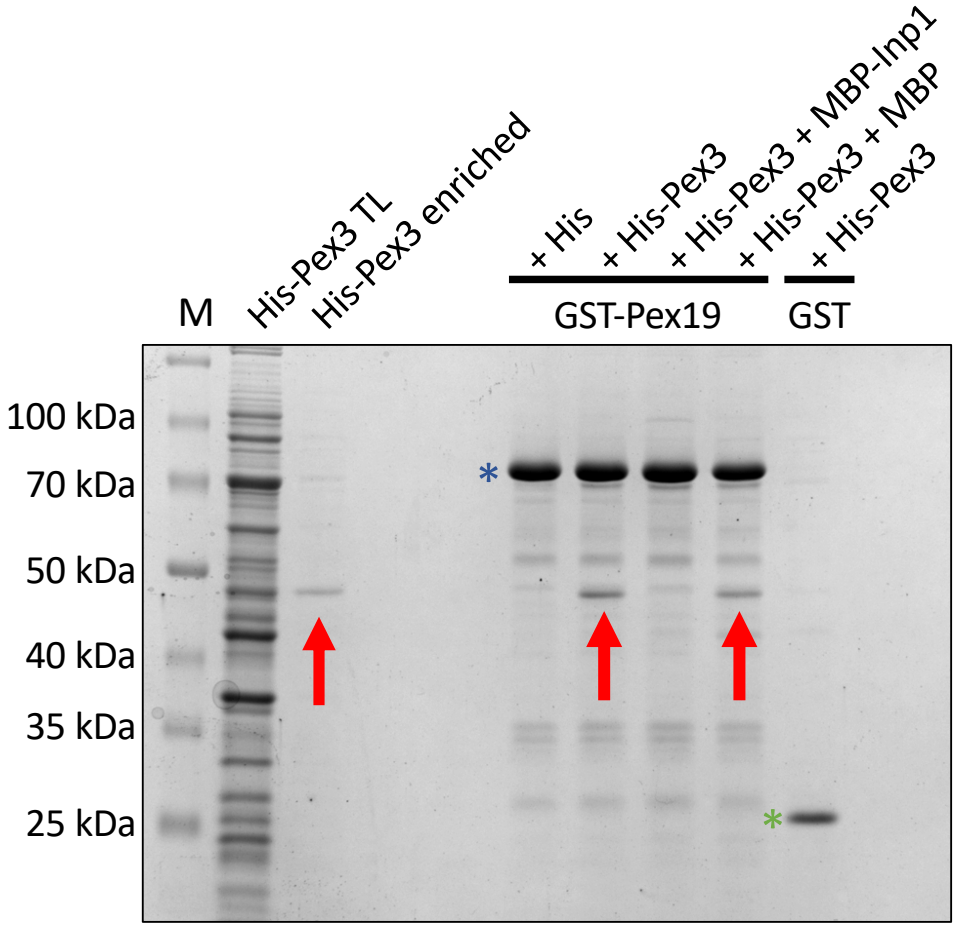

Figure 3.11 – Inp1 prevents Pex3 from binding to Pex19 *in vitro.* *E. coli* total lysates expressing His-Pex3 (40-441) or His tag only were mixed with buffer only or with *E. coli* total lysates containing either MBP-Inp1 or MBP. These mixtures were then incubated with GST-Pex19 (blue asterisk) or GST (green asterisk) immobilised on glutathione Sepharose beads. After extensive washing, including a PBS + 0.5M KCl wash, bound fractions were analysed by SDS-PAGE and Coomassie staining of the gel. A lane was included with enriched His-Pex3 as a control. M, molecular weight marker. Red arrows indicate His-Pex3.

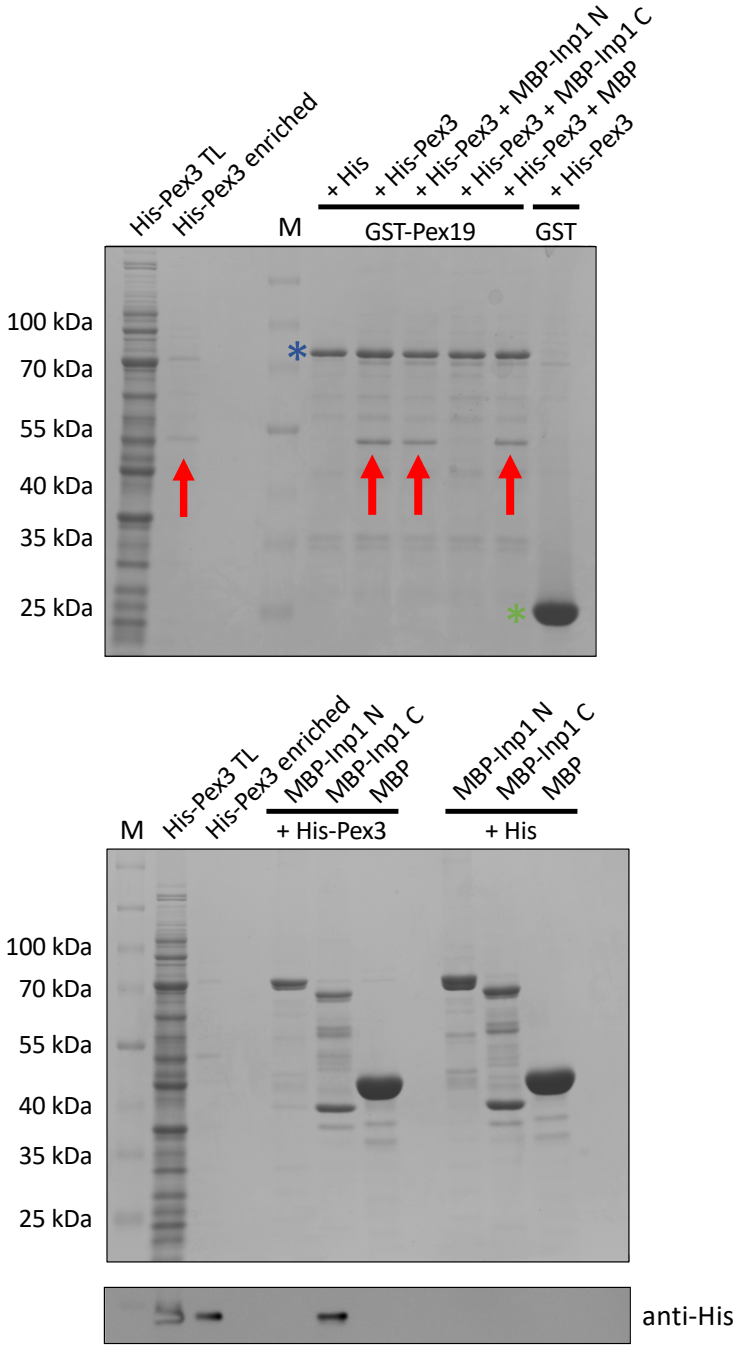

Figure 3.12 – The C-terminus of Inp1 prevents Pex3 from binding to Pex19. *E. coli* total lysates containing His-Pex3 (40-441) or His-tag only were mixed with *E. coli* total lysates containing MBP-Inp1 N (1-280), MBP-Inp1 C (281-420) or MBP. These lysates were then incubated with GST-Pex19 or GST and the mixture was immobilised on glutathione Sepharose beads. After this incubation, the unbound fraction was removed and incubated with amylose beads. The glutathione Sepharose beads and amylose beads were washed extensively. Protein was eluted from the glutathione Sepharose beads with protein loading buffer and bound fractions were analysed by SDS-PAGE and Coomassie staining of the gel (See upper gel). A lane was included with enriched His-Pex3 as a control. MBP-Inp1 C prevents binding of His-Pex3 to GST-Pex19. Protein was eluted from the amylose beads with 10mM maltose buffer and bound fractions were analysed by SDS-PAGE and Coomassie staining (See lower gel) and Western blotting with anti-His (bottom panel). M, molecular weight marker. Red arrow indicates His-Pex3. Protein visible of the gel on the right is ¼ total protein incubated with GST-Pex19. Protein visible on anti-His tag blot is 1/10.

3.3.4 *In vivo* competition between Inp1 and Pex19 can be investigated by swapping their LXXLL motifs

As discussed in Section 3.2.2, overexpression of Inp1 blocks *de novo* biogenesis of peroxisomes dependent on its LXXLL motif. This is assumed to be due high levels of Inp1 outcompeting endogenous levels of Pex19 by interacting with all available Pex3. During this study, *in vivo* and *in vitro* evidence has been obtained which supports this idea and so the converse experiment was carried out where Pex19 was overexpressed to assess if it has the ability to outcompete Inp1 (Fig 3.13).

Constitutive overexpression of Pex19 under the *TPI1* promoter in *Δpex19* cells does not have any obvious effect on the distribution of peroxisomes compared to Pex19 expressed under its endogenous promoter. Peroxisomes are retained in the mother cell and transported into the bud as in wild type cells. This implies that, despite the overabundance of Pex19, Inp1 is still able to bind to Pex3 and function in the retention of peroxisomes. The main difference in the putative Pex3 binding sites of Inp1 and Pex19 is that the central, non-leucine residues of the LXXLL motifs are NY in Inp1 and DD in Pex19. To further study the potential for Pex19 to outcompete Inp1, the LXXLL motif of Pex19 was mutated to resemble the LXXLL motif of Inp1.

Amino acids D13 and D14 of Pex19 were mutated to N and Y, respectively, and the mutant was overexpressed under the *TPI1* promoter in *Δpex19* cells co-expressing *Hc*Red-PTS1. Firstly, the protein was confirmed to be functional due to the complementation of the *Δpex19* phenotype illustrated by the presence of peroxisomes. Overexpression of wild type Pex19 did not affect peroxisome retention but interestingly, overexpression of the LNYLL mutant resulted in a partial peroxisome inheritance defect. Over half of budding cells resembled *Δinp1* cells with peroxisomes only present in the bud and a failure to retain peroxisomes in the mother cell, despite the presence of endogenous Inp1. These results show that when overexpressed, Pex19 DD13,14NY has the ability to outcompete endogenous Inp1 for interaction with Pex3.

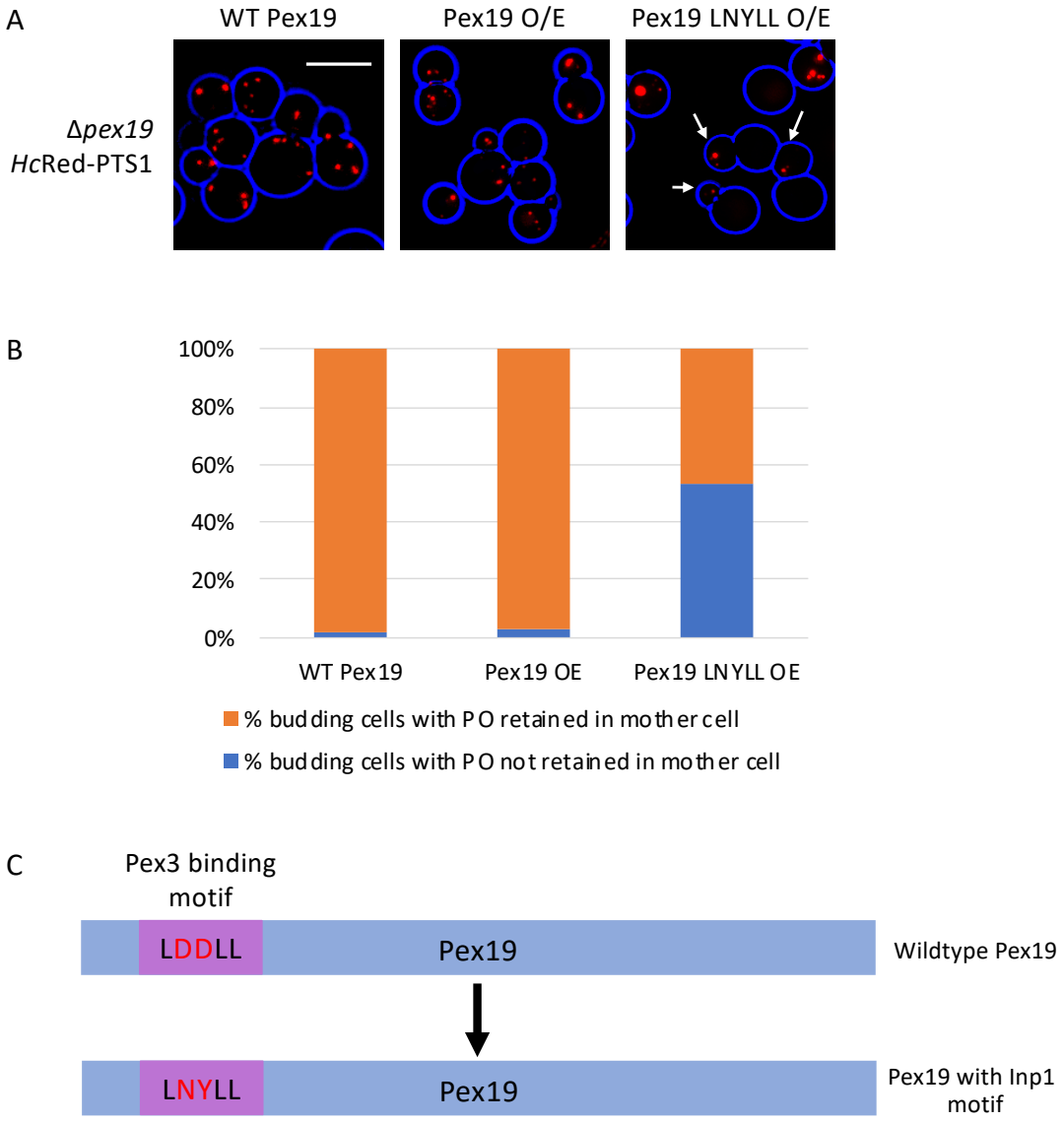

Figure 3.13 – Pex19 can out-compete endogenous Inp1 for Pex3 binding when its LXXLL motif is replaced with that of Inp1. A) Wild type Pex19 under its endogenous promoter (WT Pex19) and Pex19 or Pex19 DD13,14NY under the TPI1 overexpression promoter (Pex19 O/E and Pex19 LNYLL O/E, respectively) were co-expressed with HcRed-PTS1 in *Δpex19* cells. Cells were analysed by fluorescence microscopy. Bar, 5 µm. B) Quantitative analysis of peroxisome retention in the strains shown in A. Budding cells were scored for the presence or absence of peroxisomes in the mother cell. At least 100 budding cells were quantified for each strain. C) Schematic diagram illustrating the mutations made to the Pex3 binding motif of Pex19 with the replacement of amino acids D13 and D14 with N and Y, respectively.

3.4 Discussion

In this chapter, the role of Inp1 has been confirmed and further characterised with evidence that it is a leucine-based motif which is required for its interaction with peroxisomal Pex3 and subsequently for its correct function in peroxisome retention and positioning. A minimal region of Inp1 containing only amino acids 311-370 has previously been shown by our lab (Hutchinson, 2016), to be crucial for peroxisomal localisation and this was corroborated by yeast 2-hybrid data in which a minimal region of Inp1 corresponding to amino acids 300-378 was found to interact with Pex3.

In this study, the importance of a conserved, leucine-based motif in the interaction between Inp1 and Pex3 was confirmed and it was found that it is specifically the leucine resides which affects the peroxisomal localisation of Inp1 and its ability to bind to Pex3 *in vitro* (Fig. 3.5, 3.6, 3.7) This is supported by an independent study carried out during the course of this work which reported a random Inp1 mutant in this motif (LXXLP) that also interfered with Inp1 function by blocking recruitment of Inp1 to peroxisomes (Knoblach and Rachubinski, 2019). Taken together, this evidence is strongly suggestive that the leucine residues of the LXXLL motif of Inp1 are required for its interaction with peroxisomal Pex3 and hence for its function in peroxisomal retention.

The comparison between the LXXLL Pex3 binding motifs of Pex19 and Inp1 was confirmed with evidence that disruption of the leucine resides in the motifs of both proteins is sufficient to disrupt their respective Pex3 interaction-dependent functions (Fig. 3.4, 3.5, 3.6). Previous observations have shown that overexpression of Inp1 results in a loss of peroxisomal structures and led to a hypothesis that Inp1 and Pex19 compete for binding to Pex3 based on their analogous LXXLL motifs. Additional *in vivo* evidence was compiled to support this theory, showing that overexpression of Inp1 does indeed lead to a loss of peroxisomal structures and that this is not as a result of increased pexophagy (Fig. 3.8).

As shown in Section 3.2.4, when overexpressed, Inp1 outcompetes endogenous Pex19 for binding to Pex3 but interestingly, overexpression of wild type Pex19 does not outcompete endogenous Inp1, unless its Pex3 binding motif is replaced with that of Inp1 (Fig. 3.13). A reasonable explanation for this could be that the central two residues of the LXXLL motif (NY or DD) affect the affinity with which Inp1 or Pex19 bind to Pex3. The Asparagine and Tyrosine in Inp1's binding motif may strengthen the interaction with Pex3 compared to the two Aspartate residues present in Pex19 which may facilitate a more transient interaction. This is logical when the role of each protein is considered. Inp1 functions as a tether, securely anchoring proteins to the cell cortex for prolonged periods during cell division. Conversely, Pex19 is a cytosolic chaperone which makes temporary interactions with Pex3 as it delivers peroxisomal membrane proteins to the peroxisomal membrane. Additionally, according to datasets on the *Saccharomyces* Genome Database, endogenous levels of Inp1 are Pex3 are fairly similar, with levels of Pex19 protein suggested to be 2-5 times higher. It would be reasonable to assume that Inp1 binds to Pex3 with higher affinity to ensure it can compete with Pex19 despite its protein levels being lower. The varying amounts of endogenous proteins in combination with different Pex3 binding site affinities could maintain competition at the desired levels. This would result in a careful cellular balance of both peroxisome

retention and PMP import and ensure that Pex3 is able to maintain different peroxisomal processes through 1 binding site.

The potential for competition between Inp1 and Pex19 was also confirmed *in vitro* (Fig. 3.11, 3.12) Interestingly, it was only the C-terminal domain of Inp1 (281-420) which prevented Pex19 from binding to Pex3 and this was supported by the data presented in Fig. 3.2 which illustrated that specific binding could be shown between Pex3 and the C-terminal domain (281-420) of Inp1 but not the N-terminal domain (1-280). The existing model states that Inp1 acts as a 'molecular hinge' between peroxisomal and cortical ER-localised Pex3 and this comes from the reported observation that both the N- and C-terminal domains of Inp1 independently bind directly to Pex3 *in vitro* (Knoblach et al., 2013). As highlighted in Section 3.2.2, specific binding of the N-terminal domain of Inp1 to Pex3 was not able to be repeated under the assay conditions used in this study. Detergent-dependent aggregation of Pex3, non-specific binding or a combination of the two could form a plausible explanation as to why Pex3 binding to MBP-Inp1 1-280 is reported by Knoblach et al., 2013, but is not seen during this study in the *in vitro* binding nor the competition assays.

This chapter has partially characterised the molecular nature by which Inp1 interacts with peroxisomal Pex3 and has established that this is a motif with much similarity to that of Pex19. The next chapter serves to elucidate how the N-terminal domain of Inp1, if not via ER-bound Pex3, tethers peroxisomes to the mother cell cortex during asymmetric cell division.

Chapter 4 – Inp1 has an N-terminal lipid-binding domain that is sufficient and necessary for peroxisome retention.

4.1 Introduction

The data reported in Chapter 3 shows that Inp1 has a leucine-based motif in the C-terminal part of the protein that is required for localisation to peroxisomes via an interaction with the cytosolic domain of peroxisomal Pex3. Contrary to previously published observations (Knoblach et al., 2013), direct *in vitro* interactions between the N-terminal domain of Inp1 and Pex3 were not observed under the assay conditions of this study. As such, the data obtained in Chapter 3 are not supportive of the current model of peroxisome retention which postulates that Inp1 acts as a 'molecular hinge' between peroxisomes and the ER by interacting in trans with both ER-associated and peroxisome-associated Pex3 via N and C-terminal Pex3 binding domains (Knoblach et al., 2013).

Interestingly, further research by the same group has recently shed doubt on the simplicity of this model with the suggestion that the ER-peroxisome tether is likely to involve additional cortical factors. That study also concludes that peroxisomes are likely to be tethered to organelles other than the ER and that the role of Inp1 as a tether probably expands beyond its function in tethering peroxisomes to the ER but it may also tether peroxisomes to other organelles (Knoblach and Rachubinski, 2019). It was shown in Chapter 3 that the C-terminal part of Inp1 is required for its interaction with peroxisomal Pex3 but it is not sufficient to retain peroxisomes at the mother cell periphery. The data presented in this chapter serves to discover which part of Inp1 anchors peroxisomes at the mother cell periphery and to elucidate how Inp1, if not via ER-bound Pex3, interacts with the mother cell cortex.

4.2 The N-terminus of Inp1 is necessary and sufficient for interaction with the cell cortex

As discussed in Chapter 3, the ability of Inp1 to localise to peroxisomes is dependent upon its C-terminal LXXLL Pex3 binding motif. The truncation screen of Inp1 described in Section 3.2.1 uncovered that the C-terminus of Inp1 is required for its localisation to peroxisomes. Additionally, this screen uncovered several N-terminal truncations of Inp1 that co-localised with peroxisomal markers but, when expressed in *Δinp1* cells, failed to rescue peroxisome retention (Hutchinson, 2016). This indicates that it is the N-terminal region of Inp1 which is required for the association of peroxisomes with the mother cell cortex.

In order to identify the region of Inp1 that is necessary for peroxisome association with the cell cortex, independent of its binding to Pex3, truncations of Inp1 were fused to GFP-Pex15, a tail anchored peroxisomal membrane protein with a cytosolic facing globular domain (Elgersma et al., 1997). This created fusion proteins where Inp1 was exposed to the cytosol and anchored to the peroxisomal membrane by Pex15, with a GFP spacer moiety between

the two proteins. These fusion proteins were then co-expressed under control of the *INP1* promoter in *Δinp1* cells with *Hc*Red-PTS1 (Fig. 4.1).

First, the functionality of the chimeric protein was confirmed, as Inp1-GFP-Pex15 was able to complement the *Δinp1* phenotype and restore peroxisome retention in mother cells (Fig 4.1). Additionally, Inp1 L312_L316del (Δmotif)-GFP-Pex15 was also able to rescue peroxisome retention. This shows that the ability of Inp1 to anchor peroxisomes to the cell periphery is independent of its LXXLL Pex3 binding motif, characterised in Chapter 3.

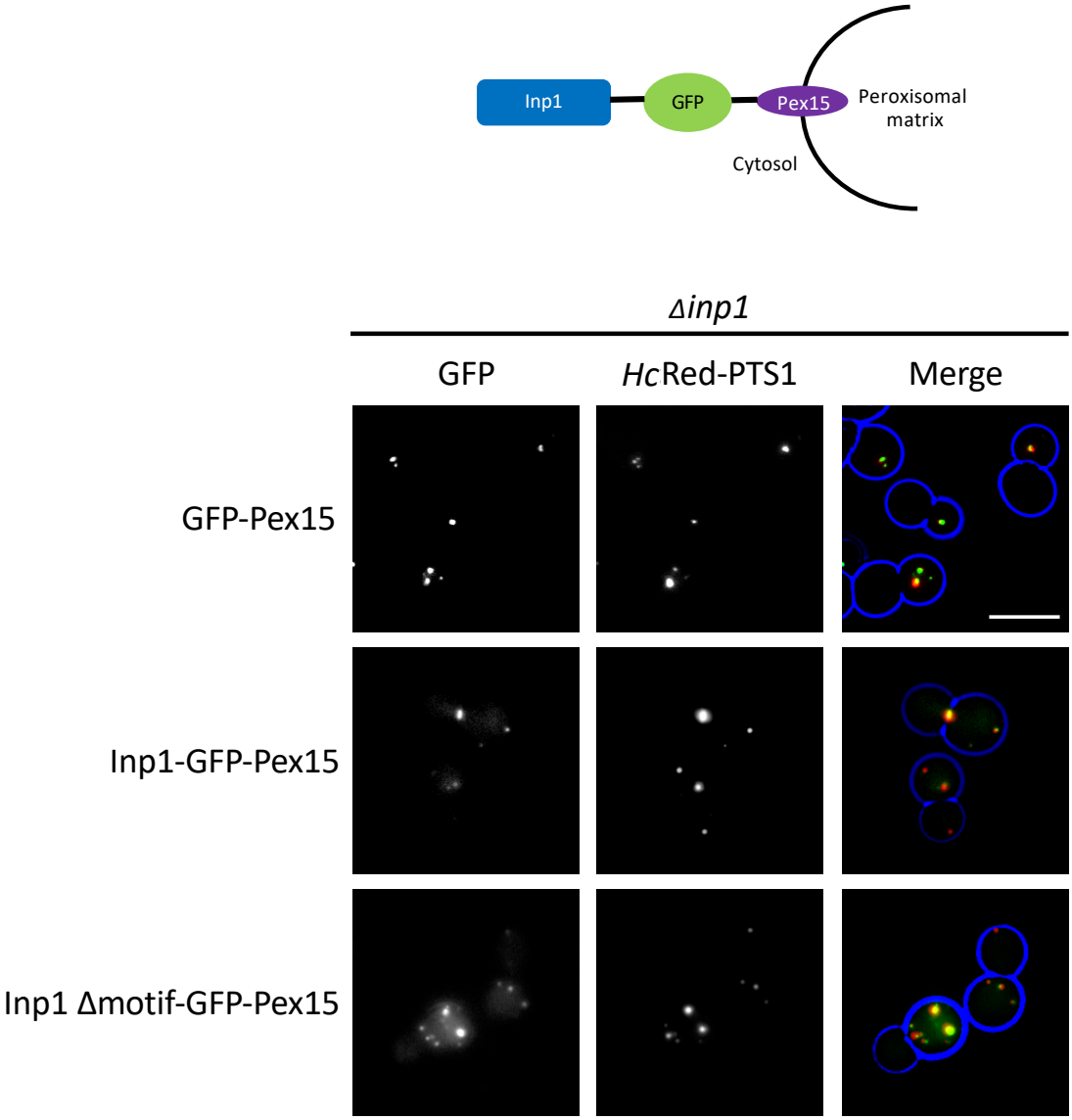

Figure 4.1 – Inp1 can restore peroxisome retention independent of its LXXLL binding motif. Inp1 or Inp1 L312_L316del (Δmotif) were fused to GFP-Pex15 and expressed under control of the *INP1* promoter in *Δinp1* cells co-expressing *Hc*Red-PTS1. Cells were analysed by fluorescence microscopy. The schematic diagram illustrates the predicted topology of the Inp1-Pex15 fusion proteins with Inp1 exposed to the cytosol and anchored to the peroxisomal membrane by Pex15 with a GFP moiety acting as a spacer between the two proteins. Bar, 5µm.

Various truncations of Inp1 were then fused to Pex15 in order to identify a minimal region required for peroxisome retention to the cell periphery. The N-terminal 100 amino acids (1-100) of Inp1 were found to be the smallest, stable truncation of Inp1 which was sufficient to rescue peroxisome retention in *Δinp1* cells (Fig. 4.2). In order to verify the role of the N-terminal 100 amino acids, Inp1 100-420-GFP was expressed in *Δinp1* cells and it was confirmed that this truncation does not rescue peroxisome retention (Fig. 4.3). It can therefore be concluded that the N-terminal 100 amino acids of Inp1 are both necessary and, when associated with the peroxisomal membrane, sufficient for retention of peroxisomes to the periphery of the cell.

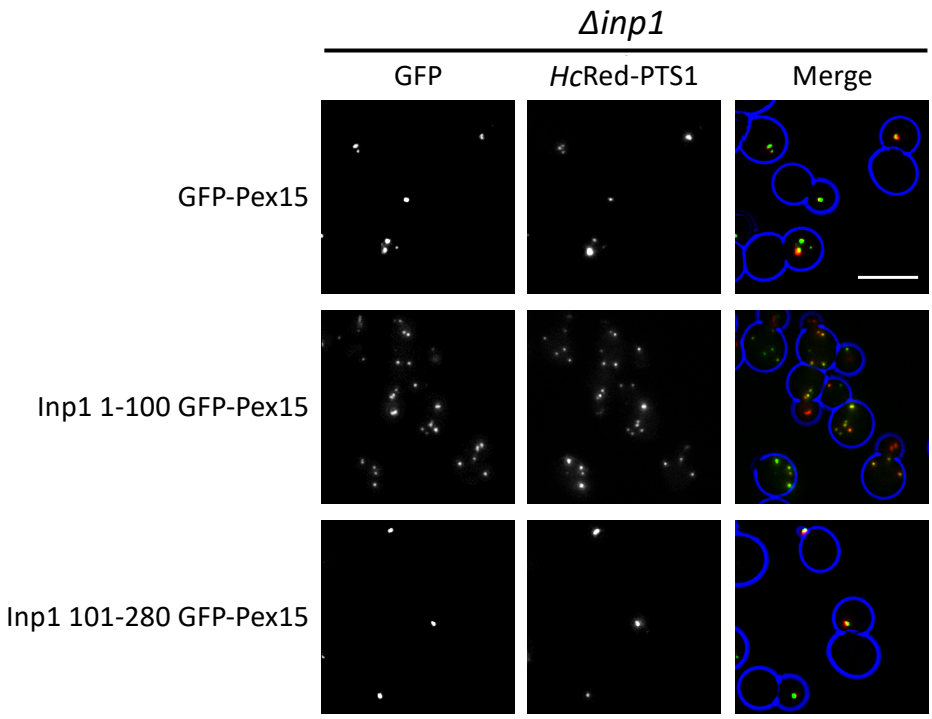

Inp1-GFP-Pex15 fusion protein	Able to restore peroxisome retention in Δ*inp1* cells?
GFP-Pex15	No
Full length Inp1	Yes
Full length Inp1 Δmotif	Yes
Inp1 1-280	Yes
Inp1 281-420	No
Inp1 1-100	Yes
Inp1 101-280	No

Figure 4.2 – The N-terminal 100 amino acids of Inp1 are sufficient for tethering of peroxisomes to the cell periphery. Truncations of Inp1 were fused to GFP-Pex15 and expressed under control of the *INP1* promoter in *Δinp1* cells co-expressing *Hc*Red-PTS1. Cells were analysed by fluorescence microscopy. The table summarises which Inp1-GFP-Pex15 fusion proteins were sufficient to rescue peroxisome retention. Cells were assessed for rescue of the *Δinp1* phenotype (obvious presence of peroxisomes in the mother cell) and at least 100 cells were counted for each fusion protein. Bar, 5µm.

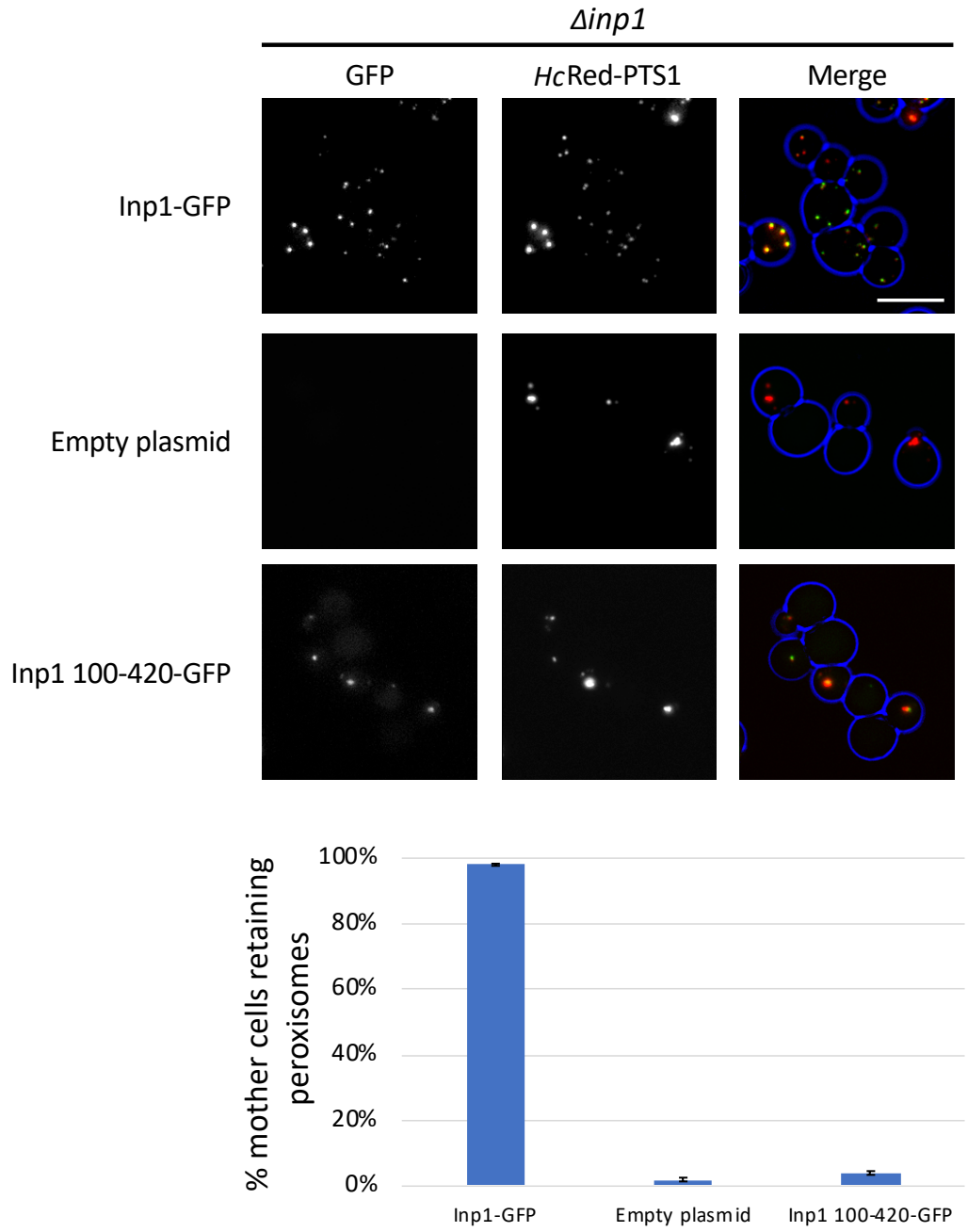

Figure 4.3 – The N-terminal 100 amino acids of Inp1 are necessary for peroxisome retention. The Inp1-GFP truncation 100-420 was expressed under control of the *INP1* promoter in *Δinp1* cells with the constitutively expressed *Hc*Red-PTS1. Cells were examined by fluorescence microscopy. Bar, 5µm. The graph shows quantitative analysis of the assay. Mating cell pairs were scored for the presence of peroxisomes in the mother cell. At least 100 budding cells were quantified for each strain. Three independent experiments were carried out. Error bars represent SEM.

4.3 The N-terminus of Inp1 contains a lipid binding domain

4.3.1 The N-terminus of Inp1 localises to the plasma membrane

As shown and discussed in Chapter 3, the N-terminus of Inp1 (amino acids 1-282) does not bind to Pex3 under the *in vitro* binding assay conditions used in this study. However, the experiments presented in Figures 4.2 and 4.3 show that the first 100 amino acids are necessary for peroxisome retention and that when fused artificially to peroxisomes, this N-terminal domain is sufficient to tether peroxisomes to the mother cell cortex. The subsequent experiments set out to characterise the anchoring function of this domain of Inp1 and to investigate what, if not Pex3, the N-terminal domain of Inp1 could be interacting with at the cell periphery.

In order to determine the sub-cellular localisation of the N-terminal domain of Inp1, the first 100 amino acids were fused to GFP and expressed under control of the inducible *GAL1/10* promoter in wild type cells. The protein was found to be cytosolic and localised to the nucleus but, surprisingly, the protein also showed plasma membrane localisation (Fig. 4.4). Nuclear localisation such as this has previously been observed with GFP fusions of proteins which contain plasma membrane-associated lipid binding domains, although the reason for this has not been established (Yu et al., 2004). This led to the hypothesis that the N-terminal domain of Inp1 has the capacity to bind to lipids and that this could facilitate an interaction between Inp1 and the plasma membrane.

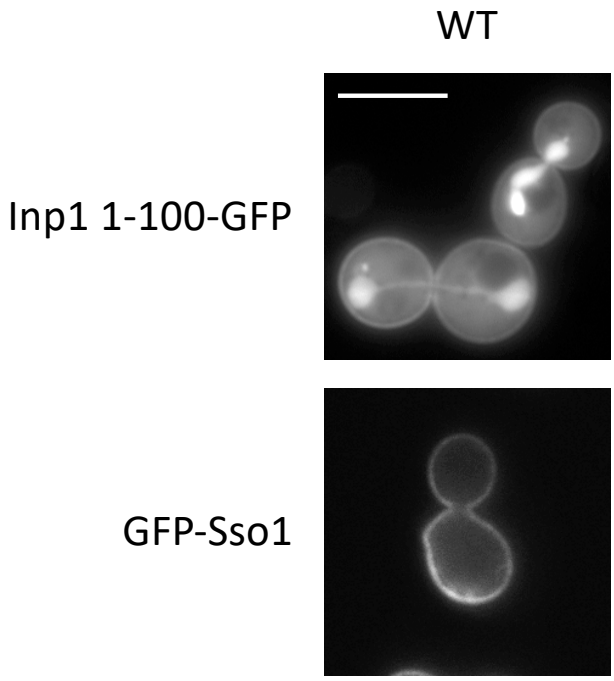

Figure 4.4 – Inp1 1-100 localises to the plasma membrane. An inducible truncation of 1-100 Inp1-GFP was expressed under control of the *GAL1/10* promoter in WT cells. GFP-Sso1 expressed under control of the *TPI1* promoter in WT cells is shown to exemplify characteristic plasma membrane localisation. A single focal plane is shown for both images. Bar, 5µm.

4.3.2 Inp1 is a lipid binding protein and is able to bind to PI(4,5)P_2

In order to test the capability of Inp1 to bind to the plasma membrane, *in vitro* lipid binding assays were carried out. In these assays, purified protein is incubated with liposomes and the mixture is subjected to ultra-centrifugation (280,000 *g*). Liposomes sediment in a pellet whilst non-bound protein will remain in the soluble supernatant fraction. Purified protein which is able to bind to the liposomes will co-sediment with the liposomes in the pellet fraction.

E. coli expressed MBP-Inp1 was bound to amylose beads, extensively washed and eluted from the beads with 10mM maltose buffer in order to obtain purified protein. Protein-free liposomes were prepared from Type I, Folch I fraction of total bovine brain lipid extract which is mainly comprised of phosphatidylinositol (PI) and phosphatidylserine (PS) (Sigma Aldrich). The purified protein was subjected to a preliminary ultra-centrifugation (350,000 *g*) to remove any aggregated protein and subsequently incubated with the Folch liposomes before ultra-centrifugation (280,000 *g*). Protein loading buffer was added to both the soluble fraction and the pellet and the total protein present in each fraction was analysed by SDS-PAGE and Coomassie staining of the gel (Fig. 4.5).

MBP was used as a control and was judged not to sediment in the presence or absence of Folch liposomes (8% and 5% total protein present in the pellet, respectively). MBP-Inp1 was clearly present in the pellet in the presence of Folch liposomes (36% total full length protein) and in the absence of liposomes was present in the pellet at a similar level to the MBP only control (7% total full length protein). This confirms that MBP-Inp1 does not aggregate upon ultra-centrifugation and identifies Inp1 as a lipid binding protein, as it is able to bind to the lipids in the Folch liposomes.

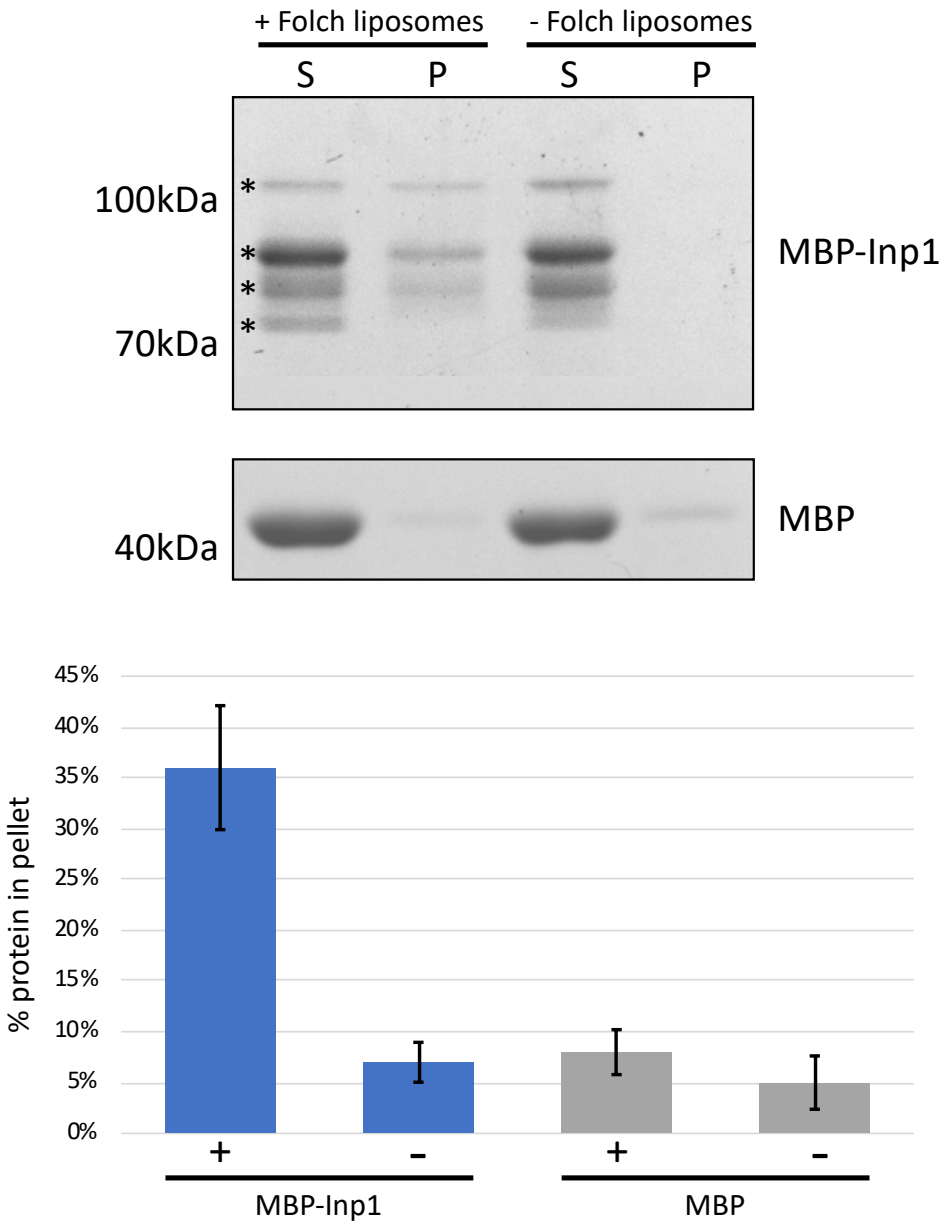

Figure 4.5 – MBP-Inp1 binds to Folch extract liposomes *in vitro*. Purified MBP-Inp1 or MBP only were incubated with Folch fraction I liposomes made from total bovine brain extract and subjected to ultra-centrifugation. Supernatant (S) and pellet (P) fractions were then analysed by SDS-PAGE and Coomassie staining. Asterisks indicate multiple MBP-Inp1 fragments. The percentage of protein present in each pellet was quantified. Each supernatant + pellet band were combined and considered to represent 100% of the protein used in the experiment (where there are multiple breakdown bands for MBP-Inp1, the top band representing full length MBP-Inp1 was used). The percentage of protein in each pellet in the presence (+) or absence (-) of the Folch liposomes is shown. The assay was performed in 3 independent experiments, error bars represent SEM.

In order to further characterise the Inp1-lipid interaction observed in Fig. 4.5, liposomes were synthesised which were comprised of 70% phosphatidylcholine (PC), 8% phosphatidylethanolamine (PE) with 22% phosphatidylinositol 4-phosphate (PI(4)P) or phosphatidylinositol 4,5-bisphosphate ($PI(4,5)P_2$). The ultra-centrifugation assays were repeated with these synthetic liposomes as described previously. Protein loading buffer was added to both the soluble fractions and the pellets and the total protein present in each fraction was analysed by SDS-PAGE and Coomassie staining of the gels (Fig. 4.6).

The MBP only control was judged not to co-sediment in the presence or absence of either of the synthetic liposomes. With PC/PE liposomes supplemented with PI(4)P, MBP-Inp1 was present in the pellet in comparative levels to the MBP control (9% and 10% total full length protein, respectively) and so it was concluded that Inp1 does not bind to PI(4)P (Fig. 4.6). However, much higher levels of MBP-Inp1 were observed in the pellet in the presence of PC/PE liposomes supplemented with $PI(4,5)P_2$ (35% total full length protein) (Fig. 4.7). MBP-Inp1 showed co-sedimentation with the PC/PE liposomes supplemented with $PI(4,5)P_2$ but not with PI(4)P, strongly indicating Inp1 has the ability to bind to $PI(4,5)P_2$ (Fig. 4.6). This result is significant as $PI(4,5)P_2$ is predominantly localised to and synthesised at the inner leaflet of the yeast plasma membrane (Yu et al., 2004; Vernay et al., 2012).

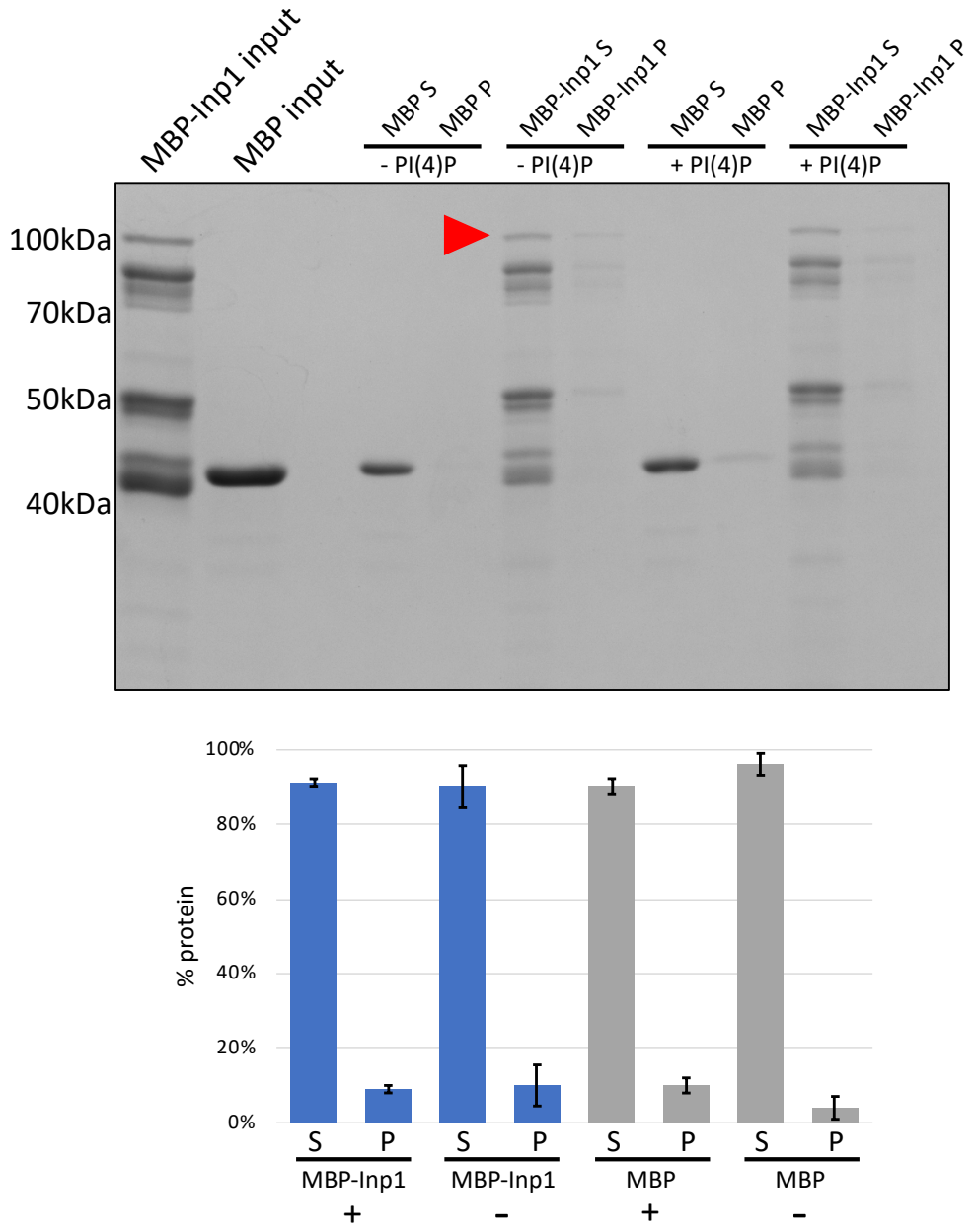

Figure 4.6 – MBP-Inp1 does not bind to PC/PE liposomes containing PI(4)P. Purified MBP-Inp1 or MBP only was incubated with liposomes made up of PC, PE and PI(4)P and subjected to ultra-centrifugation. Total protein input, supernatant (S) and pellet (P) fractions were analysed by SDS-PAGE and Coomassie staining. The percentage of protein present in each supernatant and pellet was quantified. Each supernatant + pellet band were combined and considered to represent 100% of the protein used in the experiment. Where there are multiple breakdown bands for MBP-Inp1, the top band representing full length MBP-Inp1 was used, the red arrow indicates full length MBP-Inp1. The percentage of protein in each supernatant (S) or pellet (P) in the presence (+) or absence (-) of the PI(4)P liposomes is shown. The assay was performed in 3 independent experiments, error bars represent SEM.

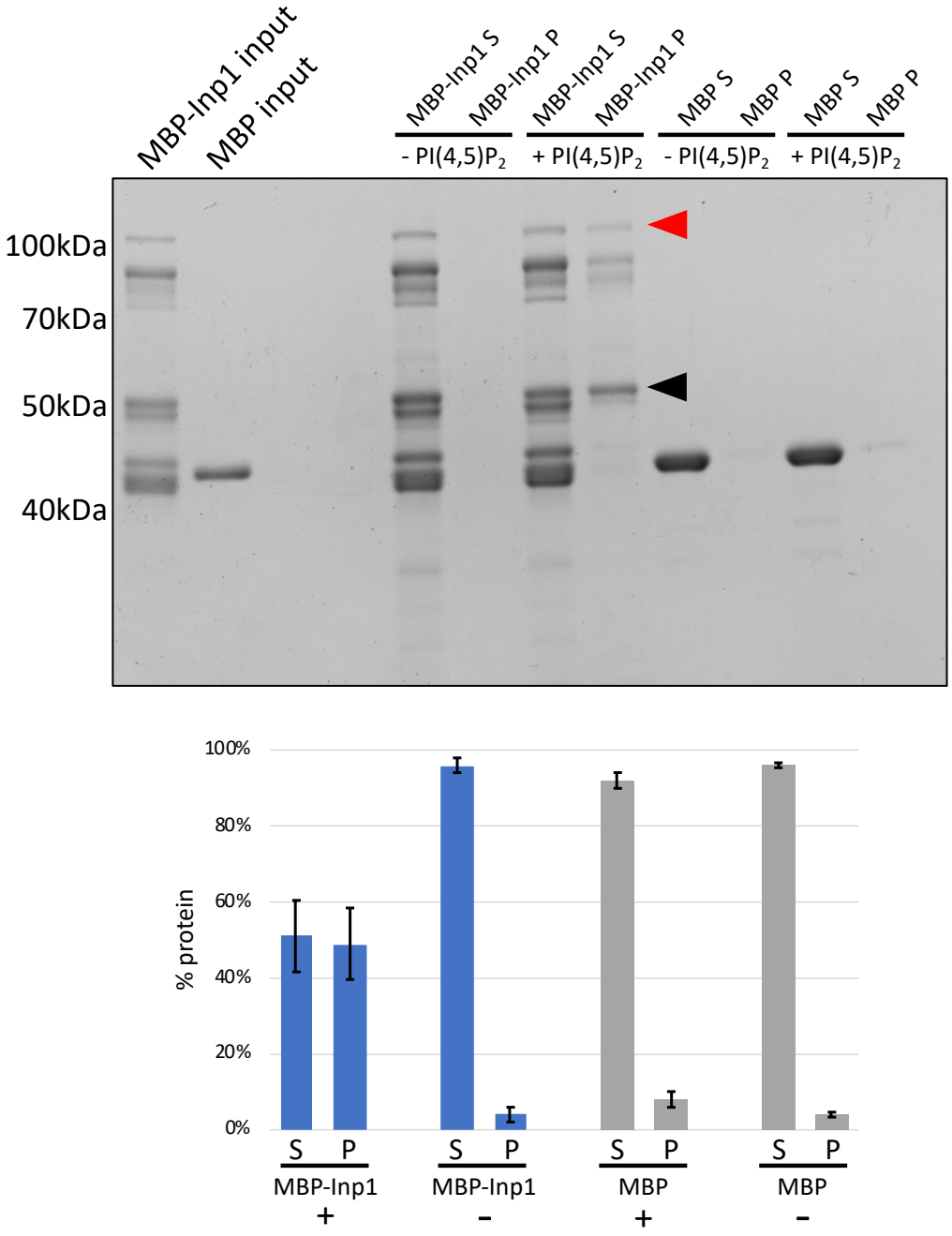

Figure 4.7 – MBP-Inp1 binds to PC/PE liposomes containing PI(4,5)P_2. Purified MBP-Inp1 or MBP only was incubated with liposomes made up of PC, PE and PI(4,5)P_2 and subjected to ultra-centrifugation. Total protein input, supernatant (S) and pellet (P) fractions were analysed by SDS-PAGE and Coomassie staining. Black arrow indicates a breakdown product truncation of MBP-Inp1 which is still able to bind to lipids containing PI(4,5)P_2. The percentage of protein present in each supernatant and pellet was quantified. Each supernatant + pellet band were combined and considered to represent 100% of the protein used in the experiment. Where there are multiple breakdown bands for MBP-Inp1, the top band representing full length MBP-Inp1 was used, the red arrow indicates full length MBP-Inp1. The percentage of protein in each supernatant (S) or pellet (P) in the presence (+) or absence (-) of the PI(4,5)P_2 liposomes is shown. The assay was performed in 6 independent experiments, error bars represent SEM.

Protein-lipid interactions at membranes can be due to non-specific, electrostatic interactions, (Lemmon, 2008), and it is plausible that such non-specific interactions between positively charged residues in Inp1 and negatively charged phospholipids, such as PI(4,5)P_2, could have been taking place in the liposome co-sedimentation assays. Although no interaction was seen between MBP-Inp1 and PI(4)P supplemented liposomes, to fully exclude that Inp1 was simply binding non-specifically to negatively charged PI(4,5)P_2, the co-sedimentation assay was repeated with PC/PE liposomes supplemented with another negatively charged phospholipid, phosphatidylserine (PS) (Fig. 4.8). Additionally, a PC/PE only control was included this time to completely exclude that MBP-Inp1 was binding to those phospholipids in the synthetic liposomes. Again, MBP-Inp1 co-sedimented with PI(4,5)P_2 containing liposomes comparatively more than with the PC/PE only control and the liposomes supplemented with PS.

As electrostatic interactions between proteins and membrane surfaces are salt sensitive, carrying out co-sedimentation assays at different salt concentrations can also indicate whether a protein is binding to the lipids in a non-specific, charge dependent manner (Saarikangas et al., 2009). Loss of interaction at a higher salt concentration indicates that the interaction between a protein and lipid is mainly mediated through non-specific electrostatic interactions. In the co-sedimentation assays carried out throughout this chapter, binding between liposomes and purified protein took place in a buffer with a final salt concentration of 180mM (20mM KCl and 160mM NaCl). Further co-sedimentation assays were subsequently carried out in buffers with gradually increasing concentrations of NaCl (200mM-350mM, data not shown), in order to assess whether binding between MBP-Inp1 and liposomes was maintained in the presence of higher concentrations of salt ions, or not.

The buffer with the highest concentration of added salt (370mM, 20mM KCl with the addition of 350mM NaCl) was sufficient to maintain MBP-Inp1 binding to PI(4,5)P_2 liposomes, albeit with a small reduction from 53% to 40% (Fig. 4.9). The maintenance of an interaction between MBP-Inp1 and PI(4,5)P_2 liposomes in high salt conditions implies that the efficient binding of Inp1 to PI(4,5)P_2 depends mainly on specific interactions but the small reduction observed could be indicative that electrostatic interactions also contribute. Conversely, the small amount of binding observed between PS liposomes and MBP-Inp1 at 180mM NaCl was depleted to a level indistinguishable from background binding under the same high salt conditions (370mM). This implies that any interactions between MBP-Inp1 and PS are mainly mediated through non-specific, electrostatic interactions.

Taken together, these results suggest that MBP-Inp1 has additional mechanisms in binding PI(4,5)P_2 beyond electrostatic interactions and indicates that there is specificity in the binding of Inp1 to the plasma membrane-associated phosphoinositide. Co-sedimentation assays performed in 370mM high salt conditions are shown in this thesis as at this concentration of salt, interactions between MBP-Inp1 and PS liposomes are lost whilst interactions with PI(4,5)P_2 liposomes are maintained. However, a full range of controls has yet to be tested in order to conclusively rule whether the binding between MBP-Inp1 and the liposomes is specific or non-specific.

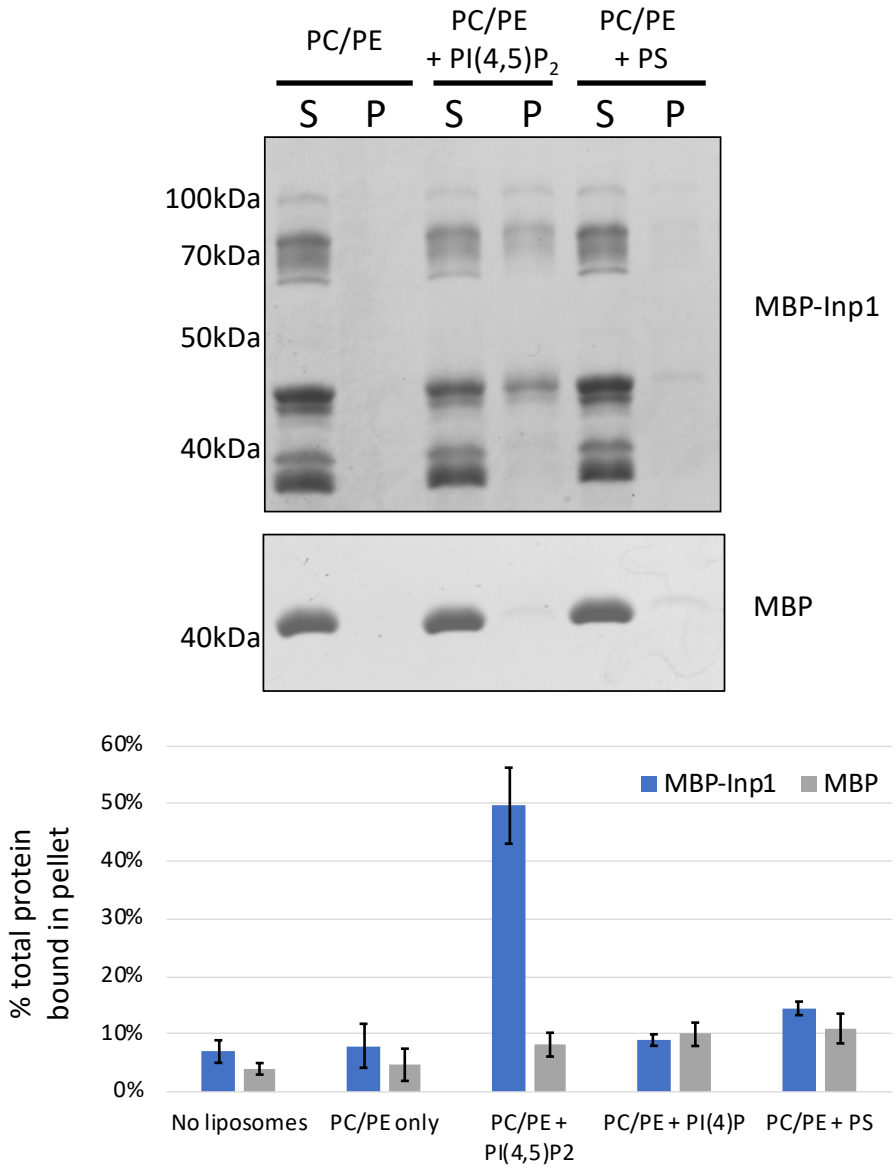

Figure 4.8 – MBP-Inp1 binds to PC/PE liposomes supplemented with PI(4,5)P_2 but not those supplemented with PS. Purified MBP-Inp1 or MBP only were incubated with liposomes made up of PC/PE +/- either 22% PI(4,5)P_2 or PS and subjected to ultra-centrifugation. Total protein input, supernatant (S) and pellet (P) fractions were analysed by SDS-PAGE and Coomassie staining. The quantitative analysis summarises the data obtained for MBP-Inp1 and MBP with various liposomes. The percentage of protein present in each pellet was quantified, each supernatant + pellet band were combined and considered to represent 100% of the protein used in the experiment. Where there are multiple breakdown bands for MBP-Inp1, the top band representing full length MBP-Inp1 was used (as indicated in Figures 4.7 and 4.8). The percentage of protein in each pellet in the presence of various liposomes is shown. Liposome binding assays were all performed in at least 3 independent experiments, error bars represent SEM.

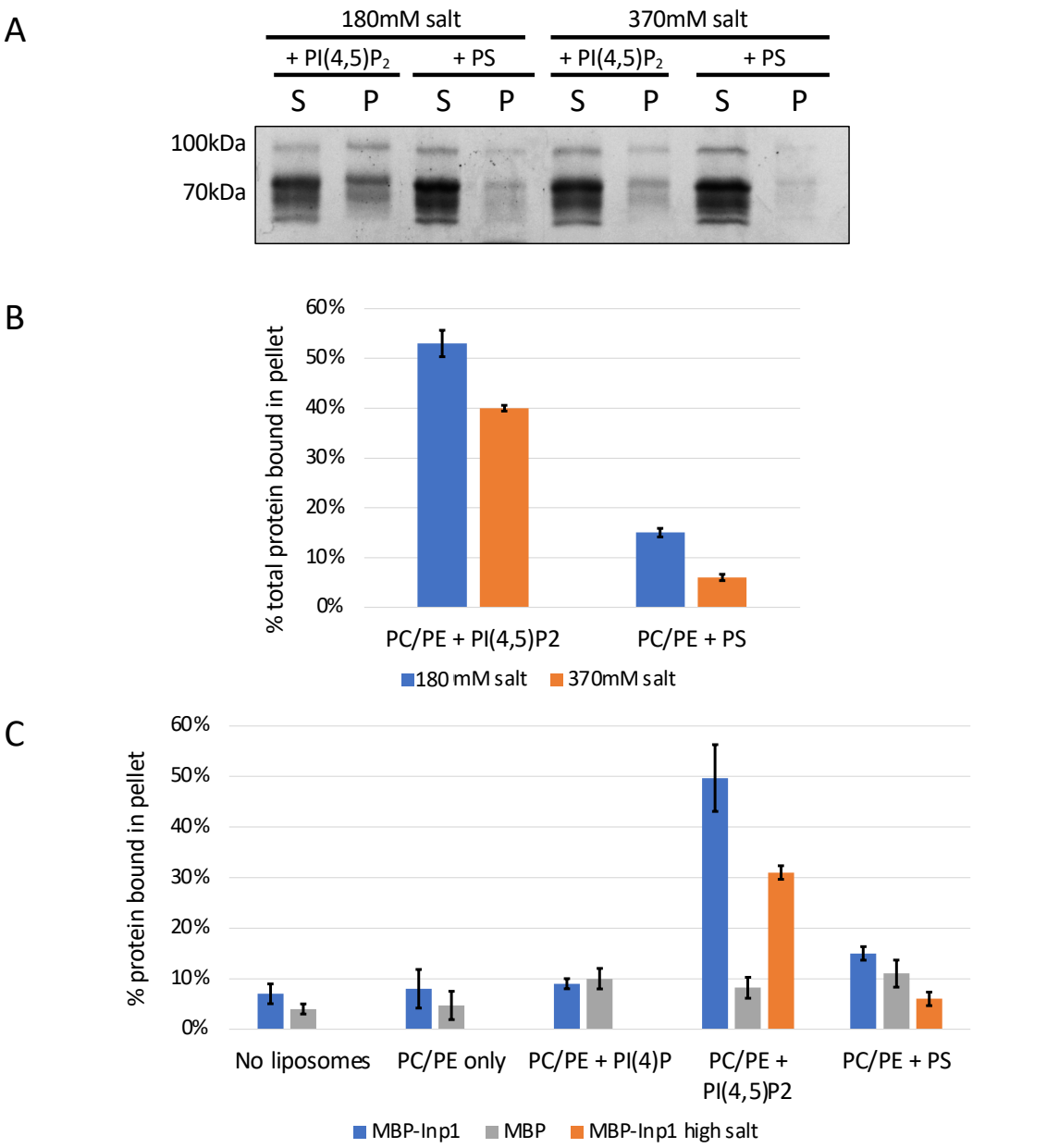

Figure 4.9 – MBP-Inp1 co-sediments with PC/PE liposomes supplemented with PI(4,5)P_2 even in high salt conditions. (A) Purified MBP-Inp1 was incubated with liposomes made up of PC/PE +/- 22% PI(4,5)P_2 or PS in the presence of either 180mM salt (20mM KCl + 160mM NaCl) or 370mM salt (20mM KCl + 350mM NaCl) and subjected to ultra-centrifugation. Total protein input, supernatant (S) and pellet (P) fractions were analysed by SDS-PAGE and Coomassie staining. (B, C) The percentage of protein present in each pellet was quantified, each supernatant + pellet band were combined and considered to represent 100% of the protein used in the experiment. Where there are multiple breakdown bands for MBP-Inp1, the top band representing full length MBP-Inp1 was used (as indicated in Figures 4.7 and 4.8). The percentage of protein in each pellet under the different NaCl conditions is shown. High salt = 370mM. Liposome binding assays were all performed in at least 3 independent experiments, error bars represent SEM.

4.3.3 The N-terminal part of Inp1 binds to PI(4,5)P_2

As seen in this study and as observed previously in independent studies, samples of purified MBP-Inp1 or GST-Inp1 contain truncated fragments (Munck et al., 2009; Knoblach et al., 2013). The presence of truncated fragments was informative in the co-sedimentation assays as some truncations were able to bind to liposomes (See black arrow in Fig. 4.7). As the MBP-fusion proteins were N-terminally tagged and since the molecular weight of MBP is 42.5kDa, it could be deduced that the N-terminal domain of Inp1 is able to bind to lipids. To test this further, N- and C-terminal truncations of Inp1 were expressed in *E. coli* and subsequently assayed for their ability to interact with PI(4,5)P_2 (Fig. 4.10, 4.11).

The N-terminal domain MBP-Inp1 1-280 binds PI(4,5)P_2 liposomes in contrast to the C-terminal domain MBP-Inp1 281-420. This confirms that the N-terminal part of Inp1 has a role in lipid binding. As Inp1 1-100-GFP was shown to localise to the plasma membrane (Section 4.3.1), MBP-Inp1 1-100 was then assayed for its ability to bind to PI(4,5)P_2 and also co-sedimented with PI(4,5)P_2 supplemented liposomes. It can be concluded that Inp1 is a lipid binding protein which binds preferentially to PI(4,5)P_2 but not PI(4)P or PS phospholipids. Additionally, the N-terminal 100 amino acids of Inp1 are sufficient for binding to PI(4,5)P_2 supplemented liposomes *in vitro*.

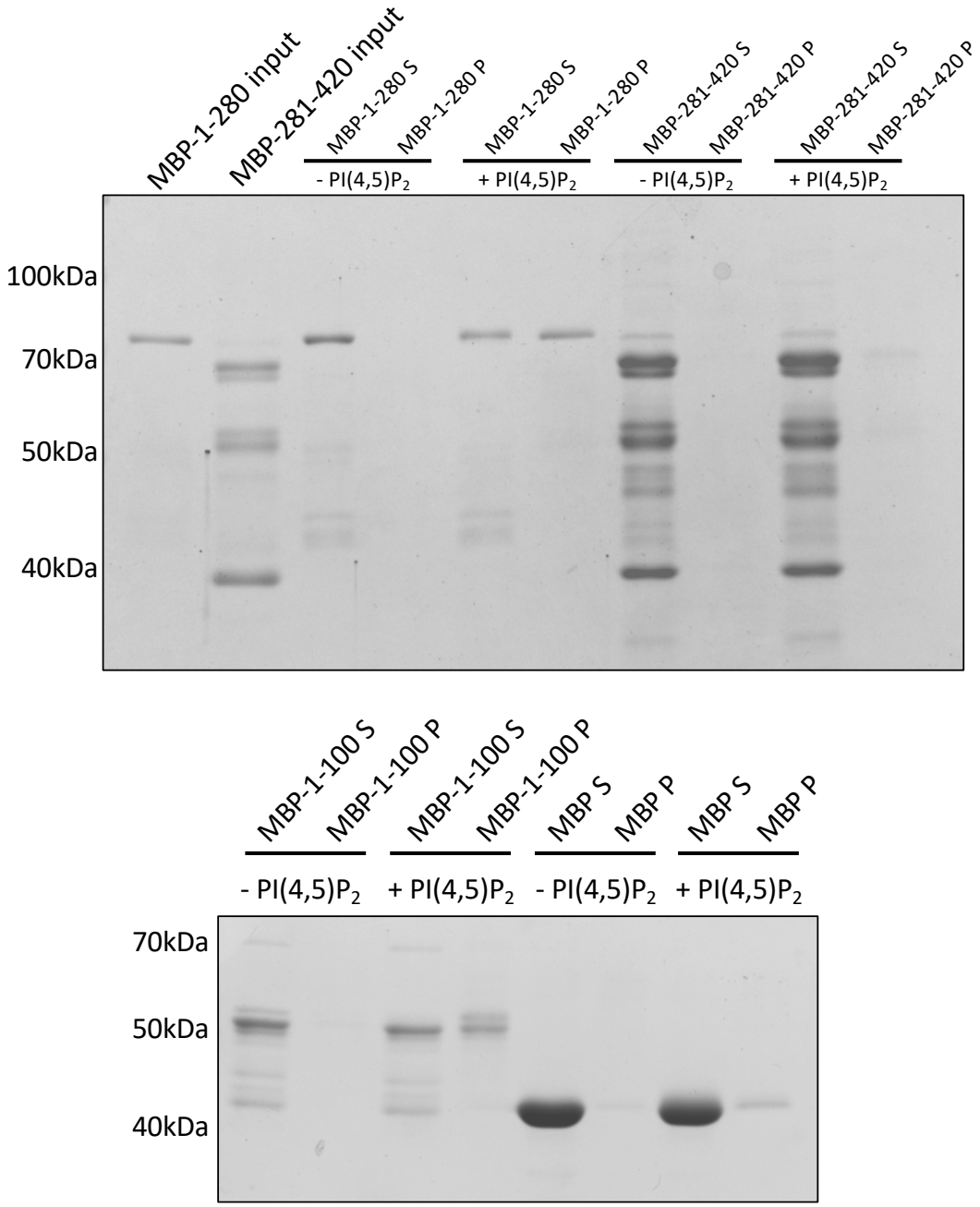

Figure 4.10 – The N-terminal truncations of MBP-Inp1 1-280 and 1-100 bind to PI(4,5)P_2 liposomes but MBP-Inp1 281-420 does not. Purified truncations of MBP-Inp1 1-280 and 281-420 (upper gel) and MBP-Inp1 1-100 (lower gel) were incubated with liposomes made up of PC, PE +/- PI(4,5)P_2 and subjected to ultracentrifugation. Supernatant (S) and pellet (P) fractions were then analysed by SDS-PAGE and Coomassie staining.

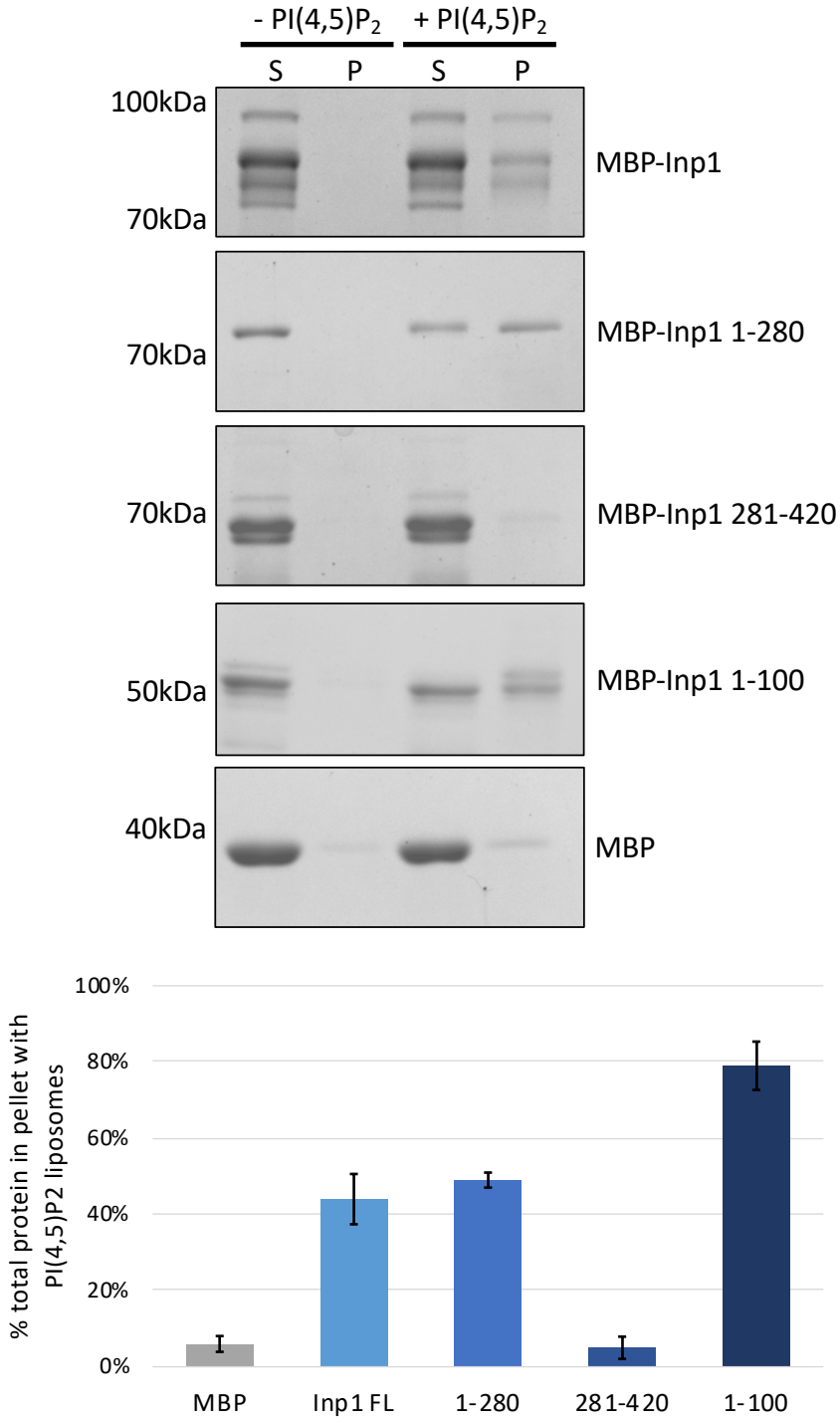

Figure 4.11 – Inp1 is a lipid binding protein, able to bind PI(4,5)P_2 via its N-terminal domain. Purified truncations of MBP-Inp1 (FL), 1-280, 281-420, 1-100 and MBP only were incubated with liposomes made up of PC, PE +/- PI(4,5)P_2 and subjected to ultracentrifugation. Supernatant (S) and pellet (P) fractions were then analysed by SDS-PAGE and Coomassie staining. The percentage of protein present in each pellet was quantified, each supernatant + pellet band were combined and considered to represent 100% of the protein used in the experiment. Where there are multiple breakdown bands for MBP-Inp1, the top band representing full length MBP-Inp1 was used (as indicated in Figures 4.7 and 4.8). For MBP-Inp1 1-100, the top band representing full length MBP-Inp1 1-100 was used. The percentage of protein in each pellet in the presence of various liposomes is shown. Liposome binding assays were all performed in at least 3 independent experiments, error bars represent SEM.

4.3.4 Reduction in cellular PI(4,5)P_2 levels results in a reduction of Inp1 1-100 localisation to the plasma membrane

The data presented in this chapter indicates that the N-terminal 100 amino acids of Inp1 localise to the plasma membrane *in vivo* and are capable of binding *in vitro* to liposomes containing PI(4,5)P_2. PI(4,5)P_2 is predominantly localised to and synthesised at the inner leaflet of the yeast plasma membrane (Yu et al., 2004; Vernay et al., 2012) and so the following experiment was carried out in order to determine how cellular PI(4,5)P_2 levels would affect the plasma membrane localisation of Inp1 1-100-GFP.

Sac1 is a phosphatidylinositol phosphate phosphatase, required for hydrolysis of PI(4)P. In *Δsac1* cells, PI(4)P accumulates to levels 20-fold higher than normal and PI(4,5)P_2 levels decrease by 75-80% (Hughes et al., 2000; Foti et al., 2001). Previously, it has been shown that other PI(4,5)P_2 binding GFP-fusion proteins are less plasma membrane localised in *Δsac1* cells (Yu et al., 2004). Likewise, when Inp1 1-100-GFP was expressed in *Δsac1* cells, a visible reduction was observed in its plasma membrane localisation (Fig. 4.12). Line scans were taken across the plasma membrane which plotted relative fluorescent intensity versus distance. For WT cells, the line scans showed defined peaks of plasma membrane enrichment, but these peaks were not observed in *Δsac1* cells. This confirmed the loss of Inp1 1-100-GFP enrichment at the plasma membrane in *Δsac1* cells compared to WT cells and strongly supports the idea that a reduction in cellular PI(4,5)P_2 results in a loss of localisation of Inp1 1-100-GFP to the plasma membrane.

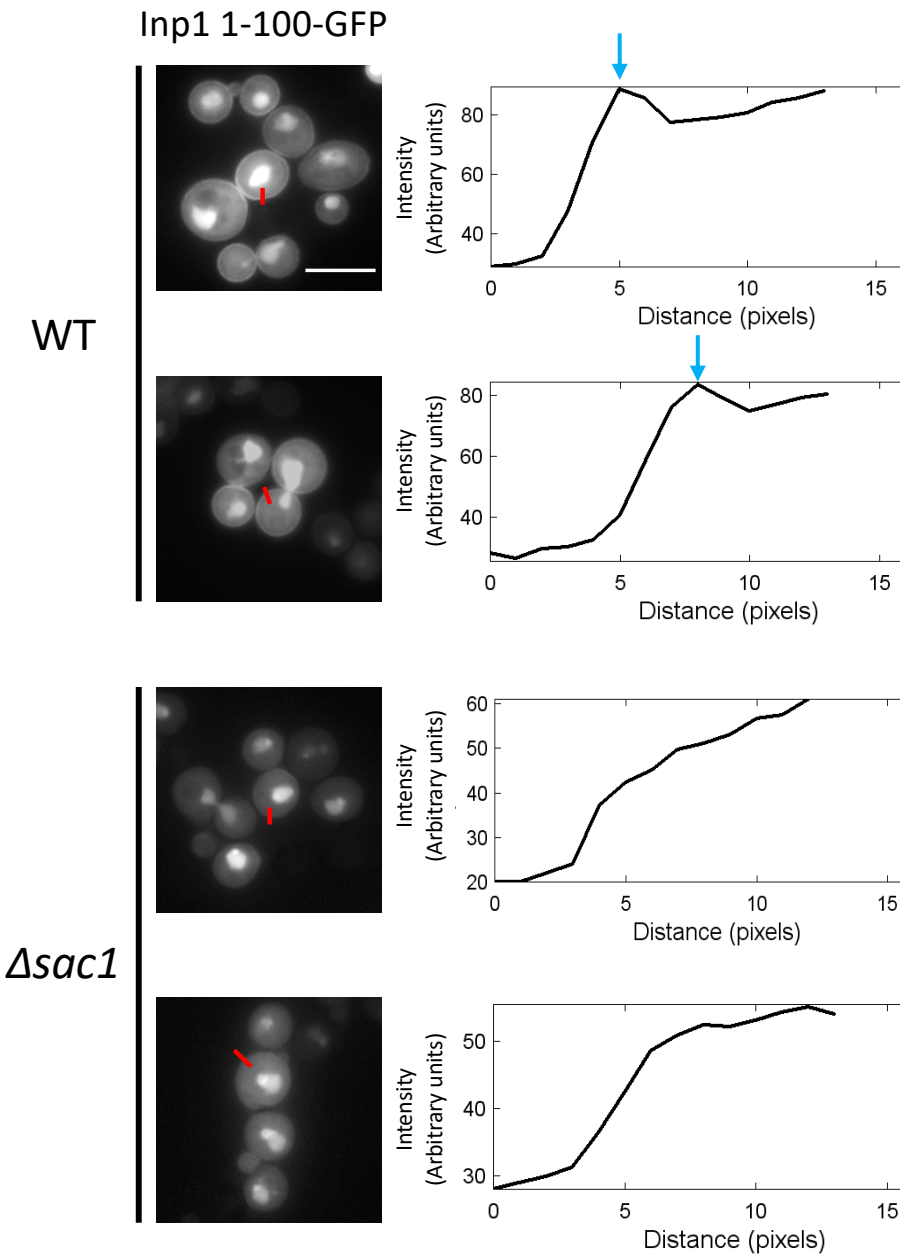

Figure 4.12 – Inp1 1-100-GFP localisation to the plasma membrane is reduced in *Δsac1* cells. An inducible truncation of Inp1 1-100-GFP was expressed in wild type and *Δsac1* cells and examined by fluorescence microscopy. The graphs show relative fluorescence intensities of Inp1 1-100-GFP across the plasma membrane. Red lines indicate where the measurements were taken from. Single focal planes are shown. Defined peaks corresponding to enrichment at the plasma membrane were observed in WT cells (blue arrows) but were not observed in *Δsac1* cells. Multiple images from the same experiment are shown. Bar, 5 µm.

4.4 Discussion

The existing model of peroxisome retention portrays Inp1 as a modular protein which anchors peroxisomes to the cell periphery via an N- and C-terminal domain (Knoblach et al., 2013). In Chapter 3, it was shown that Inp1 interacts directly with peroxisomal Pex3 via a conserved motif in its C-terminal domain. In Chapter 4, the role of the N-terminal domain of Inp1 in peroxisome retention has been characterised. By artificially attaching truncations of Inp1 to the peroxisomal membrane via Pex15, peroxisome retention could be studied independently of Inp1's interaction with peroxisomal Pex3. Through these assays, the N-terminal 100 amino acids of Inp1 were identified as being necessary and capable of peroxisome retention at the cell periphery. As such, it has been shown that Inp1 interacts with the cell periphery via its N-terminal domain and this can be genetically separated from its direct interaction with peroxisomal Pex3 via its C-terminal domain. In that respect, the current model portraying Inp1 as a modular protein seems to be correct. However, the data acquired in this study does not support the idea that the N-terminal domain of Inp1 interacts with Pex3 and identifies the N-terminus of Inp1 as a lipid binding domain that binds to $PI(4,5)P_2$ and associates with the plasma membrane.

When expressed as a GFP-fusion protein in wild type cells, the N-terminal 100 amino acids of Inp1 exhibit plasma membrane localisation (Fig. 4.4). Interestingly, they also show nuclear localisation, an observation which has been reported for other proteins upon expression of their plasma membrane binding domains and as yet is not understood (Yu et al., 2004). This additional observation supports the idea that Inp1 1-100-GFP has the capability to bind to the plasma membrane as not only does it localise there but the pattern of localisation closely resembles that of other, well characterised plasma membrane binding domains.

The hypothesis that the N-terminal 100 amino acids of Inp1 are capable of binding to the plasma membrane was supported by the *in vitro* liposome co-sedimentation assays carried out in this chapter. These showed that Inp1 is a lipid binding protein which binds to liposomes containing $PI(4,5)P_2$, a phosphoinositide which is primarily synthesised and located at the inner leaflet of the yeast plasma membrane (Yu et al., 2004; Vernay et al., 2012). A low amount of MBP-Inp1 did appear to co-sediment with liposomes supplemented with PS (Fig. 4.8, 4.9). However, as PS is mainly concentrated and highly abundant in the plasma membrane, this would not affect the final conclusion that Inp1 binds to plasma membrane lipids. Importantly, this weak interaction with PS was salt sensitive, implying that the interaction is based on non-specific, electrostatic charges. The co-sedimentation assays also showed that MBP-Inp1 interacts with $PI(4,5)P_2$ even under high salt conditions, albeit less efficiently than at 180mM salt (Fig. 4.9). The slight reduction in MBP-Inp1 co-sedimentation suggests again that electrostatic interactions do contribute in the binding of Inp1 to the liposomes, but that there is some specificity in Inp1 binding to PI(4,5)P2 containing liposomes and the interaction is not solely based on charge.

The *in vitro* lipid co-sedimentation assays also showed that it is the N-terminal domain of Inp1 that is able to bind to lipids and indeed that amino acids 1-100 possess the ability to bind to $PI(4,5)P_2$ (Fig. 4.10, 4.11). The *in vitro* work was then supported with *in vivo* data as a reduction of cellular $PI(4,5)P_2$ in *Δsac1* cells was shown to result in a reduction of Inp1 1-100-GFP localisation to the plasma membrane (Fig. 4.12). Additionally, in *Δsac1* cells, PI(4)P levels are

increased 10-20 fold with PI(4)P accumulating at the ER and vacuole (Tahirovic et al., 2005). Nonetheless, Inp1 1-100-GFP was not seen accumulating at ER or vacuolar membranes which gives additional support to the observations made in the liposome binding assays MBP-Inp1 binds to PI(4,5)P_2 and not PI(4)P. Taken together, the work presented in this chapter provides convincing evidence that the N-terminus of Inp1 is a lipid binding protein which binds to the plasma membrane.

Attempts were made during this study to further pinpoint regions in the first 100 amino acids required for peroxisomal tethering. It was found that when the first 52 amino acids of Inp1 are deleted in the endogenously expressed Inp1-GFP (Inp1 52-420-GFP), peroxisome retention is restored in *Δinp1* cells. As 100-420-GFP does not restore peroxisome retention in *Δinp1* cells (Fig. 4.3) this points to the fact that retention relies on amino acids in the 52-100 region. However, when experiments were attempted with these smaller tethers, the proteins were found to be unstable. Due to this, it was most appropriate to use amino acids 1-100 as a minimal tether as this truncation was stable and behaved as such that confident observations and conclusions could be made.

It is perhaps too simplistic to simply try and shave off more and more amino acids from the primary sequence of Inp1 in order to find a minimal tether. The tethering ability of the N-terminal domain of Inp1 most likely relies on a secondary or tertiary folded structure such as a PH domain. An archetypal PH-domain is a structural module which interacts with phosphoinositides and the majority of PH-like domains are also protein binding (Yu et al., 2004). During the course of this study, an additional, complementary study was also accepted for publication which investigates the functional role of Inp1 in *H. polymorpha* (Krikken et al., 2020). Additionally, Krikken *et al.* analyse the sequence of a middle domain (100-216) of *Hp*Inp1 and predict that it may fold as a divergent Ran-binding domain from the PH-like domain superfamily (Krikken et al., 2020). This sequence roughly aligns with *Sc*Inp1 amino acids 80-260 and so by using the truncations 1-100 and 101-280, I may have missed the presence of an orthologous domain in *Sc*Inp1. This is something which is further discussed in Section 6.1.

To summarise the results obtained in Chapter 4, Inp1 appears to be a modular protein with an N-terminal lipid binding domain and a C-terminal Pex3 binding region. This illustrates that Inp1 has the capacity to act as a molecular tether between the plasma and peroxisomal membranes by directly binding to PI(4,5)P_2 at the plasma membrane and to Pex3 on the peroxisomal membrane. In order to be considered a contact site tether, a protein must adhere to a pre-determined set of criteria (Eisenberg-Bord et al., 2016). The following Chapter serves to evidence how Inp1 qualifies as a plasma membrane-peroxisome tether.

Chapter 5 – Inp1 meets the criteria to be classed as a plasma membrane-peroxisome tether

5.1 Introduction

In recent years, it has become increasingly obvious that organelles make physical contact with each other at membrane contact sites (MCS). Membrane contact sites can be defined as cellular domains where membranes from opposing organelles are tethered in close proximity by protein or lipid interactions, resulting in the function of one or both organelles being affected (Prinz, 2014; Shai et al., 2018; Prinz et al., 2020). Research of MCS's is increasing rapidly and every organelle has now been shown to have at least one functional MCS with another organelle. Most organelles are now known to have multiple MCS's and these encompass a range of functions such as exchange of cellular materials, arrangement of the cell, organelle inheritance and fission (Valm et al., 2017; Shai et al., 2018). The characterisation of MCS's has also led to the identification of proteins that tether and regulate contact sites. However, as more contact sites are identified, there remains a range of MCS tethering factors which are as yet unknown.

As has been postulated for other organelles, yeast peroxisomes have been found to interact with many cellular structures including the plasma membrane, ER, vacuole, mitochondria and lipid bodies (Eisenberg-Bord et al., 2016; Knoblach & Rachubinski, 2019; Wu et al., 2019). Although components of some of these interorganellar peroxisomal contact sites have been identified, others are still completely uncharacterised (Shai et al., 2018). Inp1 and Pex3 are implicated as peroxisome-ER contact site proteins, although a more recent study suggests that additional components are required for peroxisome tethering to the cell cortex (Knoblach et al., 2013; Knoblach & Rachubinski, 2019). Additionally, the data obtained during this study, as presented in Chapters 3 and 4, are suggestive of an alternative model of Inp1 function involving the plasma membrane rather than the cortical ER. Although contact sites between peroxisomes and the plasma membrane have been observed, (Shai et al., 2018), any factors or tether proteins required to mediate these membrane contact sites have not yet been identified.

Contact sites between the plasma membrane and other organelles such as the ER have been more widely studied and in yeast cells, the plasma membrane and cortical ER (cER) are in very close proximity with up to 45% of the plasma membrane in contact with the cER network (Pichler et al., 2001; West et al., 2011). These areas of close contact between the two membranes create distinct, sub-cellular microenvironments and have been shown to have membrane contact sites with a third organelle, the mitochondria (Lackner et al., 2013). Cortical mitochondrial anchorage occurs via the mitochondria ER cortex anchor (MECA), a multi-subunit protein complex (Lackner et al., 2013). The core component of MECA is Num1, a cortical associated protein which binds to the mitochondrial outer membrane and the plasma membrane via two distinct lipid binding domains (Lackner et al., 2013). Although MECA is reported to be a tether between three organelle membranes, the molecular mechanisms for MECA association with the ER remain poorly understood.

The plasma membrane has been further implicated in mitochondrial tethering via site-specific mitochondrial anchorage at the mother cell tip via Mfb1 (Manford et al., 2012; Pernice et al., 2016). As the plasma membrane has been shown to be required for cortical retention and correct spatial distribution of mitochondria, this raises the possibility that organelle retention via the plasma membrane could also occur in the cases of other cortically associated organelles such as peroxisomes.

The data presented in Chapters 3 and 4 characterises Inp1 as a modular protein with an N-terminal lipid binding domain and a C-terminal peroxisomal Pex3 binding region. The N-terminal 100 amino acids of Inp1 localise to the plasma membrane, bind to liposomes containing the plasma membrane localised phosphoinositide $PI(4,5)P_2$ and can act as a minimal tether which, when artificially attached to peroxisomes, restores retention of peroxisomes to the cell periphery in *Δinp1* cells. As research into membrane contact sites grows, the research community has proposed a 'gold standard' of 3 criteria which an MCS tether protein must fulfil. Chapter 5 serves to explore whether Inp1 adheres to these pre-requisites and therefore whether Inp1 can be formally characterised as a plasma membrane-peroxisome contact site tether (Eisenberg-Bord et al., 2016).

5.2 Inp1 is in the correct sub-cellular location to be a PM-PER tether

5.2.1 Peroxisome retention at the mother cell periphery is not disrupted in cortical ER mutants.

The current model of peroxisome retention classifies Inp1 as a peroxisome-ER tether protein due to the apparent ability of Inp1 to simultaneously interact with both peroxisomal and cortical ER-associated Pex3 (Knoblach et al., 2013a). Though the role of the cortical ER (cER) in peroxisome retention has been reported, the role of the plasma membrane remains unexplored. In order to investigate the contribution of the cER to peroxisome retention, peroxisome distribution was analysed by expressing the peroxisomal matrix marker *Hc*Red-PTS1 in two mutants where the cER is disrupted. *Δrtn1/Δrtn2/Δyop1* cells do not form cortical ER tubules but instead produce ER sheets which leaves large parts of the plasma membrane free of ER (Voeltz et al., 2006). A second ER mutant, *Δscs2/Δscs22/Δist2/Δtcb1/Δtcb2/Δtcb3* was also studied. In this second strain, which will be referred to as (ΔER-PM tether), the proteins required for tethering the cortical ER to the plasma membrane are absent and so the cER is separated from the plasma membrane and accumulates in the cytoplasm, almost completely collapsed away from the cell cortex (Manford et al., 2012).

In both strains, the severe disruption of the cER does not appear to affect peroxisome partitioning with peroxisomes retained in mother cells as in wild type (Fig. 5.1). This implies that despite the absence of typical ER structures at the cell cortex, peroxisomes are still able to be retained at the cell periphery. Deletion of *INP1* in these strains results in a typical *Δinp1* phenotype with most peroxisomes present in the bud.

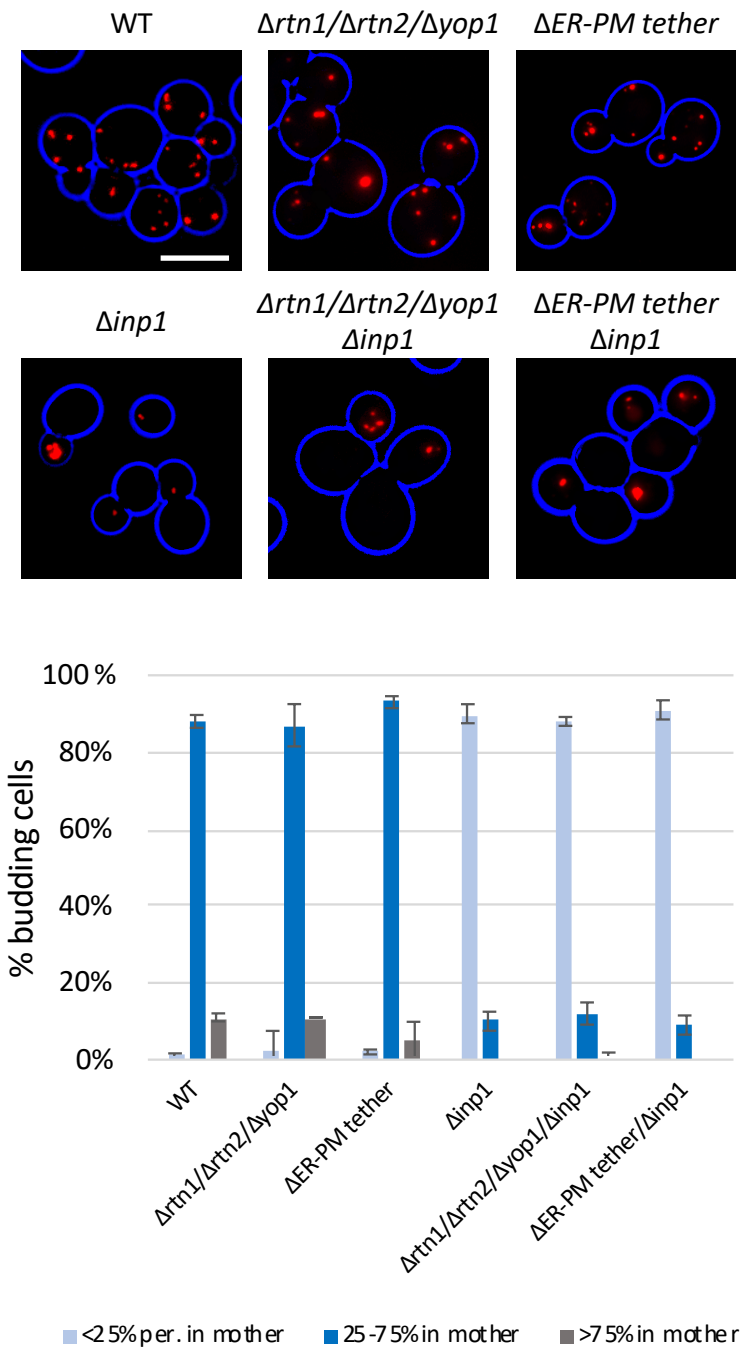

Figure 5.1 – Disruption of the cER does not affect peroxisome distribution. The peroxisomal matrix marker *Hc*Red-PTS1 was constitutively expressed in wild type (WT), *Δrtn1/Δrtn2/Δyop1*, *ΔER-PM tether*, *Δinp1*, *Δrtn1/Δrtn2/Δyop1/Δinp1* and *ΔER-PM tether/*Δinp1 cells. Cells were examined by epifluorescence microscopy. The peroxisome distribution between mother and daughter cells we analysed in the strains described. Each budding cell was scored for what percentage of its total cellular peroxisomes were present in the mother cell. Per. = peroxisomes. Over 100 budding cells were analysed for each strain. Three independent experiments were carried out. Error bars represent SEM. Bar, 5µm.

5.2.2 Peroxisomes are still present at the cell periphery in the absence of the cortical ER

In order to further visualise peroxisome localisation when the normal cellular distribution of the cortical ER is disrupted, the ER marker Sec63-mRFP, the plasma membrane marker GFP-Sso1 and the peroxisomal matrix marker blue fluorescent protein-PTS1 (BFP-PTS1) were co-expressed in *Δrtn1/Δrtn2/Δyop1* cells. As shown in Figure 5.1, peroxisomes in this mutant were normally distributed and present at the mother cell periphery. Analysis of these mutants found that peroxisomes were often seen at the exposed ends of ER sheets and 46% of budding cells contained at least one peroxisome at the cell periphery in areas devoid of ER (n=170) (Fig. 5.2).

In order to further visualise the spatial relationship between peroxisomes, the ER and the plasma membrane, line-scan analyses of the images were used to obtain plots of the relative fluorescent intensities *versus* distance. These confirmed that peroxisomes were present even in regions with little to no Sec63-mRFP signal and showed an overlap in the signal of peroxisomal foci and the plasma membrane, indicative of PM-PER contact sites.

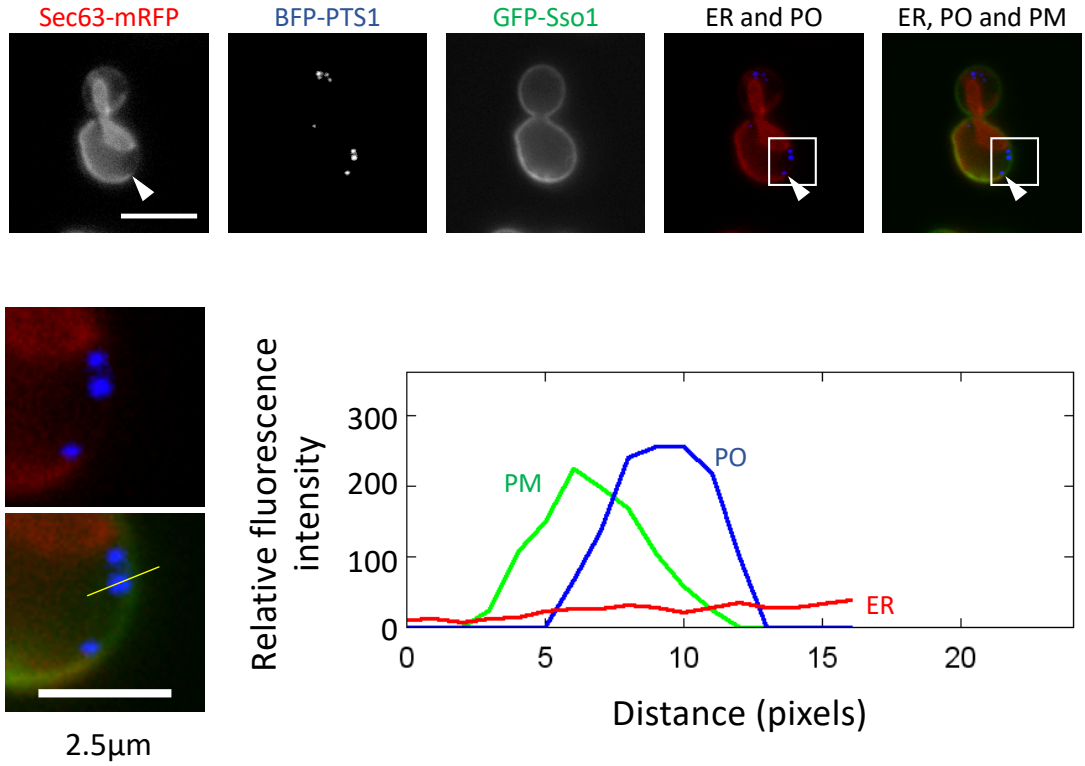

Figure 5.2 – Peroxisomes are present at the cell periphery in *Δrtn1/Δrtn2/Δyop1* cells, even in the absence of cortical ER. Sec63-mRFP, BFP-PTS1 and GFP-Sso1 were co-expressed in *Δrtn1/Δrtn2/Δyop1* cells and imaged using epifluorescence microscopy. Single focal planes are shown from the centre of the Z-stack. The white arrow highlights a peroxisome present at the end of an ER sheet. The boxed areas are magnified. The graph shows relative fluorescence intensities of the markers for the ER (red), the peroxisomal matrix (blue) and the plasma membrane (green) along a line drawn through the centre of the peroxisomal focus indicated by the yellow line on the magnification panel. Bar, 5µm except where indicated as 2.5µm.

Peroxisome localisation at the periphery of cER mutants was further visualised in the *ΔER-PM tether* strain by co-expressing the ER marker Sec63-GFP with *Hc*Red-PTS1 (Fig. 5.3). Despite a lack of cER, around half of cells (50.3%, n=150) appeared to contain at least 1 peroxisome at the cell periphery in areas devoid of detectable ER signal. When *INP1* was also deleted from the *ΔER-PM tether* strain, peroxisomes were no longer localised at the periphery but were still observed in close proximity to internal cellular ER structures in buds. It is important to acknowledge that the Axiovert microscopy images obtained during this study may have limitations and so it cannot be stated with 100% confidence that when a peroxisome appears in an area devoid of ER, that there are no traces of ER structure present. However, the images obtained do suggest that peroxisomes are able to localise to the periphery even in the absence of typical cortical ER structures and illustrate that contact between peroxisomes and the ER is able to occur even in the absence of Inp1.

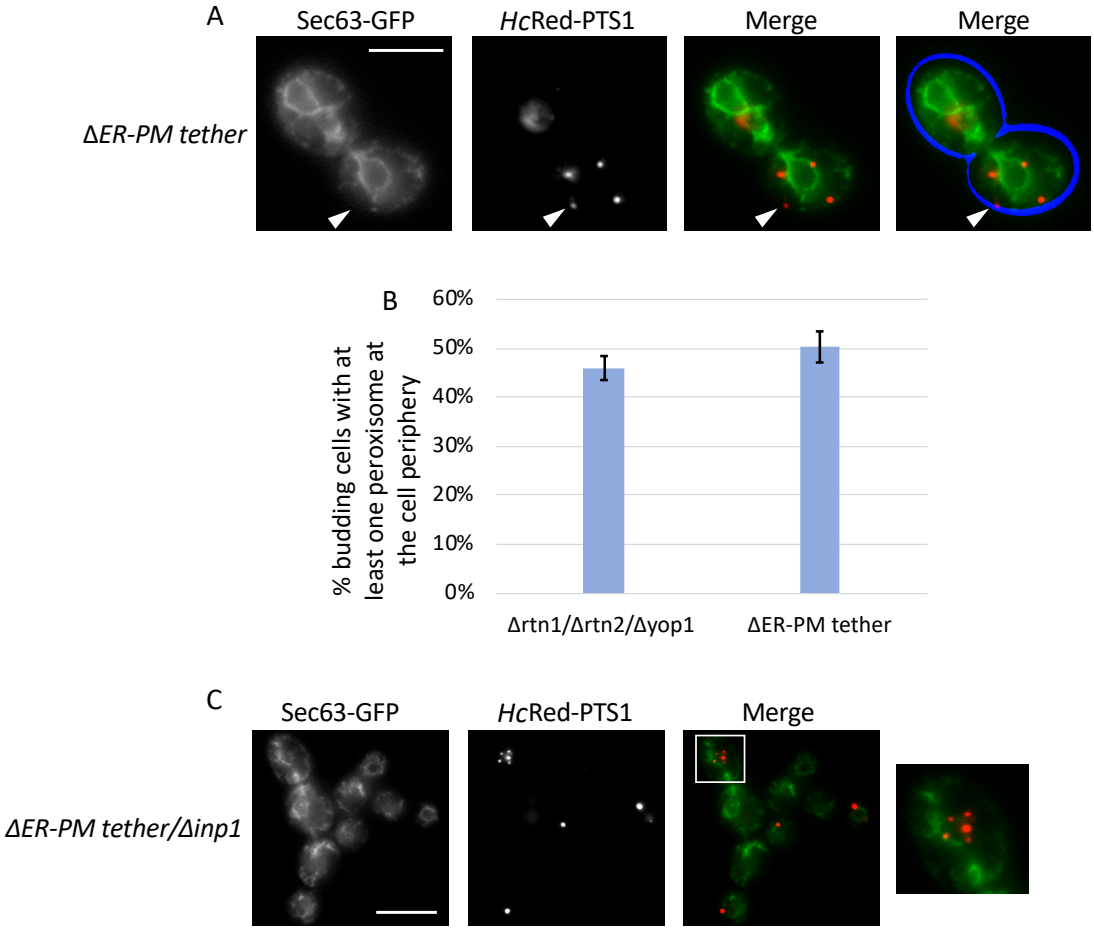

Figure 5.3 – Peroxisomes are present at the cell periphery in *ΔER-PM tether* cells, even in the absence of cortical ER. A) Sec63-GFP and *Hc*Red-PTS1 were co-expressed in *ΔER-PM tether* cells and examined by fluorescence microscopy. The white arrow highlights an example of a peroxisome which is at the cell periphery in the absence of visible ER. A single focal plane is shown from the centre of the z-stack. Border of cell is outlined in blue in the second merge image. B) Budding *Δrtn1/Δrtn2/Δyop1* or *ΔER-PM tether* cells were scored for the presence of at least one peroxisome present at the cell periphery but not associated with visible ER. Over 100 budding cells were quantified for each strain. Three independent experiments were carried out. Error bars represent SEM. C) Sec63-GFP and *Hc*Red-PTS1 were co-expressed in *ΔER-PM tether/Δinp1* cells and examined by fluorescence microscopy. The boxed area is magnified and exemplifies peroxisomes associated with a central ER structure in the absence of *INP1*. A single focal plane is shown from the centre of the z-stack. Bars, 5µm.

5.2.3 Inp1 is present in close proximity to the plasma membrane and peroxisomes

The first requirement that a protein must meet in order to be considered a *bona fide* membrane contact site tether is that it must reside in a defined location at the contact site (Eisenberg-Bord et al., 2016). In order to begin elucidating the potential for Inp1 to be a plasma membrane-peroxisome tether protein, the sub-cellular localisation of Inp1 was explored in relation to peroxisomes, the plasma membrane and the ER. First, Inp1-mCherry, Sec63-GFP and BFP-PTS1 were co-expressed in *Δrtn1/Δrtn2/Δyop1/Δinp1* cells (Fig. 5.4). Where peripheral peroxisomes could be seen localised to the exposed ends of ER sheets, (Fig. 5.4A), or in areas free of ER, Inp1 foci was always observed to be partially co-localised with peroxisomal matrix foci on the side of peroxisomes proximal to the cell periphery. Peroxisomes were often seen 'sandwiched' between the ER and the cell periphery and in these instances, peroxisomal matrix foci were consistently located between Inp1 foci and the ER. Inp1 was again proximal to the cell periphery and distal from ER sheets. Line-scan analyses were carried out which confirmed that the profiles of Inp1-mCherry were slightly juxtaposed to those of peroxisomal matrix foci but the peak intensities of Inp1-mCherry and the ER were spatially resolved indicating no physical contact (Fig. 5.4C).

Where Inp1-mCherry was co-expressed with BFP-PTS1 and the plasma membrane marker GFP-Sso1, Inp1-mCherry again partially overlapped with peroxisomal matrix foci, proximal to the cell periphery and co-localised with GFP-Sso1 at the plasma membrane (Fig. 5.5). Taken together, these observations show that Inp1 foci are present in locations closely apposed to the peroxisomal and plasma membranes but can be spatially resolved from the ER and are even seen at the cell periphery in areas devoid of cortical ER. As these images were obtained using an Axiovert microscope, it is likely that the fluorescent signals in the images appear bigger than the protein that they represent. As such, it is likely that where fluorescent signals of proteins appear to be spatially distinct, the proteins are perhaps even further apart in reality. It can therefore be concluded that Inp1 is present in the correct sub-cellular locations to be a PM-PER tether.

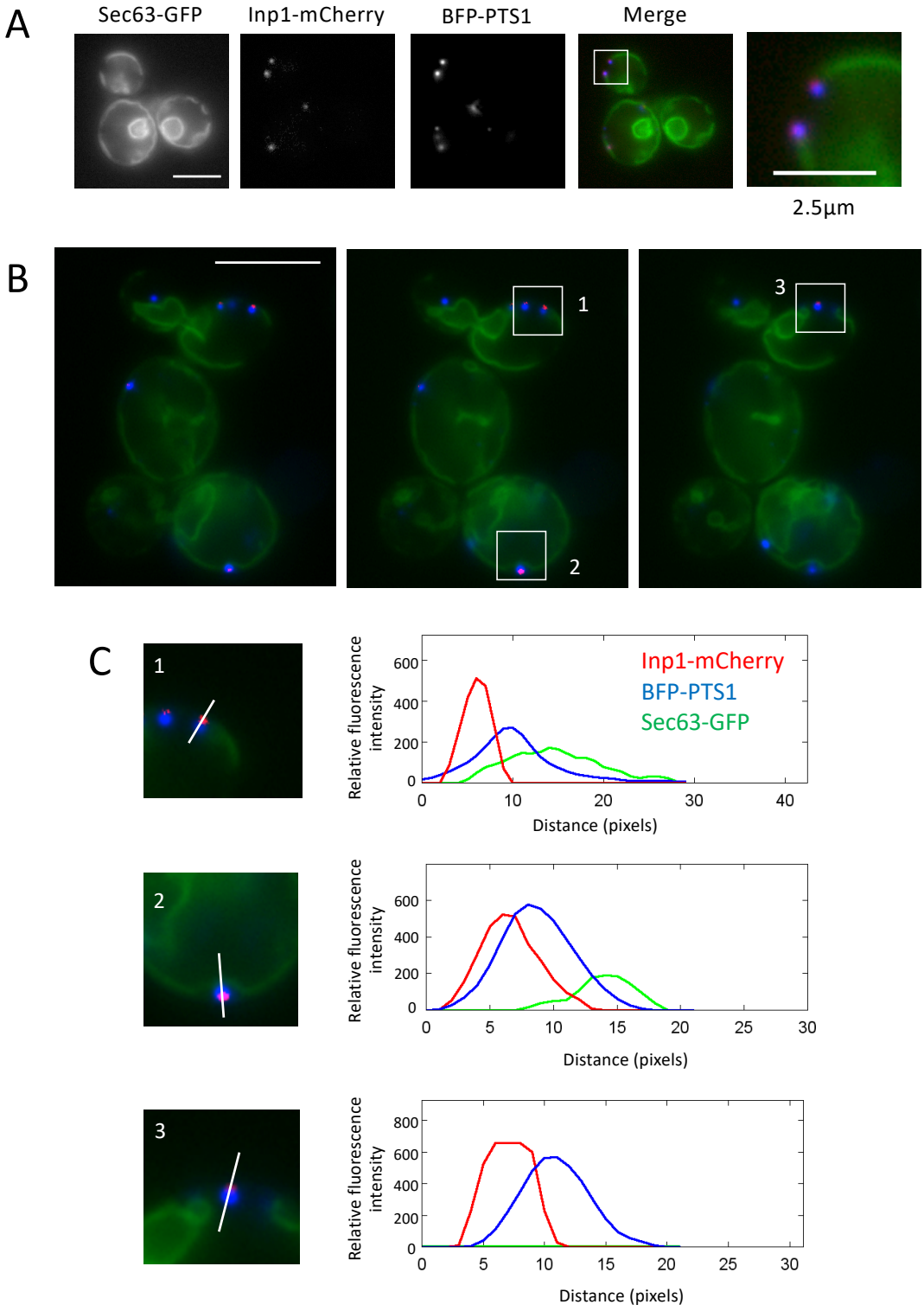

Figure 5.4 – Inp1 foci can be seen proximal to the cell periphery but distal from ER sheets. (A, B) Sec63-GFP, Inp1-mCherry and BFP-PTS1 were co-expressed in *Δrtn1/Δrtn2/Δyop1/Δinp1* cells and imaged using epifluorescence microscopy. In A, a single focal plane is shown. In B, three single, consecutive Z-stack layers of the same image are shown. The boxed areas are numbered and magnified in C. (C) The graphs show relative fluorescence intensities of the ER (green), the peroxisomal matrix (blue) and Inp1 (red) along a line drawn through the centre of peroxisomal foci, indicated by the white lines on the magnified images. Bars, 5µm except where indicated as 2.5µm.

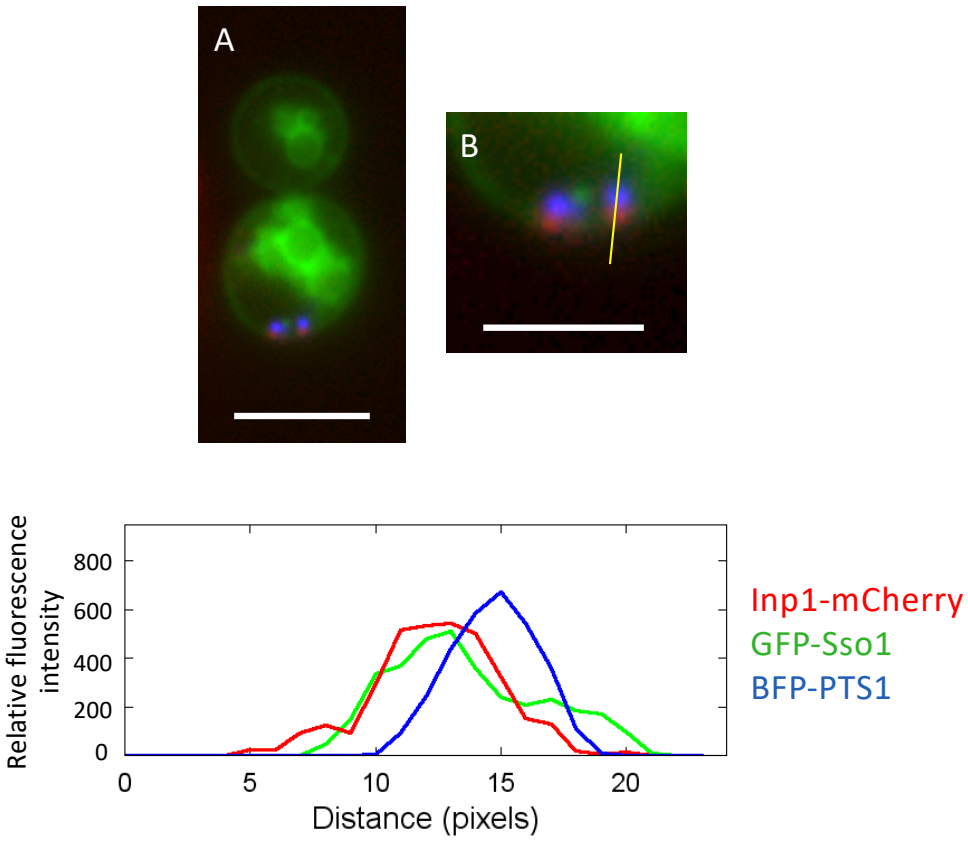

Figure 5.5 – Inp1 foci are seen juxtaposed to peroxisomal matrix markers but co-localise with the plasma membrane. GFP-Sso1, Inp1-mCherry and BFP-PTS1 were co-expressed in *Δrtn1/Δrtn2/Δyop1/Δinp1* cells and imaged using epifluorescence microscopy. A single focal plane is shown. Image B is a magnification of Image A. The graph shows relative fluorescence intensities of the plasma membrane (green), the peroxisomal matrix (blue) and Inp1 (red) along a line drawn (yellow) through the centre of the peroxisomal foci. Bars, 5 µm (A) and 2.5 µm (B).

5.3 Inp1 has the functional capacity to be considered a PM-PER tether

5.3.1 The PH domain of Num1 can act as an artificial tether to restore peroxisome retention

The second minimal requirement that a protein must fulfil in order to be considered a tether is that it must have functional activity and therefore exert a tethering force. The molecular function of a tether protein is to physically hold membranes of distinct cellular components at close distance. As such, depletion of a tether protein should result in loss of physical proximity of the two membranes. In the field of contact site research, it is regarded that the functional capacity of a protein as a contact site tether can be assayed by expression of an artificial tether. Expression of synthetic components designed to tether the respective membranes should, in theory, compensate for loss of a tether protein (Eisenberg-Bord et al., 2016).

One such example of a synthetic tether being used to establish an endogenous tethering role is in previously published work regarding Num1, a mitochondrial-plasma membrane tether (Ping et al., 2016). Num1 binds to the mitochondrial outer membrane and the plasma membrane via two distinct and characterised lipid-binding domains. In *Δnum1* cells mitochondrial tethering is defective and this phenotype can be compensated for by expression of a truncated, artificial tether comprised just of the two, lipid membrane-binding domains of Num1, spaced by a GFP moiety (Lackner et al., 2013; Ping et al., 2016).

A similar experiment was carried out as part of this study in Figure 4.2, where a minimal region of Inp1, comprised of the N-terminal 100 amino acids, was artificially attached to the peroxisomal membrane via Pex15. This minimal tether was found to be sufficient to restore peroxisome retention in *Δinp1* cells (Fig. 4.2). The functional capacity of Inp1 to be a PM-PER tether was further tested by investigating whether the *Δinp1* phenotype could be rescued by a completely artificial tether. For this, the plasma membrane-binding PH domain of Num1 (amino acids 2563-2692) was used, which has been shown to be a highly selective $PI(4,5)P_2$ binding domain (Yu et al., 2004; Tang et al., 2009). The Num1 PH domain was fused to Pex15 in the same way as the Inp1 1-100 minimal tether, with a GFP spacer moiety, and expressed under control of the *INP1* promoter in *Δinp1* cells (Fig. 5.6). This completely artificial tether was sufficient to restore peroxisome retention to the mother cell cortex in *Δinp1* cells, closely resembling the Inp1 1-100-GFP-Pex15 minimal tether. As stated above, the loss of a tether should be rescued by expression of synthetic components that are able to tether the respective membranes. As peroxisome localisation to the cell periphery was restored through expression of a tether comprising a plasma membrane-binding domain and a peroxisomal membrane-associated domain, this strongly suggests that Inp1 has the functional capacity to be a PM-PER tether.

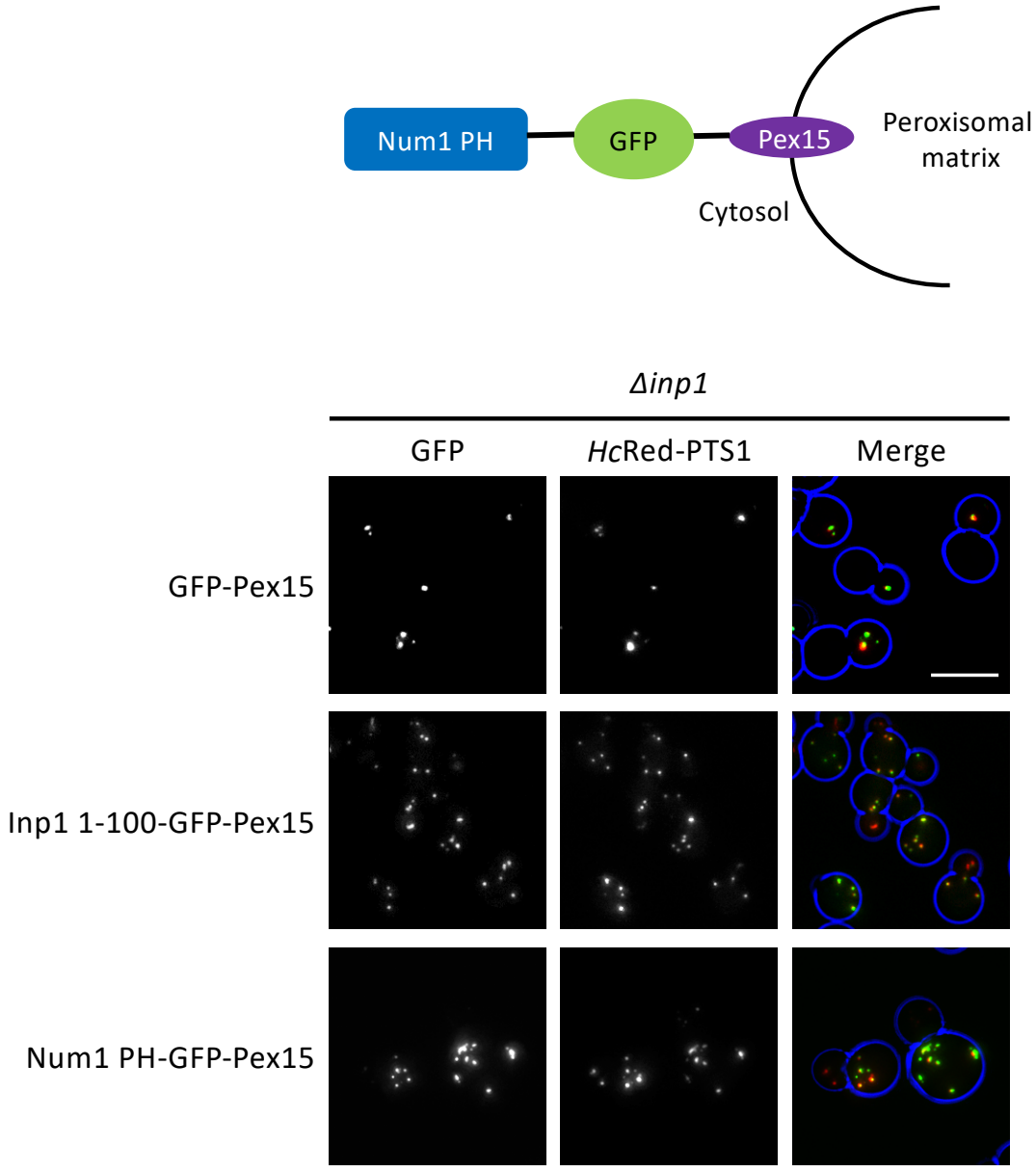

Figure 5.6 – The PH domain of Num1 can function as an artificial peroxisome tether and rescue peroxisome retention in *Δinp1* cells. The N-terminus of Inp1 (amino acids 1-100) or the PH domain of Num1 (amino acids 2563-2692) were fused to GFP-Pex15 and expressed under control of the *INP1* promoter in *Δinp1* cells with the constitutively expressed *Hc*Red-PTS1. Cells were examined by fluorescence microscopy. The diagram illustrates the predicted topology of the Num1-Pex15 fusion protein with the PH domain of Num1 exposed to the cytosol and anchored to the peroxisomal membrane by Pex15 with a GFP moiety acting as a spacer between the two proteins. Bar, 5 µm.

5.3.2 Overexpression of a minimal Inp1 tether results in an increase in PM-PER contact sites

Another method of assaying the functional ability of a tether protein is by measuring its effect on the extent of a contact site. Depletion of a tether protein may result in a loss of proximity between distinct membranes, but a complementary approach is to observe what happens when the tether is overexpressed. If overexpression of a tether protein results in an increase in the size or amount of contact sites between distinct membranes, this is a good indicator that the protein contributes to interorganellar tethering (Eisenberg-Bord et al., 2016).

In order to carry out this assay, a series of yeast strains were obtained from the laboratory of Maya Schuldiner (Weizmann Insitute of Science, Rehovet, Israel) which use a bimolecular fluorescence complementation assay to allow for visualisation of contact sites (Shai et al., 2018). Each strain contains split Venus reporters for peroxisomes and one other organelle (ER, mitochondria, plasma membrane or vacuoles). The perimeter of the peroxisomes and the other given organelle in each strain are each coated with half of a Venus fluorescence protein and at contact sites between the two organelles, the two halves of the Venus fluorescent protein interact and form a full fluorophore. This allows for the visualisation of the number or size of contact sites between organelles.

In order to measure its functional capacity, Inp1 could not simply be overexpressed in these strains as overexpression of Inp1 leads to a loss of peroxisomal structures (Fig. 3.8). As such, an alternative approach was taken and the minimal Inp1 peroxisomal tether, which has been established in this study, was overexpressed (Inp1 1-100-mRFP-Pex15). The minimal tether was first overexpressed in wild type cells which resulted in over-retention of peroxisomes in mother cells, as initial overexpression of wild type Inp1 does (Fig. S1B of Munck et al., 2009), but importantly overexpression of the minimal tether did not affect overall peroxisome number or peroxisome biogenesis (Fig. 5.7).

This minimal tether was then overexpressed in the series of split Venus reporter strains. The number of fluorescent puncta representing peroxisomal contact sites with ER, mitochondria and vacuoles were unaffected by this overexpression. On the other hand, the number of plasma membrane-peroxisome contact site reporter puncta in the cell population increased with overexpression of the minimal tether. Both the frequency of cells with PM-PER reporter signal increased as well as the number of puncta per cell (Fig. 5.8).

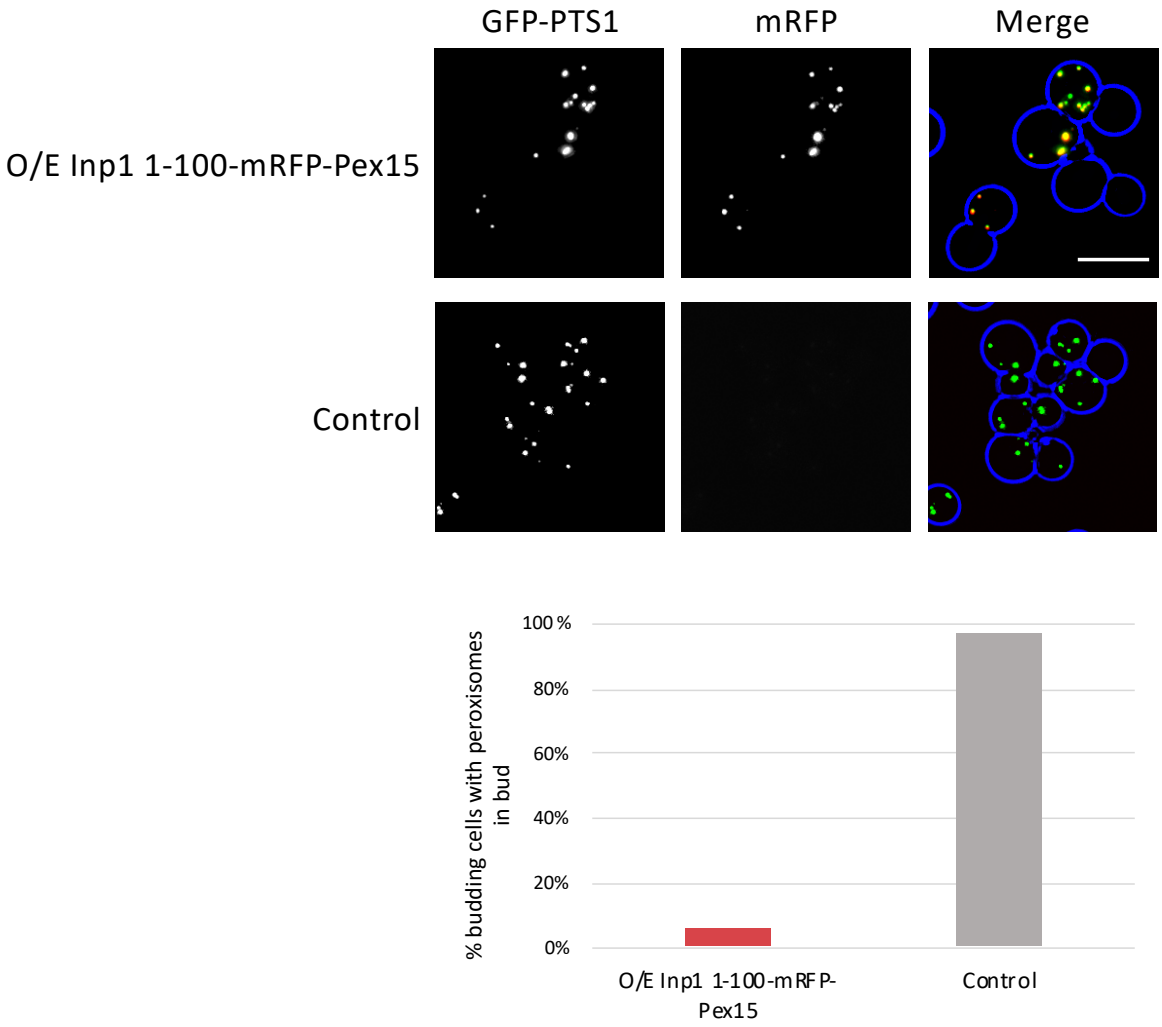

Figure 5.7 – Overexpression of the minimal tether results in over-retention of peroxisomes but does not affect peroxisome biogenesis. The N-terminus of Inp1 (amino acids 1-100) was fused to mRFP-Pex15 and overexpressed under control of the *TPI1* promoter in wild type cells with the constitutively expressed peroxisomal matrix marker GFP-PTS1. Cells were examined by fluorescence microscopy. Whole cell projections are shown. Bar, 5µm. The experiment was then quantitatively analysed by scoring budding cells for the presence of peroxisomes in the bud. At least 100 budding cells were quantified for each strain.

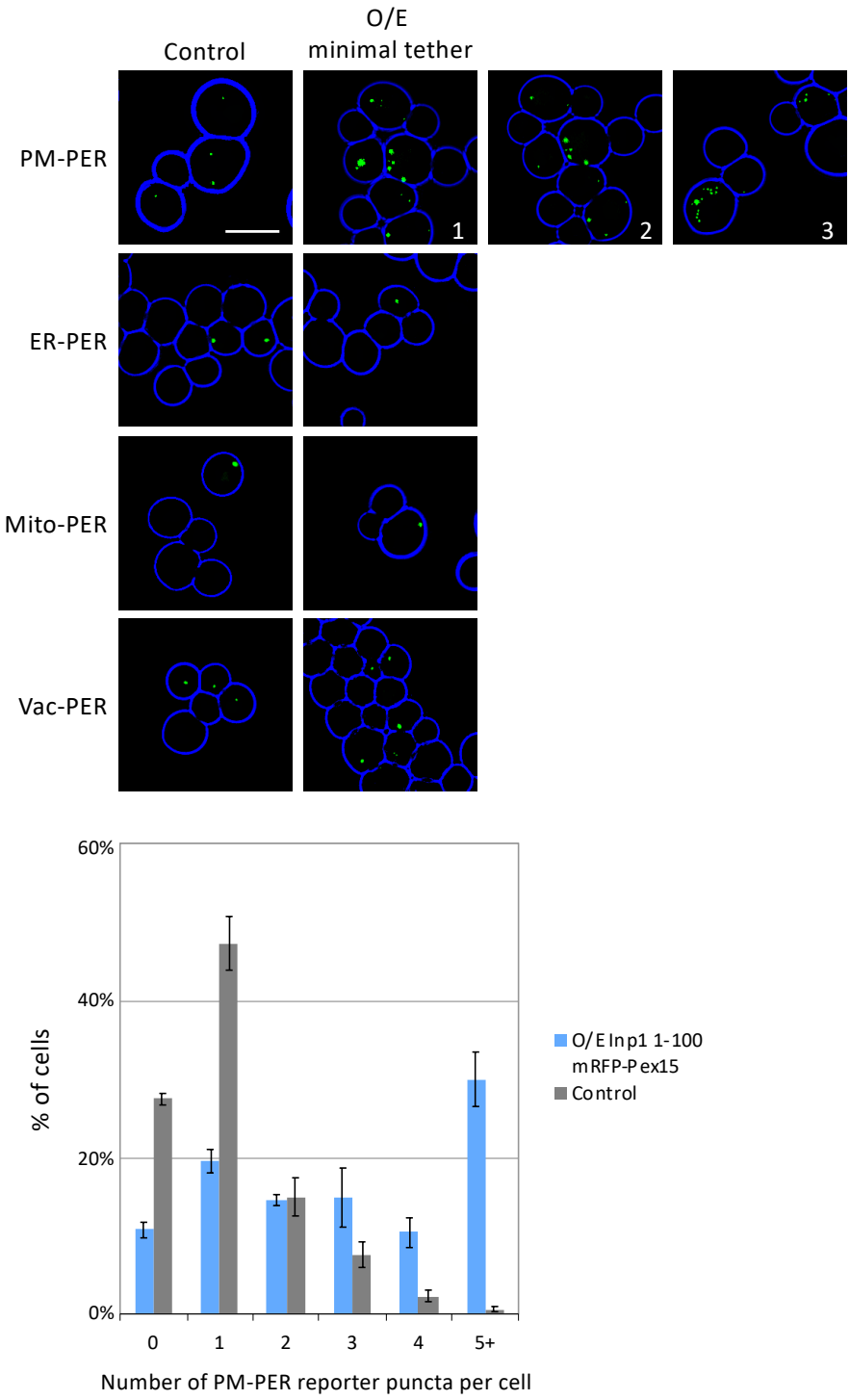

Figure 5.8 – Overexpression of the Inp1 minimal tether results in an increase in plasma membrane-peroxisome contact sites. The Inp1 1-100 truncation was fused to mRFP-Pex15 and this minimal tether was overexpressed under the control of the *TPI1* promoter in different peroxisome contact site split reporter strains. PM-PER, plasma membrane-peroxisome. ER-PER, endoplasmic reticulum-peroxisome. Mito-PER, mitochondria-peroxisome. Vac-PER, vacuole-peroxisome. Strains are described in Table 2.1, Section 2.2.1. Cells were examined by fluorescence microscopy for the presence of Venus puncta indicative of inter-organelle contact sites. Images labelled 1, 2 and 3 indicate various examples of the effect that overexpression of the minimal tether had on the PM-PER split reporter. Whole cell projections are shown. Bar, 5µm. The effect of overexpression of the minimal tether Inp1 1-100 mRFP-Pex15 on PM-PER split reporter was quantified. Over 100 cells were analysed for each strain. Three independent experiments were carried out. Error bars represent SEM.

5.3.3 The Inp1 minimal tether localises to the correct sub-cellular location to be a plasma membrane-peroxisome tether

As discussed in Section 5.2.3, one characteristic of a membrane contact site tether protein is its sub-cellular localisation to the contact site and full length Inp1-mCherry was shown to be closely apposed to the peroxisomal and plasma membranes (Fig. 5.3). The minimal Inp1 tether of amino acids 1-100, artificially attached to peroxisomes via Pex15, has been shown to be capable of restoring peroxisome localisation to the cell periphery and increasing the number of peroxisome-plasma membrane contact sites and so the sub-cellular location of this minimal tether was subsequently investigated.

To visualise the sub-cellular localisation of the minimal tether, it was first co-expressed in the cortical ER mutant *rtn1/rtn2/yop1/inp1Δ* with Sec63-GFP (Fig. 5.9A). The minimal tether was always seen to be present on the peripheral side of the ER, proximal to the plasma membrane. Quantitative analysis found that in around 49% of cells, the minimal tether was present in areas devoid of cortical ER (n=150 cells). This is comparable with the 46% of *rtn1/rtn2/yop1/inp1Δ* cells which had peripheral peroxisomes in the absence of cortical ER when expressing wild type Inp1. In order to further visualise the spatial relationship between the minimal Inp1 tether, peroxisomes and the ER, the minimal tether was co-expressed in *rtn1/rtn2/yop1/inp1Δ* cells with Sec63-GFP and BFP-PTS1 (Fig. 5.9B, C). Again, peroxisomes appeared 'sandwiched' between cortical ER and the cell periphery with the Inp1 minimal tether foci consistently juxtaposed to the peroxisomal matrix foci, closer to the cell periphery, and spatially resolved from the ER. Line scan analyses of the images confirmed that the minimal tether signal overlapped with that of the peroxisomal foci but that, as with full length Inp1, the peaks of the minimal tether and Sec63-GFP were spatially resolved. It can therefore be concluded that the N-terminal domain of Inp1, when retaining peroxisomes as a minimal tether, localises to the correct sub-cellular location to be associated with the plasma membrane.

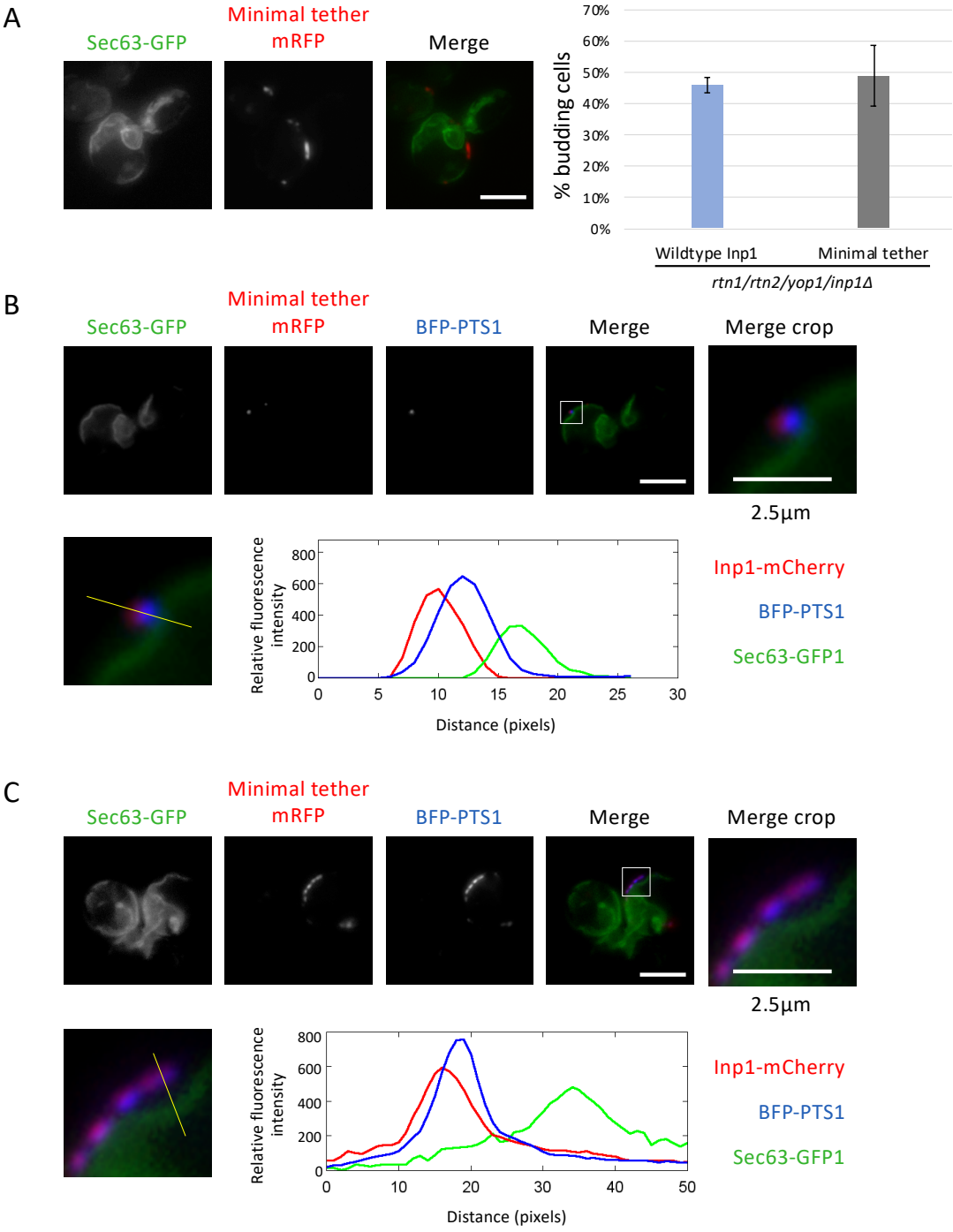

Figure 5.9 – The minimal tether Inp1 1-100-mRFP-Pex15 localises to the correct sub-cellular location to be considered a PM-PER tether. (A) Inp1 1-100-mRFP-Pex15 was overexpressed under control of the *TPI1* promoter in *rtn1/rtn2/yop1/inp1Δ* cells with Sec63-GFP and analysed using epifluorescence microscopy. Budding *rtn1/rtn2/yop1/inp1Δ* cells were scored for the presence of peroxisomes at the periphery but not associated with visible ER. Over 100 budding cells were quantified for each strain. Three independent experiments were carried out. Error bars represent SEM. (B, C) Images are taken from the same experiment. Inp1 1-100-mRFP-Pex15 was overexpressed under the control of the *TPI1* promoter in *rtn1/rtn2/yop1/inp1Δ* cells with Sec63-GFP and BFP-PTS1 and analysed using epifluorescence microscopy. The boxed areas are magnified (Merge crop). The graphs show relative fluorescence intensities of Inp1 (red), the peroxisomal matrix (blue) and the ER (green) along a line drawn through the centre of the Inp1 foci (Indicated by yellow lines). In A, B and C, single focal planes are shown. Bars, 5 µm except where indicated as 2.5 µm.

5.4 Inp1 has the structural capacity to be considered a PM-PER tether

5.4.1 Inp1 has two distinct membrane interacting domains and so meets the structural requirements to be a PM-PER tether

The third minimal requirement that a protein must fulfil in order to be considered a contact site tether is it must have the structural capacity to mediate binding to the opposing membrane of the organelles forming the contact site (Eisenberg-Bord et al., 2016). Structure function analysis must show that a protein has at least two domains, each with the ability to bind to a distinct membrane. The data obtained in this study has shown that Inp1 can interact with the plasma membrane via an N-terminal lipid-binding domain which binds to $PI(4,5)P_2$ and a C-terminal Pex3 binding domain by which Inp1 associates with the peroxisomal membrane. Taken together, the *in vivo* and *in vitro* data supports the idea that Inp1 has the structural capacity to be a plasma membrane-peroxisome tether.

A way of further analysing the structural capacity of a potential tether is by observing what happens when the putative membrane-binding domains of a tether protein are mutated. Many tether proteins are present at organellar interfaces as foci yet redistribute to different areas of the cell upon the functional loss of one membrane-binding domain. The same can also be observed with Inp1 (Fig. 5.10). Whilst wild type Inp1 can be found in foci at the interface of the peroxisomal and plasma membranes (See Figs. 5.4 and 5.5), upon deletion of the LNYLL peroxisomal Pex3 binding motif in the C-terminal domain, Inp1 foci that co-localise with peroxisomes are lost and the protein is present diffusely in the cytosol. When the N-terminal plasma membrane-binding domain (amino acids 1-100) is deleted, Inp1 still forms peroxisome-localised foci, but is unable to retain peroxisomes at the mother cell cortex. These Inp1 foci are therefore present only in the bud and are no longer in close proximity to the plasma membrane at the mother cell periphery. When either of the newly characterised Inp1 domains are mutated, Inp1 is redistributed to different sub-cellular locations. This, along with the data obtained in Chapters 3 and 4, confirms a structural capacity of Inp1 to act as a modular PM-PER tether protein between peroxisomes and the plasma membrane.

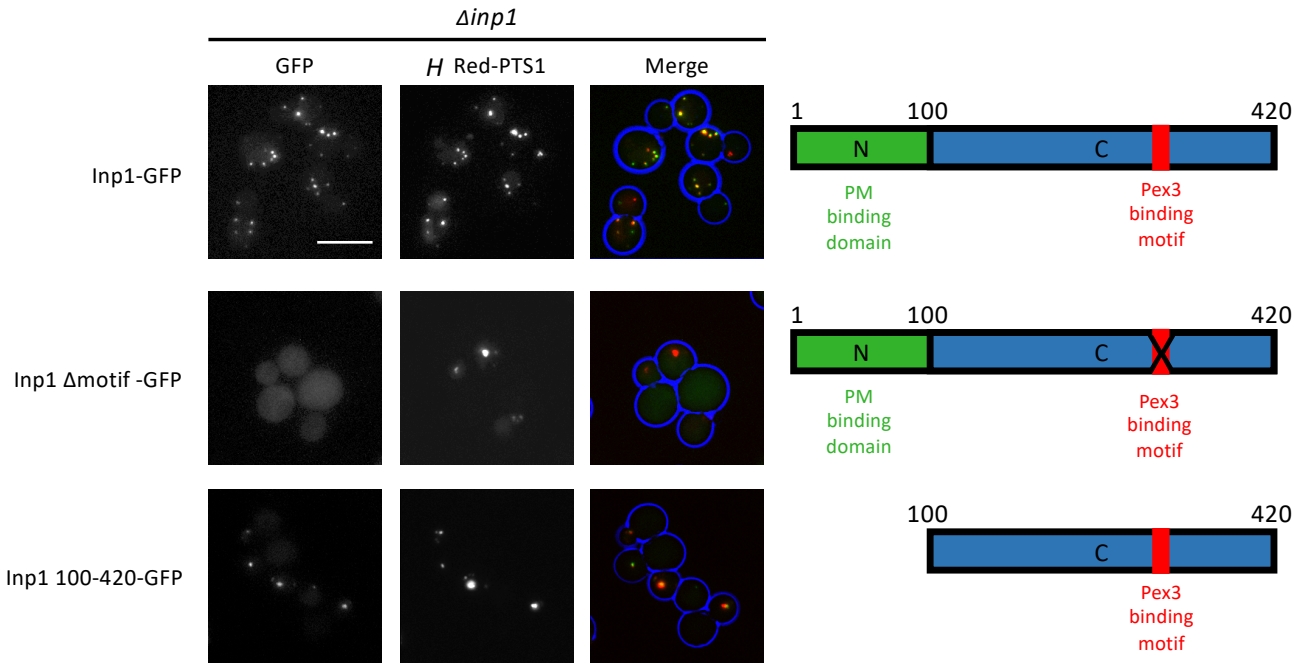

Figure 5.10 – Mutation of Inp1's functional domains results in a sub-cellular redistribution of the protein. Inp1-GFP, a leucine motif deletion (L312_L316del) (motifΔ) and Inp1 100-420-GFP were expressed under the endogenous *INP1* promoter in *Δinp1* cells with *Hc*Red-PTS1 and analysed by epifluorescence microscopy. The schematic diagrams represent a simplified domain structure of Inp1 with the N-terminal plasma membrane binding domain (amino acids 1-100) marked in green and the LNYLL Pex3 binding site (amino acids 312-316) shown in red. Bar, 5 µm.

5.4.2 The minimal tethers do not fully restore peroxisome positioning at the mother cell cortex

Previously in this study, it has been shown that minimal and artificial tethers comprised of the first 100 amino acids of Inp1 or the PH domain of Num1 are able to restore peroxisome localisation to the mother cell periphery in *Δinp1* cells when anchored into the peroxisomal membrane via Pex15 (Fig. 5.6). However, although peroxisome retention was restored, it was also observed that peroxisome distribution in these cells did not resemble that of wild type cells. A characteristic 'budneck clustering' phenotype was observed for both tethers where peroxisomes appeared to cluster at the mother cell side of the budneck. Extreme examples are shown in Fig. 5.11B. This clustering phenotype has been observed previously (Knoblach and Rachubinski, 2019). To further understand why peroxisomes cluster in the bud neck, Myo2-dependent peroxisome transport was blocked by deletion of the peroxisomal Myo2 receptor gene *INP2*. Accumulation in the bud neck was no longer observed in *Δinp1/Δinp2* cells expressing the minimal or artificial tethers, indicating that the clustering is a consequence of actin-myosin dependent transport (Fig. 5.11).

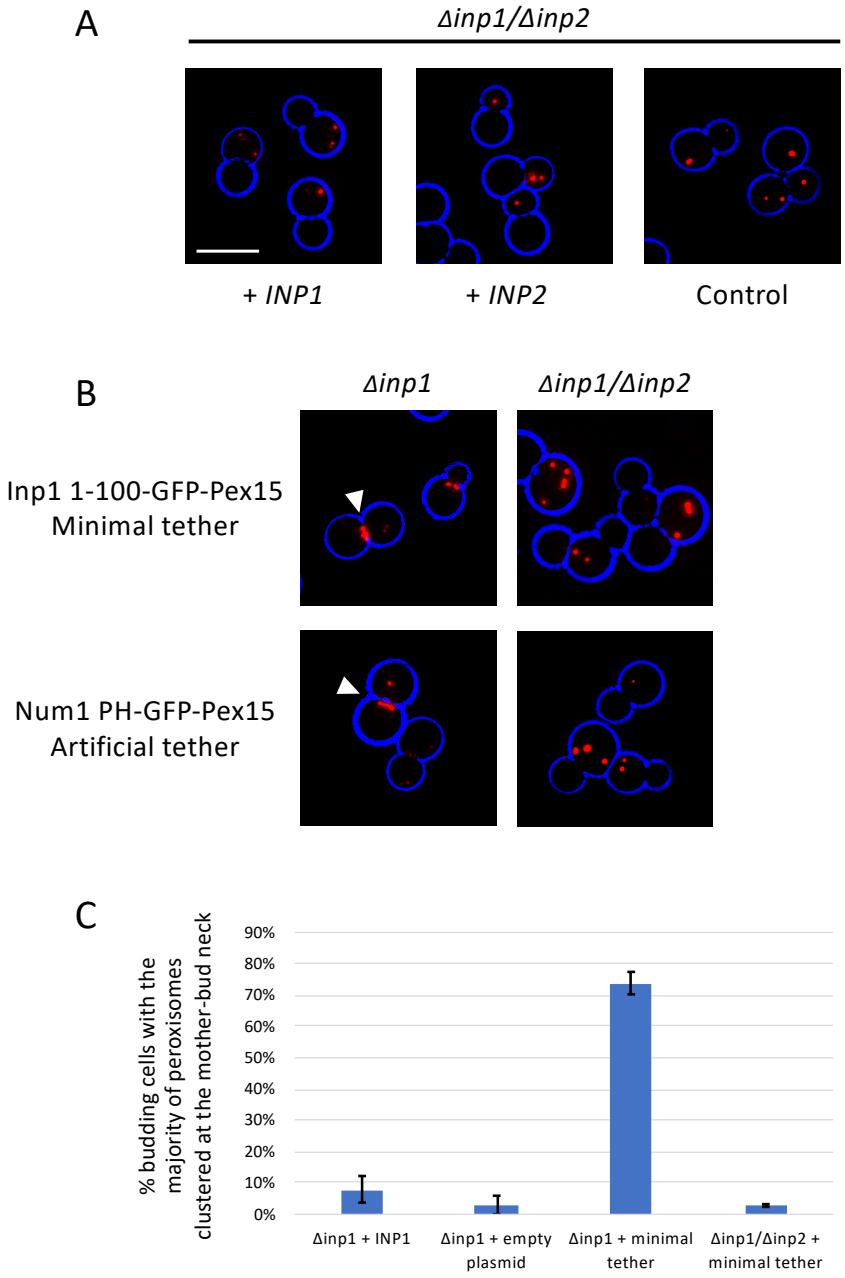

Figure 5.11 – Peroxisomes cluster at the bud neck in an *INP2* dependent manner when retention is restored by a minimal or artificial tether. (A) *Hc*Red-PTS1 was expressed in *Δinp1/Δinp2* with Inp1, Inp2 or a control plasmid in order to demonstrate the effect of restored expression of Inp1, Inp2 and a control plasmid on peroxisome localisation in *Δinp1/Δinp2* cells. (B) Inp1 1-100 GFP-Pex15 or Num1 PH-GFP-Pex15 were expressed under control of the *INP1* promoter in *Δinp1* or *Δinp1/Δinp2* cells as indicated, with the constitutively expressed *Hc*Red-PTS1. Cells showing strong phenotypic examples of bud neck clustering are shown. The white arrows indicate accumulation of peroxisomes on the mother cell side of the bud neck. Bars, 5 µm. (C) Quantification of the bud neck accumulation phenotype observed upon expression of Inp1-GFP or Inp1 1-100 GFP-Pex15 in *Δinp1* or *Δinp1/Δinp2* cells as indicated. Over 100 cells were analysed for each strain. Cells were deemed to have bud neck clustering when more than half of the peroxisomes in the cell were present at the bud neck area in the mother. Three independent experiments were carried out. Error bars represent SEM.

5.5 Discussion

The data acquired in this chapter demonstrates that Inp1 meets the requirements to be categorized as a membrane-contact site tether protein (Eisenberg-Bord et al., 2016). Inp1 can be recognised as a component of the plasma membrane-peroxisome (PM-PER) tether as, 1) it is present in the correct sub-cellular location, closely apposed to the peroxisome and plasma membranes (Fig. 5.4, 5.5). 2) Inp1 has the structural capacity to form a PM-PER tether by binding the peroxisomal membrane via a C-terminal Pex3 binding motif and by binding the plasma membrane via an N-terminal domain that binds $PI(4,5)P_2$. 3) Inp1 has the functional capacity to form a PM-PER tether. The first 100 amino acids of Inp1 or the plasma membrane-binding PH domain of Num1 can act as artificial tethers when attached to peroxisomes, which are sufficient to relocate peroxisomes to the cell periphery in *Δinp1* cells (Fig. 5.5). Additionally, overexpression of the Inp1 minimal tether (Inp1 1-100 GFP-Pex15) increases the number of PM-PER contact sites (Fig. 5.7) and when expressed in cortical ER mutants, the minimal tether localises to the side of peroxisomal foci proximal to the plasma membrane, spatially resolved from the ER (Fig. 5.8). The observations presented throughout this thesis qualify Inp1 as the first characterised PM-PER tether and support a new model for peroxisome retention (Fig. 5.11).

It has previously been reported that peroxisomes are retained at the mother cell cortex by Inp1 acting as a 'molecular hinge' and binding to both peroxisomal and ER bound Pex3 (Knoblach and Rachubinski, 2013). However, the results obtained throughout this study do not support this model. As well as a lack of evidence that the N-terminus of Inp1 binds to Pex3, it was shown that peroxisomes still localise to the periphery of the cell in mutants with severely disrupted cortical ER structures (Fig. 5.1, 5.2, 5.3). This shows that the role of the cortical ER in peroxisome tethering is not as essential as the existing model suggests. During the course of this work, another study by the same authors shed doubt on the simplicity of the existing Pex3-Inp1-Pex3 retention model with the suggestion that additional components are required for peroxisome tethering to the cell cortex. The authors (Knoblach and Rachubinski, 2019), suggest that Inp1 may function as a tether between peroxisomes and other organelles. In agreement with this postulate, I show that Inp1 is a tether protein at membrane contact sites between peroxisomes and the plasma membrane.

Although the proposed mechanisms for the existing Pex3-Inp1-Pex3 retention model do not correlate with the findings of this study, it cannot be ruled out that there are additional interactions domains elsewhere in Inp1. Whilst the artificial tethers Inp1 1-100 GFP-Pex15 and Num1 PH GFP-Pex15 restore peroxisome retention to the mother cell cortex in *Δinp1* cells, peroxisome positioning is not restored to that of wildtype cells with peroxisomes frequently seen 'clustering' at the bud neck (Fig. 5.10).

One explanation for the clustering phenotype could be that in budding yeast, $PI(4,5)P_2$ is not uniformly present around the plasma membrane and is enriched at areas of polarised growth and the bud neck (Garrenton et al., 2010). The artificial tethers are comprised of the $PI(4,5)P_2$ binding domain of Inp1 or the PH-domain of Num1 and so their expression may result in an enrichment of peroxisome tethering to sites where $PI(4,5)P_2$ is more concentrated, such as the bud neck.

Additionally, the phenotype could be due to a lack of regulation of the artificial tethers. During observation with fluorescence microscopy, the artificial tethers were seen to be visibly brighter than wild type Inp1-GFP, despite being expressed under control of the same *INP1* promoter. This is probably due to the fact that any potential regulatory machinery which exists for Inp1 would not recognise these artificial, chimeric tether proteins. As such, the tether proteins are not regulated or degraded as wild type Inp1 and so are present at higher levels than an endogenous Inp1 tether would be. In wild type yeast, it has been reported that peroxisomes with Inp1 foci attached can sometimes be observed moving along the cell cortex but being retained at the mother-bud neck interface. It seems that peroxisomes which are cortically attached via Inp1 are unable to enter the bud (Knoblach et al., 2013). The phenotype observed with the artificial tethers may be explained in the same way. There is a high cellular amount of plasma membrane-peroxisome tethers which are not broken down and so remain attached to peroxisomes. The phenotype has been shown to be dependent on Inp2 and so the peroxisomes are probably being dragged along the plasma membrane via Inp2-dependent transport towards the bud neck. These peroxisomes are unable to enter the bud due to still being cortically attached in the mother cell, hence they cluster at the mother cell bud-neck interface. (Figure 5.11).

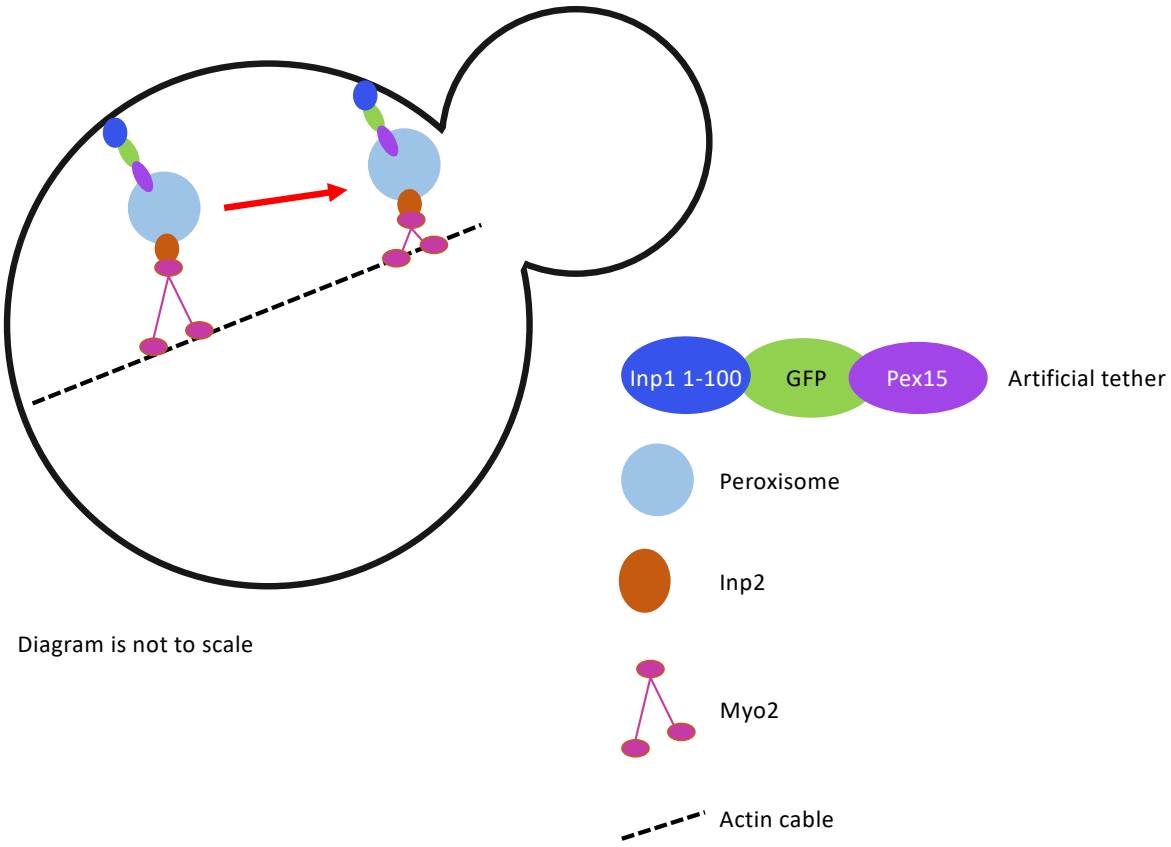

Figure 5.12 – Peroxisome clustering observed at the bud neck could be due to a lack of regulation of artificial tethers. Peroxisomes are normally transported along actin cables to the bud via Myo2 and the peroxisome-specific adaptor Inp2. Artificial tethers used in this study such as Inp1 1-100-GFP-Pex15 are likely not regulated as wild type Inp1 would be and so remain attached to peroxisomes, tethering them at the cell cortex. As peroxisomes are transported along actin cables to the bud, they may remain attached at the periphery by a tether which is not broken down or regulated properly and so gather at the bud neck, unable to enter the bud, resulting in the observed bud neck clustering phenotype.

The Inp2-dependent, 'bud neck clustering' seen upon expression of the artificial peroxisomal tethers could also suggest that the native Inp1 tether possesses additional functionality. It is known that Num1 has a dual role as a mitochondrial tether protein and as a cortical anchor for dynein attachment sites required for nuclear migration (Heil-Chapdelaine et al., 2000; Farkasovsky and Küntzel, 2001). Inp1 could also have an additional role in cortical recruitment of additional factors such as dynein, resultant in opposition to Myo2 traffic. The absence of amino acids 101-420 in the artificial tethers could mean that although the tethers can interact with lipids at the plasma membrane, the Inp1 domains required for dynein recruitment activity are absent. Therefore, the artificial tethers cannot oppose Myo2-based movement of peroxisomes which results in peroxisomes being 'dragged' along the cortex to the bud neck.

Further to the idea that the native Inp1 tether possesses further functionality, it can be hypothesised that additional contacts at the cell cortex are required in order to fix peroxisomes in the correct position. This study does not exclude that Inp1 could tether

peroxisomes via dual interaction at the cell cortex. This could be mediated by as yet unidentified factors which also reside at the mother cell cortex. Alternatively, this could be via other organelles such as the cortical ER, analogous to how mitochondria are positioned by dual interaction with the plasma membrane and the cER via MECA (Lackner et al., 2013). The existence of another three-way tether involving the cER and plasma membrane would suggest there are conserved mechanisms by which organelles make contact with each other. Inp1's role as a peroxisome tether is clear as an absence of functional Inp1 results in a complete lack of peroxisome retention in the mother cell. However, accurate peroxisome distribution at the cell periphery could also involve contact with organelles or cortical factors independent of Inp1. This will be further discussed in the following chapter.

Chapter 6 - Discussion

Initially, the primary aim of this study was to functionally characterise Inp1 in molecular detail and to investigate how Inp1 and Pex19 compete with their highly similar binding motifs for interaction with peroxisomal Pex3. However, the data that was subsequently obtained also indicated a role for Inp1 as tether protein at peroxisome-plasma membrane contact sites. The evidence presented has resulted in the proposal of a new model for peroxisome retention during asymmetric cell division with Inp1 identified as a component of the peroxisome-plasma membrane tether. The final sections of Chapters 3, 4 and 5 discuss and interpret the specific experimental data presented in each respective chapter. In this final chapter, a broader discussion will take place of the newly identified function of Inp1 as a peroxisome-plasma membrane tether and the new proposed model of peroxisome retention.

6.1 The functional domains of Inp1

Previous studies have interpreted the secondary structure of Inp1 to predict that it is a protein that can be roughly divided into two globular domains, an N-terminal domain comprised of amino acids 1-280 and a C-terminal domain comprised of amino acids 281-420 (Knoblach et al., 2013). In this study, these truncations were also used for initial functional analysis of Inp1. In Chapter 3, it was shown that Inp1 interacts directly with peroxisomal Pex3 via a conserved motif in its C-terminal domain. In Chapter 4, the N-terminal domain of Inp1 was found to be a lipid binding domain that binds to $PI(4,5)P_2$ and associates with the plasma membrane. As such, it has been shown that Inp1 interacts with the cell periphery via its N-terminus and this can be genetically separated from its direct interaction with peroxisomal Pex3 via its C-terminal domain.

Further analysis uncovered that the N-terminal 100 amino acids of Inp1 can be functionally separated as a domain which is capable of lipid binding and, when artificially attached to peroxisomes, is capable of tethering peroxisomes to the cell periphery. As discussed in Section 4.4, attempts were made during this study to further pinpoint regions in the first 100 amino acids required for peroxisomal tethering. However, when experiments were attempted with smaller tethers, the proteins were found to be unstable and as such, confident interpretations could not be made. This led to a conclusion that it is perhaps too simplistic to keep removing amino acids from a primary sequence of Inp1 in order to find a minimal tether. In order to function as a tether, the N-terminal domain of Inp1 most likely relies on a secondary or tertiary folded structure.

During the course of this study, an additional, complementary study has also been accepted for publication which investigates the functional role of Inp1 in *H. polymorpha* (Krikken et al., 2020). The authors divide *Hp*Inp1 into 3 functional domains, an N-terminal domain (amino acids 1-99), a middle homology domain (MHD) (100-216) and a C-terminal domain (217-405). As in this study, they also conclude that the N-terminal domain (1-99) of *Hp*Inp1 is required for association with the plasma membrane whilst the C-terminal domain of *Hp*Inp1 is required for peroxisome binding.

The authors observe that the N-terminal domain (1-99) of *Hp*Inp1 accumulates at the cell cortex, with higher concentrations of signal observed initially at the bud tip and then in the bud neck (Krikken et al., 2020). These observations were also made during this study, (Fig. 4.4, 4.12), and additionally, peroxisomes were seen to cluster at the bud neck when tethered to the periphery artificially by a plasma membrane-binding domain (Fig. 5.10). These observations could be explained by the fact that in budding yeast, $PI(4,5)P_2$ is not uniformly present around the plasma membrane and is enriched at areas of polarised growth and the bud neck (Garrenton et al., 2010). This pattern of enriched localisation to the bud neck has also been seen upon expression of the $PI(4,5)P_2$ binding pleckstrin homology (PH)-domain of Num1 (Tang et al., 2009).

Krikken *et al*. note that there is a high percentage of positive residues in the first 100 amino acids of *Hp*Inp1 and this is also true of *Sc*Inp1. The function of *Hp*Inp1 is affected upon substitution of these positive residues to negative ones and so it would be interesting to assay the effect that mutating these equivalent amino acids in *Sc*Inp1 has on its respective function. The positive residues could be required for binding to the plasma membrane, as is true for septins which associate specifically with $PI(4,5)P_2$ in the plasma membrane at the bud neck through positive residues in conserved, N-terminal polybasic regions (Casamayor and Snyder, 2003). The data shown in Fig. 4.8 and 4.9 is also supportive that charge plays some role in the interaction between Inp1 and $PI(4,5)P_2$. MBP-Inp1 shows clear binding to $PI(4,5)P_2$ liposomes under high salt conditions, but this is slightly reduced compared to lower salt conditions. This could be indicative that efficient binding of Inp1 to $PI(4,5)P_2$ liposomes depends mainly on specific interactions but that electrostatic interactions also contribute to binding.

Krikken *et al.* analyse the sequence of the MHD (100-216) of *Hp*Inp1 and predict that it may fold as a divergent Ran-binding domain from the PH-like domain superfamily (Krikken et al., 2020). The MHD of *Hp*Inp1 is found to contribute to peroxisome-plasma membrane contact in combination with the positive residues of the N-terminal domain and due to its predicted structural features, the authors suggest it could bind to an α-helix or proline-rich sequence but likely does not bind to the plasma membrane via anionic lipids. Whilst Krikken *et al* find that *Hp*Inp1 101-405 is able to partially rescue peroxisome retention, the same was not found for the equivalent truncation of *Sc*Inp1 in this study (100-420) (Fig. 4.3). However, retrospective analysis of the data in this thesis allows for speculation that there could also be an orthologous 'MHD' in *Sc*Inp1.

This study made use of truncations of Inp1 which provided major insights into the functionality of the protein. However, the design of these truncations may have resulted in a failure to identify additional functional domains. Structural analysis of *Hp*Inp1 100-216 shows that the MHD contains 7 β-sheets followed by an α-helix (Krikken et al., 2020). The authors align this sequence with that of other Inp1 orthologues including *Sc*Inp1 and show apparent conservation of this secondary structure (Fig. S1, Krikken et al., 2020). Retrospective analysis of the data obtained in this thesis and the work by Krikken *et al*, reveals a putative orthologous domain in *Sc*Inp1 in the region of amino acids 80-260. Through use of the truncations 1-100 and 101-280 during this study, identification of this domain may have been missed. Further work will be needed to fully characterise this putative PH-family domain of *Sc*Inp1 but it seems likely that this domain is involved in *Sc*Inp1's tethering function and could have the capabilities to bind to other proteins or cortical factors.

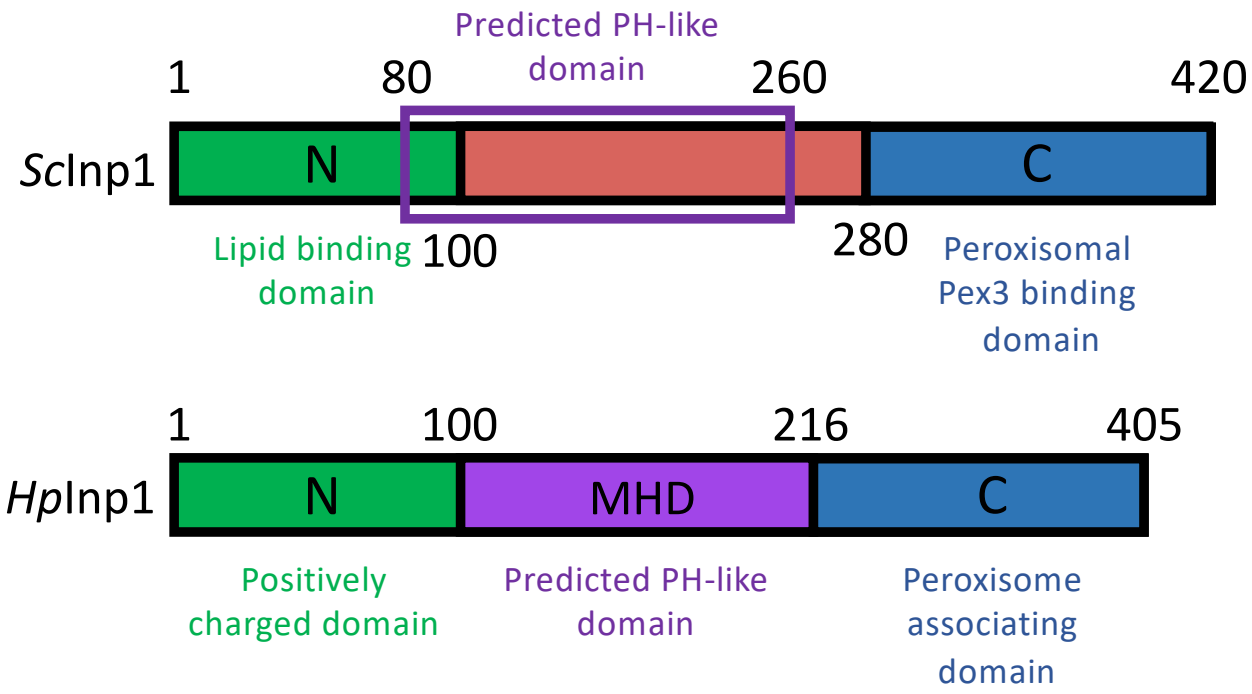

Figure 6.1 – Schematic representations of ScInp1 and HpInp1. The diagrams show an overview of the predicted domain structures of Inp1 in *S. cerevisiae* (*Sc*Inp1) and *H. polymorpha* (*Hp*Inp1). Diagrams are not to scale. For *Sc*Inp1, Green, N-terminal domain 1-100 shown to bind to lipids and localise to the plasma membrane; Purple box, the predicted PH-like domain 80-260 based on structural analysis of *Hp*Inp1, Blue, the C-terminal domain 281-420 shown to bind to be required for peroxisome association through direct binding with peroxisomal Pex3. For *Hp*Inp1, Green, the N-terminus with conserved positive charges; Red, MHD/predicted PH-like domain; Blue, C-terminal domain shown to be required for association of Inp1 with peroxisomes. Predictions for *Hp*Inp1 are based upon work by Krikken et al., 2020.

6.2 Other factors may be involved in peroxisome tethering

As reported in Chapter 5 (Fig. 5.10), peroxisomal localisation to the cell periphery can be restored in *Δinp1* cells upon expression of artificial peroxisome tethers which contain a plasma membrane-binding domain. However, the positioning of these peroxisomes is not restored to that of wildtype cells with peroxisomes frequently seen 'clustering' at the bud neck. A possible explanation for this, briefly discussed in Section 5.5, is that additional contacts at the mother cell periphery are required in order to fix peroxisomes in the correct position. Inp1 as a native tether could possess additional functionality and mediate tethering by interactions with the plasma membrane and as yet unidentified cortical factors or other organelles such as the cortical ER. Alternatively, peroxisome tethering and accurate peroxisome distribution at the cell periphery could involve contact with organelles or cortical factors independent of Inp1. This has been previously suggested by (Knoblach and Rachubinski, 2019) who hypothesise that additional components, independent of Inp1, are required for peroxisome tethering to the cell cortex.

6.2.1 Could Inp1 interact with the actin cytoskeleton?

There is dynamic cellular interplay between the plasma membrane and the underlying cortical actin cytoskeleton. Formation and elongation of actin filaments first requires actin nucleation and many of the proteins required for nucleation of actin at cortical patches are actin binding proteins which associate with $PI(4,5)P_2$ in the plasma membrane. $PI(4,5)P_2$ is considered to promote formation of actin filament structures through direct interaction with actin binding proteins and scaffolding proteins which control their sub-cellular localisation (Saarikangas et al., 2010).

This study finds Inp1 to be a $PI(4,5)P_2$ binding protein and this, combined with its sub-cellular localisation to cortical patches at the plasma membrane means that it is a plausible concept that Inp1 is also an actin binding protein. This idea is supported by observations made by Krikken *et al* who suggest that Inp1's cortical localisation is dependent on an intact actin cytoskeleton, as treatment of cells with latrunculin A results in a loss of cortical Inp1 patches, especially close to the bud neck (Krikken et al., 2020).

As a hypothetical actin binding protein, Inp1 could be involved in the marking of cortical patches from which actin nucleation can occur. Peroxisomes could then be anchored to these cortical patches in the mother cell, positioned at the 'start of the track' at points from which actin filaments then polymerise and form the track along which peroxisomes are transported. According to the *Saccharomyces* Genome Database, Inp1 genetically interacts with Las17, an actin assembly factor which nucleates actin filaments at cortical patches (Urbanek et al., 2013). Additionally, observations were made by the Schuldiner group that Bni1, a formin which nucleates the formation of linear actin filaments (Kohno et al., 1996; Pruyne et al., 2002), co-localises with peroxisomal markers (Personal communication). These observations were confirmed by the Hettema lab who then also observed that overexpression of mCherry-Bni1 affects normal peroxisomal distribution with most peroxisomes present in the mother as would be seen with Inp1 overexpression or in *Δinp2* cells (Personal communication).

This hypothetical dual role of Inp1 as an organelle tether protein and cortical actin nucleation site is reminiscent of the two roles carried out by the mitochondrial tether protein Num1. Num1 forms the core component of the mitochondrial ER cortical anchor (MECA) and is required for tethering mitochondria to the mother cell cortex during cell division. It does this through a coiled-coil domain which exhibits specificity to negatively charged, cone-shaped lipids characteristic of the mitochondrial outer membrane and a C-terminal PH domain, which binds to the plasma membrane via high specificity interactions with $PI(4,5)P_2$ (Yu et al., 2004; Ping et al., 2016). Additionally, Num1 has been shown to have an independent role in nuclear migration. In this role, Num1 is a cortical anchor for dynein and harnesses dynein-mediated microtubule sliding along the cell cortex for nuclear migration into buds (Heil-Chapdelaine et al., 2000; Farkasovsky and Küntzel, 2001). The potential link between Inp1 and actin seems promising and going forwards, this would be an interesting topic of peroxisome transport research.

6.2.2 Could Pex23 family proteins be required for correct peroxisome positioning?

In *S. cerevisiae,* the Pex23 family of proteins is comprised of Pex28, 29, 30, 31, 32 (Kiel et al., 2006). Although named as peroxins, this family of proteins localise to the ER and Pex29 and Pex30 have been shown to form complexes with the ER reticulon proteins Rtn1, Rtn2 and Yop1 (David et al., 2013; Joshi et al., 2016; Mast et al., 2016). Although present throughout the ER, Pex30 has been observed primarily in peripheral puncta in subdomains of the cortical ER, sandwiched between ER tubules and peroxisomes (Figure 5C of David et al., 2013). Peroxisomes have been observed to dynamically associate with subdomains of the ER which contain Pex29 and Pex30 and it has been reported that the absence of Pex30 and its paralogues results in increased mobility of peroxisomes, but peroxisomes are still retained at the mother cell periphery. Conversely, peroxisomes which co-localise with ER-associated Pex30 foci lack rapid movement (Munck et al., 2009; David et al., 2013; Mast et al., 2016; Knoblach and Rachubinski, 2019).

Additionally, peroxisomes are reported to cluster in *Δrtn1/Δrtn2/Δyop1* cells, (David et al., 2013), an observation which was also made during this study. Peroxisomes are still present at the cell periphery in *Δrtn1/Δrtn2/Δyop1* mutants, (Fig. 5.1, 5.2) but an absence of the reticulon proteins may disrupt the Pex30-dependent ER-peroxisome contact and this could affect peroxisome positioning. Interestingly, it has also been reported that Pex30 is capable of directly interacting with Inp1 (Fagarasanu et al., 2005). Taken together, these observations could indicate a role for Pex30 and its paralogues in the positioning and distribution of peroxisomes at the mother cell cortex which occurs in addition to the plasma membrane-peroxisome tethering achieved by Inp1.

During the writing up period of this study, an investigation into the Pex23 family orthologues in *H. polymorpha* was published which supports this hypothesis (Wu et al., 2020). The authors observe that the Pex23 family proteins *Hp*Pex24 and *Hp*Pex32 localise to ER-peroxisome contact sites and that these contacts are disrupted upon deletion of *Hp*Pex24 and *Hp*Pex32. In the absence of *Hp*Pex24 and *Hp*Pex32 defects in peroxisomal positioning and segregation are observed, and this defect is supressed upon introduction of an artificial ER-peroxisome tether. As was observed in this study (Fig. 5.3C), deletion of *H. polymorpha* Inp1 seems to have no effect on the proximity between ER and peroxisomal membranes at contact sites. The authors propose that Inp1 and the ER-localised Pex23 family proteins contribute together to peroxisome positioning at the cell cortex (Krikken et al., 2020).

ER-peroxisome contacts are also extensively observed in mammalian cells, (Valm et al., 2017), and the proteins which tether the ER and Peroxisomes at their MCS in mammalian cells were described by two independent groups. The ER resident proteins known as Vesicle associated membrane protein (VAMP)-associated proteins A and B (VAP-A and VAP-B) interact with the FFAT-like motifs of the peroxisomal membrane proteins ACBD4 and ACBD5 (Loewen and Levine, 2003; Hua et al., 2017; Costello et al., 2017a; Costello et al., 2017b).

Function of the tether has been proven as overexpression of ACBD5/VAPB increases the amount of ER-peroxisome contact sites whilst depletion of the tether reduces contact sites. The primary function of ER-peroxisome contact is proposed to be lipid transfer between the two organelles as disruption of these tethers results in decreased plasmalogen, cholesterol

and fatty acid β-oxidation levels, although direct lipid transfer activity by VAP-ACBD5 has not yet been demonstrated. (Hua et al., 2017; Yagita et al., 2017). However, both groups report that disruption of the ACBD5-VAPA/B tether results in increased motility of peroxisomes whilst attaching peroxisomes to the ER artificially appears to restrict their movement. This perhaps suggests that membrane contact sites may also regulate peroxisome motility through anchoring to the ER in mammalian cells (Hua et al., 2017; Costello et al., 2017). These observations that proteins present at peroxisome-ER contact sites affect peroxisome positioning has now been made independently in two yeast species and in mammalian cells and supports the ideas presented by Knoblach and Rachubinski, that factors, independent of Inp1, are required for correct and proper peroxisome tethering to the cell cortex (Knoblach and Rachubinski, 2019)

6.3 Final remarks

Whilst the relative contribution of other cortical components in peroxisome tethering remains unclear, Inp1 is absolutely required for peroxisome retention. The data obtained in this study identify Inp1 as a peroxisome-plasma membrane tether and demonstrates that this function allows Inp1 to fulfil its role in peroxisome retention. Looking ahead, questions remain which need to be addressed in order obtain the complete picture of how peroxisomes are retained at the cell cortex. Is the cortical ER involved, or do other cortical factors such as actin or as yet unidentified factors contribute to peroxisome positioning? If so, which domains of Inp1 do they interact with? Or are there additional cortical-peroxisomal interactions required for peroxisome tethering which occur independent of Inp1? These questions and more could all be addressed by further research in the field in order to clarify how peroxisomes are properly tethered and positioned. This work provides the first molecular description of a peroxisome-plasma membrane tether and characterises how Inp1 interacts with the opposing membranes. This is a major development in elucidating the mechanisms of peroxisome tethering at the cell cortex and has allowed for the proposal of a new model for peroxisome retention (Fig. 6.2).

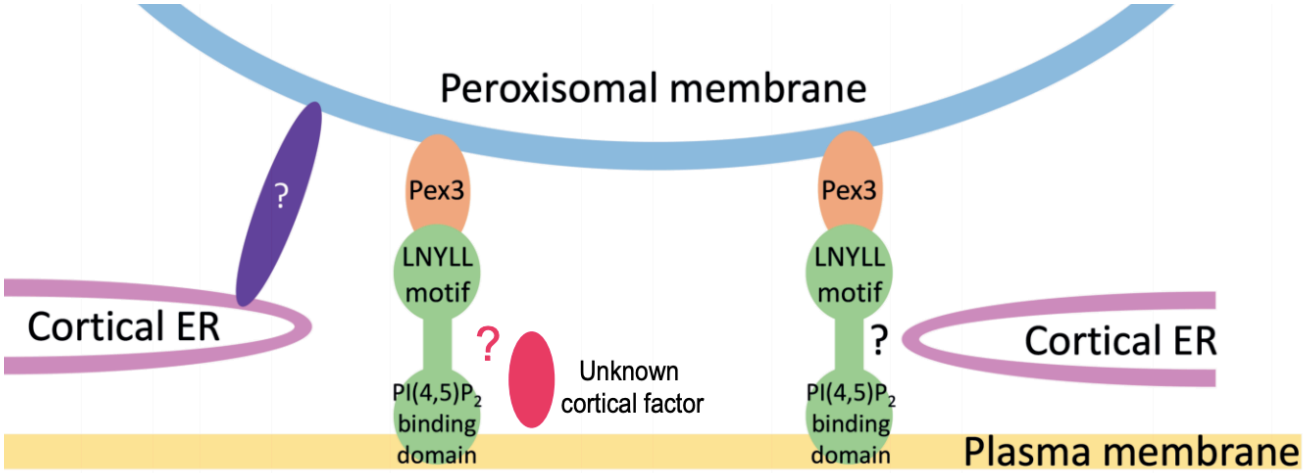

Figure 6.2 – Models of peroxisome tethering to the mother cell cortex (Hulmes et al., 2020). Inp1 is a PM-PER tether which bridges peroxisomes and the plasma membrane by interacting with peroxisomal Pex3 via a conserved LNYLL motif and with the plasma membrane via an N-terminal domain that binds PI(4,5)P_2. This PM-PER tether is required for peroxisome retention. Additional peroxisome contacts with cortical structures may contribute to peroxisome positioning or distribution at the mother cell cortex. Interaction with the cortical ER (cER) could occur via Inp1 and not-yet-identified factors (indicated by black question mark). Inp1 could also be in contact with cortical structures/factors independent of the cER such as actin (indicated by the red oval and red question mark). Peroxisome contact with the cER could also occur independently of Inp1 and via additional unidentified factors such as Pex30 and/or its paralogues (indicated by the purple oval and white question mark).

References

Agranoff, B. W., Bradley, R. M., and Brady, R. O., (1958). The enzymatic synthesis of inositol phosphatide. *The Journal of Biological Chemistry*, *233*(5), 1077–1083.

Agrawal, G., Shang, H. H., Xia, Z.-J., and Subramani, S. (2017). Functional regions of the peroxin Pex19 necessary for peroxisome biogenesis. *The Journal of Biological Chemistry*, *292*(27), 11547–11560.

Al-Saryi, N. A., Al-Hejjaj, M. Y., Van Roermund, C. W. T., Hulmes, G. E., Ekal, L., Payton, C., … Hettema, E. H. (2017). Two NAD-linked redox shuttles maintain the peroxisomal redox balance in Saccharomyces cerevisiae. *Scientific Reports*, *7*(1), 11868.

Audhya, A., and Emr, S. D. (2002). Stt4 Pl 4-kinase localizes to the plasma membrane and functions in the Pkc1-mediated MAP kinase cascade. *Developmental Cell*, *2*(5), 593–605.

Balla, T., Szentpetery, Z., and Kim, Y. J. (2009). Phosphoinositide signaling: new tools and insights. *Physiology*, Vol. 24, 231–244.

Baudhuin, P., Beaufay, H., and De Duve, C. (1965). Combined biochemical and morphological study of particulate fractions from rat liver: Analysis of Preparations Enriched in Lysosomes or in Particles Containing Urate Oxidase, D-Amino Acid Oxidase, and Catalase. *The Journal of Cell Biology*, *26*(1), 219–243.

Bernhard, W., and Rouiller, C. (1956). Close topographical relationship between mitochondria and ergastoplasm of liver cells in a definite phase of cellular activity. *The Journal of Biophysical and Biochemical Cytology*, *2*(4, Suppl), 73–78.

Besprozvannaya, M., Dickson, E., Li, H., Ginburg, K. S., Bers, D. M., Auwerx, J., and Nunnari, J. (2018). GRAM domain proteins specialize functionally distinct ER-PM contact sites in human cells. *ELife*, *7*.

Binns, D., Januszewski, T., Chen, Y., Hill, J., Markin, V. S., Zhao, Y., … Goodman, J. M. (2006). An intimate collaboration between peroxisomes and lipid bodies. *Journal of Cell Biology*, *173*(5), 719–731.

Birschmann, I., Stroobants, A. K., van den Berg, M., Schäfer, A., Rosenkranz, K., Kunau, W.-H., and Tabak, H. F. (2003). Pex15p of Saccharomyces cerevisiae provides a molecular basis for recruitment of the AAA peroxin Pex6p to peroxisomal membranes. *Molecular Biology of the Cell*, *14*(6), 2226–2236.

Braverman, N., Dodt, G., Gould, S. J., and Valle, D. (1998). An isoform of pex5p, the human PTS1 receptor, is required for the import of PTS2 proteins into peroxisomes. *Human Molecular Genetics*, *7*(8), 1195–1205.

Braverman, N. E., D'Agostino, M. D., and MacLean, G. E. (2013). Peroxisome biogenesis disorders: Biological, clinical and pathophysiological perspectives. *Developmental Disabilities Research Reviews*, *17*(3), 187–196.

Brown, F. R., McAdams, A. J., Cummins, J. W., Konkol, R., Singh, I., Moser, A. B., and Moser, H. W. (1982). Cerebro-hepato-renal (Zellweger) syndrome and neonatal adrenoleukodystrophy: similarities in phenotype and accumulation of very long chain fatty acids. *The Johns Hopkins Medical Journal*, *151*(6), 344–351.

Burnett, S. F., Farré, J. C., Nazarko, T. Y., and Subramani, S. (2015). Peroxisomal Pex3 activates selective autophagy of peroxisomes via interaction with the pexophagy receptor Atg30. *Journal of Biological Chemistry*, *290*(13), 8623–8631.

Casamayor, A., and Snyder, M. (2003). Molecular Dissection of a Yeast Septin: Distinct Domains Are Required for Septin Interaction, Localization, and Function. *Molecular and Cellular Biology*, *23*(8), 2762–2777.

Chang, J., Mast, F. D., Fagarasanu, A., Rachubinski, D. A., Eitzen, G. A., Dacks, J. B., and Rachubinski, R. A. (2009). Pex3 peroxisome biogenesis proteins function in peroxisome inheritence as class V myosin receptors. *Journal of Cell Biology, 187(2),* 233-246.

Chang, C. L., Weigel, A. V., Ioannu, M. S., Passoli, H. A., … Lippincott-Schwartz, J. (2019). Spastin tethers lipid droplets to peroxisomes and directs fatty acid trafficking through ESCRT-III. *Journal of Cell Biology, 218(8), 2583-2599.*

Chen, D. C., Yang, B. C., and Kuo, T. T. (1992). One-step transformation of yeast in stationary phase. *Current Genetics*, *21*(1), 83–84.

Cockcroft, S., and Raghu, P. (2018). Phospholipid transport protein function at organelle contact sites. *Current Opinion in Cell Biology*, *53*, 52–60.

Copeland, D. E., and Dalton, A. J. (1959). An association between mitochondria and the endoplasmic reticulum in cells of the pseudobranch gland of a teleost. *The Journal of Biophysical and Biochemical Cytology*, *5*(3), 393–396.

Costello, J. L., Castro, I. G., Hacker, C., Schrader, T. A., Metz, J., Zeuschner, D., … Schrader, M. (2017). ACBD5 and VAPB mediate membrane associations between peroxisomes and the ER. *Journal of Cell Biology*, *216*(2), 331–342.

Costello, J. L., Castro, I. G., Schrader, T. A., Islinger, M., and Schrader, M. (2017). Peroxisomal ACBD4 interacts with VAPB and promotes ER-peroxisome associations. *Cell Cycle*, Vol. 16, 1039–1045.

Csordás, G., Renken, C., Várnai, P., Walter, L., Weaver, D., Buttle, K. F., … Hajnóczky, G. (2006). Structural and functional features and significance of the physical linkage between ER and mitochondria. *Journal of Cell Biology*, *174*(7), 915–921.

Csordás, G., Várnai, P., Golenár, T., Roy, S., Purkins, G., Schneider, T. G., … Hajnóczky, G. (2010). Imaging Interorganelle Contacts and Local Calcium Dynamics at the ER-Mitochondrial Interface. *Molecular Cell*, *39*(1), 121–132.

David, C., Koch, J., Oeljeklaus, S., Laernsack, A., Melchior, S., Wiese, S., … Brocard, C. (2013). A combined approach of quantitative interaction proteomics and live-cell imaging reveals a regulatory role for endoplasmic reticulum (ER) Reticulon Homology Proteins in peroxisome biogenesis. *Molecular and Cellular Proteomics*, *12*(9), 2408–2425.

De Duve, C., and Baudhuin, P. (1966). Peroxisomes (microbodies and related particles). *Physiol Rev*, *46*(2), 323–357.

Dickson, E. J., and Hille, B. (2019). Understanding phosphoinositides: Rare, dynamic, and essential membrane phospholipids. *Biochemical Journal*, Vol. 476, 1–23.

Distel, B., Erdmann, R., Gould, S. J., Blobel, G., Crane, D. I., Cregg, J. M., … Veenhuis, M. (1996). A unified nomenclature for peroxisome biogenesis factors. *The Journal of Cell Biology*, *135*(1), 1–3.

Dyer, J. M., McNew, J. A., and Goodman, J. M. (1996). The sorting sequence of the peroxisomal integral membrane protein PMP47 is contained within a short hydrophilic loop. *Journal of Cell Biology*, *133*(2), 269–280.

Eisenberg-Bord, M., Shai, N., Schuldiner, M., and Bohnert, M. (2016). A Tether Is a Tether Is a Tether: Tethering at Membrane Contact Sites. *Developmental Cell*, Vol. 39, 395–409.

El Magraoui, F., Bäumer, B. E., Platta, H. W., Baumann, J. S., Girzalsky, W., and Erdmann, R. (2012). The RING-type ubiquitin ligases Pex2p, Pex10p and Pex12p form a heteromeric complex that displays enhanced activity in an ubiquitin conjugating enzyme-selective manner. *FEBS Journal*, *279*(11), 2060–2070.

Elgersma, Y., Kwast, L., van den Berg, M., Snyder, W. B., Distel, B., Subramani, S., and Tabak, H. F. (1997). Overexpression of Pex15p, a phosphorylated peroxisomal integral membrane protein required for peroxisome assembly in S.cerevisiae, causes proliferation of the endoplasmic reticulum membrane. *The EMBO Journal*, *16*(24), 7326–7341.

Elgersma, Y., van den Berg, M., Tabak, H. F., and Distel, B. (1993). An efficient positive selection procedure for the isolation of peroxisomal import and peroxisome assembly mutants of Saccharomyces cerevisiae. *Genetics*, *135*(3), 731–740.

Erdmann, R., Veenhuis, M., Mertens, D., and Kunau, W. H. (1989). Isolation of peroxisome-deficient mutants of Saccharomyces cerevisiae. *Proceedings of the National Academy of Sciences*, *86*(14), 5419–5423.

Erdmann, R., and Schliebs, W. (2005). Peroxisomal matrix protein import: The transient pore model. *Nature Reviews Molecular Cell Biology*, Vol. 6, 738–742.

Fagarasanu, A., Fagarasanu, M., Eitzen, G. A., Aitchison, J. D., and Rachubinski, R. A. (2006). The Peroxisomal Membrane Protein Inp2p Is the Peroxisome-Specific Receptor for the Myosin V Motor Myo2p of Saccharomyces cerevisiae. *Developmental Cell*, *10*(5), 587–600.

Fagarasanu, A., Mast, F. D., Knoblach, B., and Rachubinski, R. A. (2010). Molecular mechanisms of organelle inheritance: Lessons from peroxisomes in yeast. *Nature Reviews Molecular Cell Biology*, Vol. 11, 644–654.

Fagarasanu, M., Fagarasanu, A., and Rachubinski, R. A. (2006). Sharing the wealth: Peroxisome inheritance in budding yeast. *Biochimica et Biophysica Acta - Molecular Cell Research*, Vol. 1763, 1669–1677.

Fagarasanu, M., Fagarasanu, A., Tam, Y. Y. C., Aitchison, J. D., and Rachubinski, R. A. (2005). Inp1p is a peroxisomal membrane protein required for peroxisome inheritance in *Saccharomyces cerevisiae*. *The Journal of Cell Biology*, *169*(5), 765–775.

Fan, J., Li, X., Issop, L., Culty, M., and Papadopoulos, V. (2016). ACBD2/ECI2-mediated peroxisome-mitochondria interactions in leydig cell steroid biosynthesis. *Molecular Endocrinology*, *30*(7), 763–782.

Fang, Y., Morrell, J. C., Jones, J. M., and Gould, S. J. (2004). PEX3 functions as a PEX19 docking factor in the import of class I peroxisomal membrane proteins. *The Journal of Cell Biology*, *164*(6), 863–875.

Farkasovsky, M. and Küntzel, H. (2001). Cortical Num1p interacts with the dynein intermediate chain Pac11p and cytoplasmic microtubules in budding yeast. *Journal of Cell Biology, 152(2),* 251-262.

Fidaleo, M. (2010). Peroxisomes and peroxisomal disorders: the main facts. *Experimental and Toxicologic Pathology : Official Journal of the Gesellschaft Für Toxikologische Pathologie*, *62*(6), 615–625.

Foti, M., Audhya, A., and Emr, S. D. (2001). Sac1 lipid phosphatase and Stt4 phosphatidylinositol 4-kinase regulate a pool of phosphatidylinositol 4-phosphate that functions in the control of the actin cytoskeleton and vacuole morphology. *Molecular Biology of the Cell*, *12*(8), 2396–2411.

Gandre-Babbe, S., and van der Bliek, A. M. (2008). The novel tail-anchored membrane protein Mff controls mitochondrial and peroxisomal fission in mammalian cells. *Molecular Biology of the Cell*, *19*(6), 2402–2412.

Garrenton, L. S., Stefan, C. J., McMurray, M. A., Emr, S. D., and Thorner, J. (2010). Pheromone-induced anisotropy in yeast plasma membrane phosphatidylinositol- 4,5-bisphosphate distribution is required for MAPK signaling. *Proceedings of the National Academy of Sciences of the United States of America*, *107*(26), 11805–11810.

Gietz, R. D., and Akio, S. (1988). New yeast-Escherichia coli shuttle vectors constructed with in vitro mutagenized yeast genes lacking six-base pair restriction sites. *Gene*, *74*(2), 527–534.

Gietz, R. D., and Woods, R. A. (2002). Transformation of yeast by lithium acetate/single-stranded carrier DNA/polyethylene glycol method. *Methods in Enzymology*, *350*, 87–96.

Gotte, K., Girzalsky, W., Linkert, M., Baumgart, E., Kammerer, S., Kunau, W. H., and Erdmann, R. (1998). Pex19p, a farnesylated protein essential for peroxisome biogenesis. *Molecular and Cellular Biology*, *18*(1), 616–628.

Gould, S J, Keller, G. A., Hosken, N., Wilkinson, J., and Subramani, S. (1989). A conserved tripeptide sorts proteins to peroxisomes. *The Journal of Cell Biology*, *108*(5), 1657–1664.

Gould, Stephen J., McCollum, D., Spong, A. P., Heyman, J. A., and Subramani, S. (1992). Development of the yeast Pichia pastoris as a model organism for a genetic and molecular analysis of peroxisome assembly. *Yeast*, *8*(8), 613–628.

Gouveia, A. M., Reguenga, C., Oliveira, M. E., Sa-Miranda, C., and Azevedo, J. E. (2000). Characterization of peroxisomal Pex5p from rat liver. Pex5p in the Pex5p-Pex14p membrane complex is a transmembrane protein. *The Journal of Biological Chemistry*, *275*(42), 32444–32451.

Gray, E. G. (1963). Electron microscopy of presynaptic organelles of the spinal cord. *Journal of Anatomy*, *97*(Pt 1), 101–106.

Hanahan, D. (1983). Studies on transformation of Escherichia coli with plasmids. *Journal of Molecular Biology*, *166*(4), 557–580.

Hariri, H., Speer, N., Bowerman, J., Rogers, S., Fu, G., Reetz, E., … Henne, W. M. (2019). Mdm1 maintains endoplasmic reticulum homeostasis by spatially regulating lipid droplet biogenesis. *Journal of Cell Biology*, *218*(4), 1319–1334.

Heil-Chapdelaine, R. A., Oberle, J. R., and Cooper, J. A. (2000). The cortical protein Num1p is essential for dynein dependent interactions of microtubules with the cortex. *Journal of Cell Biology, 151(6),* 1337-1344.

Hettema, E. H., Girzalsky, W., van Den Berg, M., Erdmann, R., and Distel, B. (2000). Saccharomyces cerevisiae pex3p and pex19p are required for proper localization and stability of peroxisomal membrane proteins. *The EMBO Journal*, *19*(2), 223–233.

Hettema, E. H., Erdmann, R., van der Klei, I. J., and Veenhuis, M. (2014). Evolving models for peroxisome biogenesis. *Current Opinions in Cell Biology, 29(100),* 25-30.

Hoepfner, D., Schildknegt, D., Braakman, I., Philippsen, P., and Tabak, H. F. (2005). Contribution of the endoplasmic reticulum to peroxisome formation. *Cell*, *122*(1), 85–95.

Hoepfner, D., Van Den Berg, M., Philippsen, P., Tabak, H. F., and Hettema, E. H. (2001). A role for Vps1p, actin, and the Myo2p motor in peroxisome abundance and inheritance in Saccharomyces cerevisiae. *Journal of Cell Biology*, *155*(6), 979–990.

Höhfeld, J., Veenhuis, M., and Kunau, W. H. (1991). PAS3, a Saccharomyces cerevisiae gene encoding a peroxisomal integral membrane protein essential for peroxisome biogenesis. *The Journal of Cell Biology*, *114*(6), 1167–1178.

Honsho, M, Tamura, S., Shimozawa, N., Suzuki, Y., Kondo, N., and Fujiki, Y. (1998). Mutation in PEX16 is causal in the peroxisome-deficient Zellweger syndrome of complementation group D. *American Journal of Human Genetics*, *63*(6), 1622–1630.

Honsho, Masanori, and Fujiki, Y. (2001). Topogenesis of peroxisomal membrane protein requires a short, positively charged intervening-loop sequence and flanking hydrophobic segments: Study using human membrane protein PMP34. *Journal of Biological Chemistry*, *276*(12), 9375–9382.

Hua, R., Cheng, D., Coyaud, É., Freeman, S., Di Pietro, E., Wang, Y., … Kim, P. K. (2017). VAPs and ACBD5 tether peroxisomes to the ER for peroxisome maintenance and lipid homeostasis. *Journal of Cell Biology*, *216*(2), 367–377.

Hughes, W. E., Cooke, F. T., and Parker, P. J. (2000). Sac phosphatase domain proteins. *The Biochemical Journal*, *350 Pt 2*(Pt 2), 337–352.

Hulmes, G. E., Hutchinson, J. D., Dahan, N., Nuttall, J., Allwood, E. G., Ayscough, K. R., and Hettema, E. H. (2020) The Pex3/Inp1 complex tethers yeast peroxisomes to the plasma membrane. *Journal of Cell Biology.* DOI: 10.1083/jcb.201906021

Hutchinson, J. D. (2016). Investigating the Interactions of Pex3p in *Saccharomyces cerevisiae*. (PhD Thesis).

Jones, J. M., Morrell, J. C., and Gould, S. J. (2004). PEX19 is a predominantly cytosolic chaperone and import receptor for class 1 peroxisomal membrane proteins. *Journal of Cell Biology*, *164*(1), 57–67.

Joshi, A. S., Huang, X., Choudhary, V., Levine, T. P., Hu, J., and Prinz, W. A. (2016). A family of membrane-shaping proteins at ER subdomains regulates pre-peroxisomal vesicle biogenesis. *Journal of Cell Biology*, *215*(4), 515–529.

Joshi, S., Agrawal, G., and Subramani, S. (2012). Phosphorylation-dependent Pex11p and Fis1p interaction regulates peroxisome division. *Molecular Biology of the Cell*, *23*(7), 1307–1315.

Kakimoto, Y., Tashiro, S., Kojima, R., Morozumi, Y., Endo, T., and Tamura, Y. (2018). Visualizing multiple inter-organelle contact sites using the organelle-Targeted split-GFP system. *Scientific Reports*, *8*(1), 1–13.

Kawamoto, R. M., Brunschwig, J. P., Kim, K. C., and Caswell, A. H. (1986). Isolation, characterization, and localization of the spanning protein from skeletal muscle triads. *Journal of Cell Biology*, *103*(4), 1405–1414.

Keller, G.-A., Gould, S., Delucat, M., and Subramani, S. (1987). Firefly luciferase is targeted to peroxisomes in mammalian cells. *Cell Biology*, *84*, 3264–3268.

Kiel, J. A. K. W., Veenhuis, M., and van der Klei, I. J. (2006). PEX genes in fungal genomes: common, rare or redundant. *Traffic (Copenhagen, Denmark)*, *7*(10), 1291–1303.

Kim, P. K., Mullen, R. T., Schumann, U., and Lippincott-Schwartz, J. (2006). The origin and maintenance of mammalian peroxisomes involves a de novo PEX16-dependent pathway from the ER. *Journal of Cell Biology*, *173*(4), 521–532.

Kim, Y. J., Guzman-Hernandez, M. L., and Balla, T. (2011). A highly dynamic ER-derived phosphatidylinositol-synthesizing organelle supplies phosphoinositides to cellular membranes. *Developmental Cell*, *21*(5), 813–824.

Klouwer, F. C. C., Berendse, K., Ferdinandusse, S., Wanders, R. J. A., Engelen, M., and Poll-The, B. T. (2015). Zellweger spectrum disorders: clinical overview and management approach. *Orphanet Journal of Rare Diseases*, *10*(1), 151.

Knoblach, B., and Rachubinski, R. A. (2015). Motors, Anchors, and Connectors: Orchestrators of Organelle Inheritance. *Annual Review of Cell and Developmental Biology*, *31*(1), 55–81.

Knoblach, B., and Rachubinski, R. A. (2019). Determinants of the assembly, integrity and maintenance of the endoplasmic reticulum-peroxisome tether. *Traffic*, *20*(3), 213–225.

Knoblach, B., Sun, X., Coquelle, N., Fagarasanu, A., Poirier, R. L., and Rachubinski, R. A. (2013). An ER-peroxisome tether exerts peroxisome population control in yeast. *EMBO Journal*, *32*(18), 2439–2453.

Koch, J., Pranjic, K., Huber, A., Ellinger, A., Hartig, A., Kragler, F., and Brocard, C. (2010). PEX11 family members are membrane elongation factors that coordinate peroxisome proliferation and maintenance. *Journal of Cell Science*, *123*(19), 3389–3400.

Kohno, H., Tanaka, K., Mino, A., Umikawa, M., Imamura, H., Fujiwara, T., … Takai, Y. (1996). Bni1p implicated in cytoskeletal control is a putative target of Rho1p small GTP binding protein in Saccharomyces cerevisiae. *The EMBO Journal*, *15*(22), 6060–6068.

Kornmann, B., Osman, C., and Walter, P. (2011). The conserved GTPase Gem1 regulates endoplasmic reticulum-mitochondria connections. *Proceedings of the National Academy of Sciences of the United States of America*, *108*(34), 14151–14156.

Kragt, A., Voorn-Brouwer, T., Van Den Berg, M., and Distel, B. (2005). Endoplasmic reticulum-directed Pex3p routes to peroxisomes and restores peroxisome formation in a Saccharomyces cerevisiae pex3Δ strain. *Journal of Biological Chemistry*, *280*(40), 34350–34357.

Krikken, A. M., Huala, W., de Boer, R., Devos, D. P., Levine, T. P., and van der Klei, I. J. (2020). Peroxisome retention involves Inp1-dependent peroxisome-plasma membrane contact sites in yeast. *Journal of Cell Biology. 219(10).*

Kuravi, K., Nagotu, S., Krikken, A. M., Sjollema, K., Deckers, M., Erdmann, R., … van der Klei, I. (2006). Dynamin-related proteins Vps1p and Dnm1p control peroxisome abundance in Saccharomyces cerevisiae. *Journal of Cell Science*, *119*(19), 3994–4001.

Lackner, L. L., Ping, H., Graef, M., Murley, A., and Nunnari, J. (2013). Endoplasmic reticulum-associated mitochondria-cortex tether functions in the distribution and inheritance of mitochondria. *Proceedings of the National Academy of Sciences of the United States of America*, *110*(6), E458-67.

Lam, S. K., Yoda, N., and Schekman, R. (2011, April 5). A vesicle carrier that mediates peroxisome protein traffic from the endoplasmic reticulum. *Proceedings of the National Academy of Sciences of the United States of America*, Vol. 108, E51–E52.

Lazarow, P. B., and Fujiki1, Y. (1985). Biogenesis of peroxisomes. *Annual Reviews of Cell Biology, 1,* 489-530.

Lemmon, M. A. (2008). Inner leaflet Membrane recognition by phospholipid-binding domains. *Nature Reviews Molecular Cell Biology, 9(2),* 99-111.

Lewis, S. C., Uchiyama, L. F., and Nunnari, J. (2016). ER-mitochondria contacts couple mtDNA synthesis with Mitochondrial division in human cells. *Science*, *353*(6296).

Li, X., and Gould, S. J. (2003). The dynamin-like GTPase DLP1 is essential for peroxisome division and is recruited to peroxisomes in part by PEX11. *Journal of Biological Chemistry*, *278*(19), 17012–17020.

Liu, H., Tan, X., Veenhuis, M., McCollum, D., and Cregg, J. M. (1992). An efficient screen for peroxisome-deficient mutants of Pichia pastoris. *Journal of Bacteriology*, *174*(15), 4943–4951.

Loewen, C., and Levine, T. (2005). A highly conserved binding site in VAP for the FFAT motif of lipid binding proteins. *The Journal of Biological Chemistry*, *280*(14), 14097–14104.

Longtine, M. S., McKenzie, A., Demarini, D. J., Shah, N. G., .. Pringle, J. R. (1998). Additional modules for versatile and economical PCR-based gene deletion and modification in *Saccharomyces cerevisiae*. *Yeast, 14(10),* 953-961.

Manford, A. G., Stefan, C. J., Yuan, H. L., MacGurn, J. A., and Emr, S. D. (2012). ER-to-Plasma Membrane Tethering Proteins Regulate Cell Signaling and ER Morphology. *Developmental Cell*, *23*(6), 1129–1140.

Mast, F. D., Herricks, T., Strehler, K. M., Miller, L. R., Saleem, R. A., Rachubinski, R. A., and Aitchison, J. D. (2018). ESC RT-III is required for scissioning new peroxisomes from the endoplasmic reticulum. *Journal of Cell Biology*, *217*(6), 2087–2102.

Mast, F. D., Jamakhandi, A., Saleem, R. A., Dilworth, D. J., Rogers, R. S., Rachubinski, R. A., and Aitchison, J. D. (2016). Peroxins Pex30 and Pex29 dynamically associate with reticulons to regulate peroxisome biogenesis from the endoplasmic reticulum. *Journal of Biological Chemistry*, *291*(30), 15408–15427.

Matsumoto, N., Tamura, S., and Fujiki, Y. (2003). The pathogenic peroxin Pex26p recruits the Pex1p–Pex6p AAA ATPase complexes to peroxisomes. *Nature Cell Biology*, *5*(5), 454–460.

Matsuzono, Y., Kinoshita, N., Tamura, S., Shimozawa, N., Hamasaki, M., Ghaedi, K., … Fujiki, Y. (1999). Human PEX19: cDNA cloning by functional complementation, mutation analysis in a patient with zellweger syndrome, and potential role in peroxisomal membrane assembly. *Proceedings of the National Academy of Sciences of the United States of America*, *96*(5), 2116–2121.

Matsuzono, Y., Matsuzaki, T., and Fujiki, Y. (2006). Functional domain mapping of peroxin Pex19p: Interaction with Pex3p is essentail for function and translocation. *Journal of Cell Science*, *119*(17), 3539–3550.

Mayerhofer, P. U., Bañó-Polo, M., Mingarro, I., and Johnson, A. E. (2016). Human Peroxin PEX3 Is Co-translationally Integrated into the ER and Exits the ER in Budding Vesicles. *Traffic*, *17*(2), 117–130.

Meinecke, M., Bartsch, P., and Wagner, R. (2016). Peroxisomal protein import pores. *Biochimica et Biophysica Acta - Molecular Cell Research*, *1863*(5), 821–827.

Meinecke, M., Cizmowski, C., Schliebs, W., Krüger, V., Beck, S., Wagner, R., and Erdmann, R. (2010). The peroxisomal importomer constitutes a large and highly dynamic pore. *Nature Cell Biology*, *12*(3), 273–277.

Miyata, N., and Fujiki, Y. (2005). Shuttling mechanism of peroxisome targeting signal type 1 receptor Pex5: ATP-independent import and ATP-dependent export. *Molecular and Cellular Biology*, *25*(24), 10822–10832.

Morand, O., Allen, L., Zoeller, R., and Raetz, C. (1990). A rapid selection for animal cell mutants with defective peroxisomes. *Biochimica et Biophysica Acta (BBA) - General Subjects*, *1034*(2), 132–141.

Motley, A. M., Galvin, P. C., Ekal, L., Nuttall, J. M., and Hettema, E. H. (2015). Reevaluation of the role of Pex1 and dynamin-related proteins in peroxisome membrane biogenesis. *The Journal of Cell Biology*, *211*(5), 1041–1056.

Motley, A. M., and Hettema, E. H. (2007). Yeast peroxisomes multiply by growth and division. *The Journal of Cell Biology*, *178*(3), 399–410.

Motley, A. M., Nuttall, J. M., and Hettema, E. H. (2012). Pex3-anchored Atg36 tags peroxisomes for degradation in *Saccharomyces cerevisiae*. *The EMBO Journal*, *31*(13), 2852–2868.

Motley, A. M., Ward, G. P., and Hettema, E. H. (2008). Dnm1p-dependent peroxisome fission requires Caf4p, Mdv1p and Fis1p. *Journal of Cell Science*, *121*(10), 1633–1640.

Munck, J. M., Motley, A. M., Nuttall, J. M., and Hettema, E. H. (2009). A dual function for Pex3p in peroxisome formation and inheritance. *The Journal of Cell Biology*, *187*(4), 463–471.

Muntau, A. C., Mayerhofer, P. U., Paton, B. C., Kammerer, S., and Roscher, A. A. (2000). Defective peroxisome membrane synthesis due to mutations in human PEX3 causes Zellweger syndrome, complementation group G. *American Journal of Human Genetics*, *67*(4), 967–975.

Muntau, A. C., Roscher, A. A., Kunau, W. H., and Dodt, G. (2003). The interaction between human PEX3 and PEX19 characterized by fluorescence resonance energy transfer (FRET) analysis. *European Journal of Cell Biology*, *82*(7), 333–342.

Nascimento, A. F., Trindade, D. M., Tonoli, C. C., de Giuseppe, P. O., … Murakami, M. T. (2013). Structural insights into functional overlapping and differentiation among myosin V motors. *The Journal of Biological Chemistry*, *288*(47), 34131–34145.

Otzen, M., Rucktäschel, R., Thoms, S., Emmrich, K., Krikken, A. M., Erdmann, R., and van der Klei, I. J. (2012). Pex19p contributes to peroxisome inheritance in the association of peroxisomes to Myo2p. *Traffic (Copenhagen, Denmark)*, *13*(7), 947–959.

Pan, X., Roberts, P., Chen, Y., Kvam, E., Shulga, N., Huang, K., … Goldfarb, D. S. (2000). Nucleus-vacuole junctions in Saccharomyces cerevisiae are formed through the direct interaction of Vac8p with Nvj1p. *Molecular Biology of the Cell*, *11*(7), 2445–2457.

Pernice, W. M., Vevea, J. D., and Pon, L. A. (2016). A role for Mfb1p in region-specific anchorage of high-functioning mitochondria and lifespan in Saccharomyces cerevisiae. *Nature Communications*, *7*, 10595.

Petriv, O. I., Tang, L., Titorenko, V. I., and Rachubinski, R. A. (2004). A New Definition for the Consensus Sequence of the Peroxisome Targeting Signal Type 2. *Journal of Molecular Biology*, *341*(1), 119–134.

Pichler, H., Gaigg, B., Hrastnik, C., Achleitner, G., Kohlwein, S. D., Zellnig, G., … Daum, G. (2001). A subfraction of the yeast endoplasmic reticulum associates with the plasma membrane and has a high capacity to synthesize lipids. *European Journal of Biochemistry*, *268*(8), 2351–2361.

Ping, H. A., Kraft, L. M., Chen, W. T., Nilles, A. E., and Lackner, L. L. (2016). Num1 anchors mitochondria to the plasma membrane via two domains with different lipid binding specificities. *Journal of Cell Biology*, *213*(5), 513–524.

Pinto, M. P., Grou, C. P., Fransen, M., Sá-Miranda, C., and Azevedo, J. E. (2009). The cytosolic domain of PEX3, a protein involved in the biogenesis of peroxisomes, binds membrane lipids. *BBA - Molecular Cell Research*, *1793*, 1669–1675.

Platta, H. W., El Magraoui, F., Bäumer, B. E., Schlee, D., Girzalsky, W., and Erdmann, R. (2009). Pex2 and pex12 function as protein-ubiquitin ligases in peroxisomal protein import. *Molecular and Cellular Biology*, *29*(20), 5505–5516.

Platta, H. W., and Erdmann, R. (2007). The peroxisomal protein import machinery. *FEBS Letters*, Vol. 581, 2811–2819.

Platta, H. W., Grunau, S., Rosenkranz, K., Girzalsky, W., and Erdmann, R. (2005). Functional role of the AAA peroxins in dislocation of the cycling PTS1 receptor back to the cytosol. *Nature Cell Biology*, *7*(8), 817–822.

Poirier, Y., Antonenkov, V. D., Glumoff, T., and Hiltunen, J. K. (2006). Peroxisomal β-oxidation—A metabolic pathway with multiple functions. *Biochimica et Biophysica Acta (BBA) - Molecular Cell Research*, *1763*(12), 1413–1426.

Poll-The, B. T., Saudubray, J. M., Ogier, H. A., Odièvre, M., Scotto, J. M., Monnens, L., … Schutgens, R. B. (1987). Infantile Refsum disease: an inherited peroxisomal disorder. Comparison with Zellweger syndrome and neonatal adrenoleukodystrophy. *European Journal of Pediatrics*, *146*(5), 477–483.

Prinz, W. A. (2014). Bridging the gap: Membrane contact sites in signaling, metabolism, and organelle dynamics. *Journal of Cell Biology*, Vol. 205, 759–769.

Prinz, W. A., Toulmay, A., and Balla, T. (2020). The functional universe of membrane contact sites. *Nature Reviews Molecular Cell Biology*, Vol. 21, 7–24.

Pruyne, D., Evangelista, M., Yang, C., Bi, E., Zigmond, S., Bretscher, A., and Boone, C. (2002). Role of formins in actin assembly: Nucleation and barbed-end association. *Science*, *297*(5581), 612–615.

Rhodin, J. (1954). Correlation of ultrastructural organization and function in normal and experimentally changed proximal convoluted tubule cells of the mouse kidney. *Doctoral Thesis., Karolinska Institutet, Stockholm, Aktiebolaget Godvil*, *1*.

Rizzuto, R., Brini, M., Murgia, M., and Pozzan, T. (1993). Microdomains with high Ca2+ close to IP3-sensitive channels that are sensed by neighboring mitochondria. *Science*, *262*(5134), 744–747.

Rosenberg, A. H., Lade, B. N., Dao-shan, C., Lin, S. W., Dunn, J. J., and Studier, F. W. (1987). Vectors for selective expression of cloned DNAs by T7 RNA polymerase. *Gene*, *56*(1), 125–135.

Saarikangas, J., Zhao, H., and Lappalainen, P. (2010). Regulation of the actin cytoskeleton-plasma membrane interplay by phosphoinositides. *Physiological Reviews*, Vol. 90, 259–289.

Saarikangas, J., Zhao, H., Pykäläinen, A., Laurinmäki, P., Mattila, P. K., Kinnunen, P. K. J., … Lappalainen, P. (2009). Molecular Mechanisms of Membrane Deformation by I-BAR Domain Proteins. *Current Biology*, *19*(2), 95–107.

Sacksteder, K. A., Jones, J. M., South, S. T., Li, X., Liu, Y., and Gould, S. J. (2000). PEX19 binds multiple peroxisomal membrane proteins, is predominantly cytoplasmic, and is required for peroxisome membrane synthesis. *Journal of Cell Biology*, *148*(5), 931–944.

Santos, M., Imanaka, T., Shio, H., Small, G., and Lazarow, P. (1988). Peroxisomal membrane ghosts in Zellweger syndrome--aberrant organelle assembly. *Science*, *239*(4847), 1536–1538.

Saraya, R., Cepińska, M. N., Kiel, J. A. K. W., Veenhuis, M., and van der Klei, I. J. (2010). A conserved function for Inp2 in peroxisome inheritance. *Biochimica et Biophysica Acta*, *1803*(5), 617–622.

Sato, Y., Shibata, H., Nakatsu, T., Nakano, H., Kashiwayama, Y., Imanaka, T., and Kato, H. (2010). Structural basis for docking of peroxisomal membrane protein carrier Pex19p onto its receptor Pex3p. *The EMBO Journal*, *29*(24), 4083–4093.

Schmidt, F., Dietrich, D., Eylenstein, R., Groemping, Y., Stehle, T., and Dodt, G. (2012). The role of conserved PEX3 regions in PEX19-binding and peroxisome biogenesis. *Traffic (Copenhagen, Denmark)*, *13*(9), 1244–1260.

Schmidt, F., Treiber, N., Zocher, G., Bjelic, S., Steinmetz, M. O., Kalbacher, H., … Dodt, G. (2010). Insights into peroxisome function from the structure of PEX3 in complex with a soluble fragment of PEX19. *Journal of Biological Chemistry*, *285*(33), 25410–25417.

Schrader, M., Bonekamp, N. A., and Islinger, M. (2012). Fission and proliferation of peroxisomes. *Biochimica et Biophysica Acta, 1822(9),* 1343-1357.

Schuldiner, M., Metz, J., Schmid, V., Denic, V., Rakwalska, M., Schmitt, H. D., … Weissman, J. S. (2008). The GET Complex Mediates Insertion of Tail-Anchored Proteins into the ER Membrane. *Cell*, *134*(4), 634–645.

Scorrano, L., De Matteis, M. A., Emr, S., Giordano, F., Hajnóczky, G., Kornmann, B., … Schuldiner, M. (2019). Coming together to define membrane contact sites. *Nature Communications*, *10*(1), 1–11.

Sellers, J. R., and Veigel, C. (2006). Walking with myosin V. *Current Opinion in Cell Biology*, Vol. 18, 68–73.

Shai, N., Yifrach, E., van Roermund, C. W. T., Cohen, N., Bibi, C., IJlst, L., … Zalckvar, E. (2018). Systematic mapping of contact sites reveals tethers and a function for the peroxisome-mitochondria contact. *Nature Communications*, *9*(1), 1761.

Shibata, H., Kashiwayama, Y., Imanaka, T., and Kato, H. (2004). Domain architecture and activity of human Pex19p, a chaperone-like protein for intracellular trafficking of peroxisomal membrane proteins. *Journal of Biological Chemistry*, *279*(37), 38486–38494.

Shimozawa, N., Suzuki, Y., Zhang, Z., Imamura, A., Ghaedi, K., Fujiki, Y., and Kondo, N. (2000). Identification of PEX3 as the gene mutated in a Zellweger syndrome patient lacking peroxisomal remnant structures. *Human Molecular Genetics*, *9*(13), 1995–1999.

Smith, J. J. and Aitchison, J. D. (2013). Peroxisomes take shape. *Nature Reviews Molecular Cell Biology, 14(12),* 803-817.

South, S. T., and Gould, S. J. (1999). Peroxisome synthesis in the absence of preexisting peroxisomes. *Journal of Cell Biology*, *144*(2), 255–266.

Studier, F. W., and Moffatt, B. A. (1986). Use of bacteriophage T7 RNA polymerase to direct selective high-level expression of cloned genes. *Journal of Molecular Biology*, *189*(1), 113–130.

Sugiura, A., Mattie, S., Prudent, J., and McBride, H. M. (2017). Newly born peroxisomes are a hybrid of mitochondrial and ER-derived pre-peroxisomes. *Nature, 542, 251-254.*

Swayne, T. C., Zhou, C., Boldogh, I. R., Charalel, J. K., McFaline-Figueroa, J. R., Thoms, S., … Pon, L. A. (2011). Role for cER and Mmr1p in anchorage of mitochondria at sites of polarized surface growth in budding yeast. *Current Biology*, *21*(23), 1994–1999.

Swinkels, B. W., Gould, S. J., and Subramani, S. (1992). Targeting efficiencies of various permutations of the consensus C-terminal tripeptide peroxisomal targeting signal. *FEBS Letters*, *305*(2), 133–136.

Tahirovic, S., Schorr, M., and Mayinger, P. (2005). Regulation of intracellular phosphatidylinositol-4-phosphate by the Sac1 lipid phosphatase. *Traffic*, *6*(2), 116–130.

Tam, Y. Y. C., Fagarasanu, A., Fagarasanu, M., and Rachubinski, R. A. (2005). Pex3p initiates the formation of a preperoxisomal compartment from a subdomain of the endoplasmic reticulum in Saccharomyces cerevisiae. *Journal of Biological Chemistry*, *280*(41), 34933–34939.

Tanaka, C., Tan, L. J., Mochida, K., Kirisako, H., Koizumi, M., Asai, E., … Nakatogawa, H. (2014). Hrr25 triggers selective autophagy-related pathways by phosphorylating receptor proteins. *Journal of Cell Biology*, *207*(1), 91–105.

Tang, X., Punch, J. J., and Lee, W.-L. (2009). A CAAX motif can compensate for the PH domain of Num1 for cortical dynein attachment. *Cell Cycle (Georgetown, Tex.)*, *8*(19), 3182–3190.

Thoms, S., Harms, I., Kalies, K. U., and Gärtner, J. (2012). Peroxisome Formation Requires the Endoplasmic Reticulum Channel Protein Sec61. *Traffic*, *13*(4), 599–609.

Titorenko, V. I., Smith, J. J., Szilard, R. K., and Rachubinski, R. A. (1998). Pex20p of the Yeast Yarrowia lipolytica Is Required for the Oligomerization of Thiolase in the Cytosol and for Its Targeting to the Peroxisome. *The Journal of Cell Biology*, *142*(2), 403–420.

Tsukamoto, T., Yokota, S., and Fujiki, Y. (1990). Isolation and characterization of Chinese hamster ovary cell mutants defective in assembly of peroxisomes. *The Journal of Cell Biology*, *110*(3), 651–660.

Urbanek, A. N., Smith, A. P., Allwood, E. G., Booth, W. I., and Ayscough, K. R. (2013). A novel actin-binding motif in Las17/WASP nucleates actin filaments independently of Arp2/3. *Current Biology, 23(3),* 196-203.

Urquhart, A. J., Kennedy, D., Gould, S. J., and Crane, D. I. (2000). Interaction of Pex5p, the type 1 peroxisome targeting signal receptor, with the peroxisomal membrane proteins Pex14p and Pex13p. *Journal of Biological Chemistry*, *275*(6), 4127–4136.

Ušaj, M. M., Brložnik, M., Kaferle, P., Žitnik, M., … Petrovič, U. (2015). Genome-Wide Localization Study of Yeast Pex11 Identifies Peroxisome-Mitochondria Interactions through the ERMES Complex. *Journal of Molecular Biology, 427(11),* 2072-2087.

Valm, A. M., Cohen, S., Legant, W. R., Melunis, J., Hershberg, U., Wait, E., … Lippincott-Schwartz, J. (2017). Applying systems-level spectral imaging and analysis to reveal the organelle interactome. *Nature*, Vol. 546, 162–167.

Van Der Zand, A., Braakman, I., and Tabak, H. F. (2010). Peroxisomal membrane proteins insert into the endoplasmic reticulum. *Molecular Biology of the Cell*, *21*(12), 2057–2065.

Van Der Zand, A., Gent, J., Braakman, I., and Tabak, H. F. (2012). Biochemically distinct vesicles from the endoplasmic reticulum fuse to form peroxisomes. *Cell*, *149*(2), 397–409.

Veenhuis, M., Mateblowski, M., Kunau, W. H., and Harder, W. (1987). Proliferation of microbodies inSaccharomyces cerevisiae. *Yeast*, *3*(2), 77–84.

Vernay, A., Schaub, S., Guillas, I., Bassilana, M., and Arkowitz, R. A. (2012). A steep phosphoinositide bis-phosphate gradient forms during fungal filamentous growth. *Journal of Cell Biology*, *198*(4), 711–730.

Voeltz, G. K., Prinz, W. A., Shibata, Y., Rist, J. M., and Rapoport, T. A. (2006). A class of membrane proteins shaping the tubular endoplasmic reticulum. *Cell*, *124*(3), 573–586.

Walch-Solimena, C., and Novick, P. (1999). The yeast phosphatidylinositol-4-OH kinase Pik1 regulates secretion at the Golgi. *Nature Cell Biology*, *1*(8), 523–525.

Wanders, R. J. A. (2014). Metabolic functions of peroxisomes in health and disease. *Biochimie*, *98*, 36–44.

Wanders, R. J. A., and Waterham, H. R. (2006). Peroxisomal disorders: the single peroxisomal enzyme deficiencies. *Biochimica et Biophysica Acta*, *1763*(12), 1707–1720.

Wang, Songyu, Tukachinsky, H., Romano, F. B., and Rapoport, T. A. (2016). Cooperation of the ER-shaping proteins atlastin, lunapark, and reticulons to generate a tubular membrane network. *ELife*, *5*(September).

Waterham, H. R., Ferdinandusse, S., and Wanders, R. J. A. (2016). Human disorders of peroxisome metabolism and biogenesis. *Biochimie et Biophysica Acta, 1863(5),* 922-933.

West, M., Zurek, N., Hoenger, A., and Voeltz, G. K. (2011). A 3D analysis of yeast ER structure reveals how ER domains are organized by membrane curvature. *Journal of Cell Biology*, *193*(2), 333–346.

Williams, C., van den Berg, M., Geers, E., and Distel, B. (2008). Pex10p functions as an E3 ligase for the Ubc4p-dependent ubiquitination of Pex5p. *Biochemical and Biophysical Research Communications*, *374*(4), 620–624.

Wu, F., de Boer, R., Krikken, A., Akşit, A., Bordin, N., Devos, D., and van der Klei, I. (2020). Pex24 and Pex32 are required to tether peroxisomes to the ER for organelle biogenesis, positioning and segregation. *Journal of Cell Science*, jcs.246983.

Wu, H., de Boer, R., Krikken, A. M., Akşit, A., Yuan, W., and van der Klei, I. J. (2019). Peroxisome development in yeast is associated with the formation of Pex3-dependent peroxisome-vacuole contact sites. *Biochimica et Biophysica Acta - Molecular Cell Research*, *1866*(3), 349–359.

Yagita, Y., Shinohara, K., Abe, Y., Nakagawa, K., Al-Owain, M., Alkuraya, F. S., and Fujiki, Y. (2017). Deficiency of a Retinal Dystrophy Protein, Acyl-CoA Binding Domain-containing 5 (ACBD5), Impairs Peroxisomal β-Oxidation of Very-long-chain Fatty Acids. *Journal of Biological Chemistry*, *292*(2), 691–705.

Yu, J. W., Mendrola, J. M., Audhya, A., Singh, S., Keleti, D., DeWald, D. B., … Lemmon, M. A. (2004). Genome-wide analysis of membrane targeting by S. cerevisiae pleckstrin homology domains. *Molecular Cell*, *13*(5), 677–688.